

Masterthesis

GLUINO ANNIHILATION INTO GLUONS AT NEXT TO LEADING ORDER

Anne Poppe
Münster, January 17, 2023

Institut for Theoretical Physics

First examiner: Prof. Dr. Michael Klasen
Second examiner: PD Dr. Karol Kovařík

Contents

1	Introduction	1
2	Supersymmetry	2
2.1	Supersymmetric Algebra	2
2.2	Wess-Zumino model	3
2.3	Supersymmetric gauge theory	4
2.4	Minimal Supersymmetric Standard Model	5
2.5	Soft SUSY Breaking	6
2.6	Mass matrices	6
2.6.1	Gluino sector	6
2.6.2	Squark sector	7
3	Dark matter	9
3.1	Observational evidence	9
3.2	Candidates	10
3.3	Boltzmann equation and freeze-out mechanism	11
4	DM@NLO	16
5	Gluino Annihilation into Gluons	17
5.1	Leading Order Contributions	17
5.2	Next-to-leading order contributions	19
6	Color decomposition	24
6.1	Color of tree level	27
7	Next-to-leading order computations	28
7.1	Superficial degree of divergence	28
7.2	Dimensional Regularization	29
7.3	Passarino-Veltman integrals	30
7.3.1	Scalar integrals	31
7.3.2	Tensor integrals and reduction	34
7.4	Renormalization	36
7.4.1	Minimal subtraction	37
7.4.2	On-shell subtraction	37
7.4.3	Gluon sector	38
7.4.4	Ghost sector	39
7.4.5	Gluino sector	39
7.4.6	Correction of α_s	41
7.4.7	Vertex counterterms	41
7.5	Infrared divergencies	42
8	Numerical results	46

9	Conclusion	47
A	Collection of Formulas	48
A.1	Dirac Algebra in D Dimensions	48
A.1.1	Dirac Matrices	48
A.1.2	Completeness Relations	48
A.1.3	Traces	48
A.1.4	Dirac Equation	48
A.2	SU(N) Algebra	49
A.3	Feynman parametrization	49
B	Feynman rules	50
B.1	Propagators	50
B.2	Couplings	50
B.3	Counterterms	52
C	Calculations for color basis	53
D	Virtual corrections	54
D.1	Self energies	55
D.1.1	Gluon self energy	55
D.1.2	Ghost	58
D.1.3	Gluino self energy	59
D.2	Vertex Corrections	60
D.2.1	Gluino-gluon Vertex	60
D.3	Box diagrams	69

1 Introduction

The existence of dark matter was proposed almost ninety years ago. Since then many observations confirmed this hypothesis, however without determining the nature of dark matter. As Standard Model physics alone cannot explain all observations connected to dark matter, there are plenty of suggestions of new physics to account for the observations. The most convincing extensions of the Standard Model are also able to present solutions for other phenomena the Standard Model cannot describe.

One well-known extension is the Supersymmetry, which is based on a symmetry between bosonic and fermionic states. This theory predicts quite a number of new fields which come along with a great number of free parameters. When opting for a parameter constellations, where one of the neutralinos happens to be the lightest supersymmetric particle, this offers a viable dark matter candidate. In addition to that, Supersymmetry is well motivated by plenty theoretical reasons. In chapter 2 the concept of supersymmetric theories will be illustrated by presenting some simplified models. These will lead to the particle content of the Minimal Supersymmetric Standard Model (MSSM).

Chapter 3 lists some observational evidences for dark matter and introduces the Λ CDM model. It follows a discussion of possible dark matter candidates. Assuming dark matter consists of WIMPs (as for example the LSP) the production of dark matter can be described by the freeze-out mechanism. Depending on the choice of parameters not only the cross sections of LSP annihilation is relevant for the relic density predicted by the freeze-out mechanism, but also coannihilations and annihilations of other supersymmetric particles. For this thesis we want to assume that the mass of the gluino is only slightly higher than the mass of the LSP. In this case the annihilation of gluinos into gluons affects the dark matter relic density significantly.

To test certain parameter scenarios to match the dark matter abundance measured by the Planck observatory, cross sections of the relevant processes have to be known to a certain precision. The goal of DM@NLO is to provide all those cross sections at next to leading order.

In chapter 6 the color basis for the gluino annihilation into gluons is deduced. Then the thesis focuses on how to deal with the virtual divergencies appearing in NLO calculations. Chapter 7 discusses the principles of dimensional regularization, Passarino-Veltman reduction and the renormalization of the fields and masses relevant for this thesis. At the end the contributions of the different NLO corrections are shown graphically for one specific scenario of parameters.

2 Supersymmetry

Today's Standard Model is doing an excellent job with describing numerous phenomena of particle physics with great precision. However there are some open questions that cannot be answered using the Standard Model, e.g. the Hierarchy Problem or the existence of Dark Matter. Due to the great success of building a theory based upon symmetries (namely space-time and gauge symmetries) the idea is to embed the Standard Model into a larger symmetry.

How to construct a suitable algebra as the basis of supersymmetry is shown in the first section of this chapter. Then the Wess-Zumino model, describing how to supersymmetrize spinor and scalar fields, will be considered. After presenting also how a supersymmetric gauge field is designed, we can combine those concepts to set up the MSSM (based on [1]). At the end of the chapter the mass eigenstates of the sparticles relevant for this thesis are summarized.

2.1 Supersymmetric Algebra

When thinking about extending the Standard Model, it is instructive to consider possible extensions of the corresponding algebra, i.e. the Poincaré algebra. The known generators of the Poincaré group are the 4-momentum operator P^μ which generates space-time translations and $M_{\mu\nu}$ which generates the boosts and rotations of Lorentz transformations. The Coleman-Mandula theorem states that (under some general assumptions) the combination of the Poincaré group and an internal symmetry group has to be the direct product of both. In other words all conserved quantities other than P^μ and $M_{\mu\nu}$ have to be scalars, the generators of the gauge symmetries. This result is therefore also known as the No-go theorem.

Later Haag, Lopuszanski and Sohnius found a loop-hole and proved that you can add fermionic (2 component spinor) generators Q_α instead of bosonic (scalar) ones. These supersymmetry generators satisfy the anticommutation relation

$$\{Q_\alpha, \bar{Q}_\beta\} = 2\gamma_{\alpha\beta}^\mu P_\mu. \quad (2.1)$$

Notice that the anticommutator of the two fermionic operators leads to a bosonic operator, which establishes the connection between fermionic and bosonic parts of the algebra. Supersymmetry algebra is obviously not a direct product of the Poincaré group and an internal symmetry group, as Q on the one hand affects gauge symmetries, while its anticommutator has an impact on space-time. Since the introduction of the supersymmetry generator Q_α requires additional degrees of freedom, one has to extend the known 4-dimensional space-time to superspace, where the Q_α then act on the four 'new' fermionic dimensions.

As Q_α generates a conserved symmetry and is of spinorial nature, also the following commutation relations hold:

$$[Q_\alpha, H] = 0 \quad (2.2)$$

$$[Q_\alpha, M_{\mu\nu}] = (\sigma_{\mu\nu})_{\alpha\beta} Q_\beta \quad (2.3)$$

One can show, that the SUSY operator acting on a particle state changes the spin of the field by $\frac{1}{2}$. Therefore applying Q to fermions of the Standard Model will create the scalar sfermions, applying Q to the SM gauge bosons creates fermionic gauginos. These superpartners possess all properties of their corresponding SM particle, except for their spin of course. In the Standard Model left chiral fields form $SU(2)_L$ doublets, while right chiral fields are singlets under $SU(2)_L$. Thus also the superpartners of left (right) chiral fields are arranged in $SU(2)_L$ doublets (singlets), the so called left (right) chiral supermultiplets. Before introducing the full particle content of the MSSM, we take a short step-by-step approach describing the supersymmetric models for chiral fields and gauge fields independently.

2.2 Wess-Zumino model

In 1974 Wess and Zumino developed the first supersymmetric quantum field theory consisting of a Weyl spinor, a real scalar and a pseudoscalar field. In a free theory those transform under the following SUSY transformations:

$$\delta A = \bar{\epsilon}\Psi \quad (2.4)$$

$$\delta B = i\epsilon\gamma_5\Psi \quad (2.5)$$

$$\delta\Psi = -i\epsilon(A + i\gamma_5 B) \quad (2.6)$$

where ϵ is a constant infinitesimal Majorana spinor. If one now defines the SUSY generator as $\delta A = \bar{\epsilon}QA$, this will yield to the same anticommutation relation already stated in equation (2.1).

When taking also interactions into account, one introduces two more auxiliary real scalar fields F and G to adapt the degrees of freedom to those of the off-shell fermion. After applying the Euler-Lagrange equations to these fields, the equations of motion will remove the unphysical auxiliary fields from the Lagrangian, which then reads

$$\begin{aligned} \mathcal{L} = & \underbrace{\frac{1}{2}(\partial_\mu A)(\partial^\mu A) + \frac{1}{2}(\partial_\mu B)(\partial^\mu B) + \frac{i}{2}\bar{\Psi}\not{\partial}\Psi}_{\text{kinetic terms}} - \underbrace{\frac{1}{2}m\bar{\Psi}\Psi - \frac{1}{2}m^2(A^2 + B^2)}_{\text{mass terms}} \\ & - \underbrace{m\frac{\lambda}{\sqrt{2}}A(A^2 + B^2) - \frac{\lambda^2}{4}(A^2 + B^2)^2 - \frac{\lambda}{\sqrt{2}}\bar{\Psi}(A - i\gamma_5 B)\Psi}_{\text{interaction terms}} \end{aligned} \quad (2.7)$$

Notice that all fields have the same mass m and all interactions have the same coupling constant λ .

As the model should describe a pair of fermion and sfermion, it is useful to combine the two real fields A and B to one complex scalar field

$$\phi = \frac{1}{\sqrt{2}}(A + iB). \quad (2.8)$$

In addition we now use the Weyl notation $\Psi = \begin{pmatrix} \psi \\ \chi \end{pmatrix}$, where now Ψ represents the fermion and ϕ the sfermion. The SUSY transformations then read

$$\delta\phi = \epsilon\chi \quad (2.9)$$

$$\delta\chi = -i\sigma^\mu i\sigma_2 \epsilon^* \partial_\mu \phi + \epsilon F. \quad (2.10)$$

This illustrates the transition from the scalar field ϕ to the chiral spinor field χ under SUSY transformation and vice versa, so that Q connects the SM multiplets to the supermultiplets. The whole Lagrangian can then also be expressed as

$$\begin{aligned} \mathcal{L}_{\text{chiral}} = & \underbrace{(\partial_\mu \phi)(\partial^\mu \phi) + \chi i \bar{\sigma}^\mu \partial_\mu \chi}_{\text{kintic terms}} \quad \underbrace{-m^2 \phi^2 - \frac{1}{2} \left(m \chi^T (-i\sigma_2) \chi + h.c. \right)}_{\text{mass terms}} \\ & \underbrace{-\frac{1}{2} \left(m y^* \phi \phi^{\dagger 2} + h.c. \right)}_{\text{cubic sfermion interaction}} \quad \underbrace{-\frac{1}{4} y^2 \phi^2 \phi^{\dagger 2}}_{\text{quartic sfermion interaction}} \quad \underbrace{-\frac{1}{2} (y \phi \chi \cdot \chi + h.c.)}_{\text{Yukawa-type interaction}}. \end{aligned} \quad (2.11)$$

2.3 Supersymmetric gauge theory

In analogue to the Wess-Zumino model the next goal is to build a supersymmetric model for a gauge field A and its superpartner, the gaugino λ . As usual we define the field strength tensor for the non-abelian $SU(N)$ gauge theory as

$$F_{\mu\nu}^a = \partial_\mu A_\nu^a - \partial_\nu A_\mu^a - g\epsilon^{abc} A_\mu^b A_\nu^c \quad (2.12)$$

where a, b, c run from 1 to $N^2 - 1$ and ϵ denotes the corresponding structure constant of the gauge group. Considering also the off-shell case, the gauge field acquires a third, longitudinal degree of freedom in addition to the two transverse ones. This leads again to the introduction of an auxiliary real scalar field D , which is in line with the third degree of freedom. The SUSY transformation of the gauge and the gaugino fields are

$$\delta A^{\mu,a} = \epsilon^\dagger \bar{\sigma}^\mu \lambda^a + \lambda^{a\dagger} \bar{\sigma}^\mu \epsilon \quad (2.13)$$

$$\delta \lambda^a = \frac{1}{2} i \sigma^\mu \bar{\sigma}^\nu \epsilon F_{\mu\nu}^a + \epsilon D^a. \quad (2.14)$$

This shows how the gauge field transits into a Majorana spinor describing the gaugino and vice versa. The fields come together in the Lagrangian as

$$\mathcal{L}_{\text{gauge}} = -\frac{1}{4} F_{\mu\nu}^a F^{\mu\nu,a} + i \lambda^{a\dagger} \bar{\sigma}^\mu (D_\mu \lambda)^a + \frac{1}{2} D^a D^a \quad (2.15)$$

where $\sigma^\mu = (1, \vec{\sigma})$ and $\bar{\sigma}^\mu = (1, -\vec{\sigma})$. The covariant derivate has to be chosen to $D_\mu = \partial_\mu + ig\epsilon^{abc} A_\mu^b$ to preserve the gauge invariance of the Lagrangian.

As a next step towards the MSSM we now want to combine the fermions and sfermion of the Wess-Zumino model with the gauge fields and gauginos. In order to maintain

gauge invariance the partial derivative in the Wess-Zumino Lagrangian (2.11) is substituted by the covariant derivative $D_\mu = \partial_\mu + igA_\mu^a T^a$, which leads to interaction terms between the fermions/sfermions and the gauge fields. Possible interaction terms between the fermions/sfermions and the gauginos have to respect not only Lorentz and gauge invariance, but also renormalizability and invariance under SUSY transformations, which restricts those couplings. The combined Lagrangian of chiral and gauge fields therefore looks like

$$\begin{aligned} \mathcal{L}_{\text{chiral \& gauge}} = & \mathcal{L}_{\text{chiral}}(\partial_\mu \rightarrow D_\mu) + \mathcal{L}_{\text{gauge}} \\ & - \sqrt{2}g \left((\phi^\dagger T^a \chi) \cdot \lambda^a + \lambda^{a\dagger} \cdot (\chi^\dagger T^a \phi) \right) - g(\phi^\dagger T^a \phi) D^a. \end{aligned} \quad (2.16)$$

The arbitrary field D can be eliminated by using the equation of motion obtained by the Euler-Lagrange equation.

2.4 Minimal Supersymmetric Standard Model

The MSSM now is the supersymmetric extension of the Standard Model that needs least possible new fields, which means introducing just one SUSY generator Q . This assigns a supersymmetric bosonic degree of freedom to every fermionic one of the Standard Model and vice versa. For every gauge boson this leads to one gaugino. The fermions however come together with two sfermions respectively, labeled after the chirality of their partners. Additional to that we have to assume a second complex Higgs doublet, instead of just one as in the SM. All those supermultiplet fields are displayed in Table 1 and 2.

Let us now consider Spontaneous Symmetry Breaking in the MSSM. As in the Standard Model the Higgs mechanism produces three Goldstone bosons that give mass to the W and Z bosons, which leaves five massive Higgs fields. The charged ones we call H^\pm while the neutral ones are h^0 , H^0 and A^0 . The mass of the lightest Higgs field h^0 should of course fit the measured Higgs mass of $m_h = 125 \text{ GeV}$ to give a reasonable model. The mass eigenstates of gauginos and Higgsinos are gained by mixing fields with the same quantum numbers. Hence the charged fields \tilde{H}_u^+ , \tilde{H}_d^- , \tilde{W}^+ and \tilde{W}^- mix to charginos $\tilde{\chi}_{1,2}^\pm$, while the neutral fields \tilde{H}_u^0 , \tilde{H}_d^0 , \tilde{W}^0 and \tilde{B} mix to neutralinos $\tilde{\chi}_{1,2,3,4}^0$. The latter are of Majorana nature.

Another important aspect of the MSSM is the conservation of R-parity

$$R = (-1)^{3B+L+2s}, \quad (2.17)$$

where B is the baryon number, L the lepton number and s the spin of the particle. With this definition all Standard Model particles (including the second Higgs doublet) have $R = 1$ and all SUSY partners have $R = -1$. If this quantity is now conserved, it follows that sparticles can only be created and annihilated in pairs. After the decay of one single SUSY particle, there has to be one (or a higher odd number of) lighter sparticles among the decay products. For the lightest supersymmetric particle (LSP) this implicates stability.

names	symbol	spin 0	spin $\frac{1}{2}$
squarks, quarks ($\times 3$ families)	Q \bar{u} \bar{d}	$(\tilde{u}_L, \tilde{d}_L)$ \tilde{u}_R \tilde{d}_R	(u_L, d_L) $(u_R)^c$ $(d_R)^c$
sleptons, leptons ($\times 3$ families)	L \bar{e}	$(\tilde{\nu}_L, \tilde{e}_L)$ \tilde{e}_R	(ν_L, e_L) $(e_R)^c$
higgs, higgsinos	H_u H_d	(H_u^+, H_u^0) (H_d^0, H_d^-)	$(\tilde{H}_u^+, \tilde{H}_u^0)$ $(\tilde{H}_d^0, \tilde{H}_d^-)$

Table 1: Chiral supermultiplet fields in the MSSM. Taken from [2]

names	spin $\frac{1}{2}$	spin 1
gluinos, gluons	\tilde{g}	g
winos, W bosons	$\tilde{W}^\pm, \tilde{W}^0$	W^\pm, W^0
bino, B boson	\tilde{B}	B

Table 2: Gauge supermultiplet fields in the MSSM. Taken from [2]

2.5 Soft SUSY Breaking

If SUSY would be an exact symmetry, supersymmetric partners of SM particles should have been measured in experiments by now, as their mass would be at the same scale. Since this is not the case, one introduces SUSY breaking terms in the Lagrangian of the MSSM. In order to avoid additional divergencies one limits oneself to super-renormalizable terms (also called soft), which still leaves a number of 105 parameters for forming all possible soft SUSY breaking terms.

By taking also phenomenological constraints into account one can reduce the number of free parameters. The pMSSM is fixed by 19 parameters under the assumptions of no new sources of CP-violation, no Flavor Changing Neutral Currents and universality of first and second generation. Those¹ are listed in table 3.

2.6 Mass matrices

2.6.1 Gluino sector

The masses of gluinos are easy to extract from the Lagrangian as gauge eigenstates and mass eigenstates are the same in this case. The corresponding soft SUSY-breaking term is

$$\mathcal{L}_{\text{gluino mass}} = -\frac{1}{2}(M_3 \tilde{g}^a \tilde{g}^a + \text{h.c.}) \quad (2.18)$$

¹Note, that there are several possibilities for choosing this parameter set. In some of the literature used for the mass matrices other conventions were used.

$\tan(\beta)$	ratio of the VEVs of the two Higgs doublets
m_{A^0}	mass of the pseudoscalar Higgs boson
μ	Higgsino mass parameter
M_1	bino mass parameter
M_2	wino mass parameter
M_3	gluino mass parameter
$M_{\tilde{q}_L}, M_{\tilde{u}_R}, M_{\tilde{d}_R}$	first and second generation squark masses
$M_{\tilde{l}_L}, M_{\tilde{t}_R}$	first and second generation slepton masses
$M_{\tilde{q}_{3L}}, M_{\tilde{t}_R}, M_{\tilde{b}_R}$	third generation squark masses
$M_{\tilde{\tau}_L}, M_{\tilde{\tau}_R}$	third generation slepton masses
A_t, A_b, A_τ	third generation trilinear couplings

Table 3: The 19 parameters of the pMSSM

with $a = 1, \dots, 8$ and \tilde{g}^a being a L-type spinor. So the gluino mass parameter $|M_3|$ is the gluino mass itself.

2.6.2 Squark sector

The mass eigenstates of the quarks are defined as

$$\begin{pmatrix} \tilde{q}_1 \\ \tilde{q}_2 \end{pmatrix} = \begin{pmatrix} \cos \theta_q & \sin \theta_q \\ -\sin \theta_q & \cos \theta_q \end{pmatrix} \begin{pmatrix} \tilde{q}_L \\ \tilde{q}_R \end{pmatrix} \quad (2.19)$$

where the mixing angle is defined such that the mass matrix diagonalizes

$$\begin{pmatrix} \cos \theta_q & \sin \theta_q \\ -\sin \theta_q & \cos \theta_q \end{pmatrix} \begin{pmatrix} m_{\tilde{q}_L}^2 & m_{\tilde{q}_{LR}}^2 \\ m_{\tilde{q}_{LR}^*}^2 & m_{\tilde{q}_R}^2 \end{pmatrix} \begin{pmatrix} \cos \theta_q & \sin \theta_q \\ -\sin \theta_q & \cos \theta_q \end{pmatrix} = \begin{pmatrix} m_{\tilde{q}_1}^2 & 0 \\ 0 & m_{\tilde{q}_2}^2 \end{pmatrix}. \quad (2.20)$$

The entries of the mixing matrix are often also denoted as

$$\begin{pmatrix} \cos \theta_q & \sin \theta_q \\ -\sin \theta_q & \cos \theta_q \end{pmatrix} = \begin{pmatrix} R_{1L} & R_{1R} \\ R_{2L} & R_{2R} \end{pmatrix} = \begin{pmatrix} R_{11} & R_{12} \\ R_{21} & R_{22} \end{pmatrix}. \quad (2.21)$$

For identifying the mass matrix of squarks several terms of the MSSM-Lagrangian have to be considered (those can be looked up in e.g. [13]). Since one of the premises of the pMSSM is to introduce no Flavor Changing Neutral Currents, the only possible mixing of

squarks is the one of \tilde{q}_L and \tilde{q}_R . The relevant terms of the Lagrangian read

$$\mathcal{L}_{\tilde{q} \text{ mass}} = - \sum_q m_q^2 (\tilde{q}_L^* \tilde{q}_L + \tilde{q}_R^* \tilde{q}_R) \quad (2.22)$$

$$\mathcal{L}_{\tilde{q}\tilde{q}} = -M_Z^2 \cos 2\beta \left[(T_{3q} - \sin^2 \theta_W Q_q) \tilde{q}_L^* \tilde{q}_L + \sin^2 \theta_W Q_q \tilde{q}_R^* \tilde{q}_R \right] \quad (2.23)$$

$$\mathcal{L}_{\tilde{q}_L \tilde{q}_R} = m_u \mu \cot \beta (\tilde{u}_R^* \tilde{u}_L + \tilde{u}_L^* \tilde{u}_R) + m_d \mu \tan \beta (\tilde{d}_R^* \tilde{d}_L + \tilde{d}_L^* \tilde{d}_R) \quad (2.24)$$

$$\mathcal{L}_{\text{soft}} = - \sum_{\tilde{q}_i} \tilde{m}_{\tilde{q}_i}^2 \tilde{q}_i^* \tilde{q}_i + m_u A_u \tilde{u}_R^* \tilde{u}_L + m_d A_d \tilde{d}_R^* \tilde{d}_L + \text{h.c.} + [\dots] \quad (2.25)$$

where T_{3q} is the third component of the weak isospin, θ_W the Weinberg angle, Q_q the electric charge of the quark, $\tilde{m}_{\tilde{q}_i}^2$ the soft SUSY breaking mass terms and $A_{u,d}$ the trilinear coupling constants. These lead to the following mass matrix

$$M_{\tilde{q}}^2 = \begin{pmatrix} m_{\tilde{q}_L}^2 & m_{\tilde{q}_{LR}}^2 \\ m_{\tilde{q}_{LR}}^{2*} & m_{\tilde{q}_R}^2 \end{pmatrix} \quad (2.26)$$

with

$$m_{\tilde{q}_L}^2 = \tilde{m}_{\tilde{q}_L}^2 + m_q^2 + M_Z^2 \cos 2\beta (T_{3q} - \sin^2 \theta_W Q_q) \quad (2.27)$$

$$m_{\tilde{q}_R}^2 = \tilde{m}_{\tilde{q}_R}^2 + m_q^2 + M_Z^2 \cos 2\beta \sin^2 \theta_W Q_q \quad (2.28)$$

$$m_{\tilde{u}_{LR}}^2 = -m_u (\mu \cot \beta + A_u^*) \quad (2.29)$$

$$m_{\tilde{d}_{LR}}^2 = -m_d (\mu \tan \beta + A_d^*) \quad (2.30)$$

To gain the masses of \tilde{q}_1 and \tilde{q}_2 like in equation (2.20) one can use

$$m_{\tilde{q}_{1,2}} = \sqrt{\frac{1}{2} \left(\text{Tr } M_{\tilde{q}}^2 \pm \sqrt{\text{Tr}^2 M_{\tilde{q}}^2 - 4 \det M_{\tilde{q}}^2} \right)} \quad (2.31)$$

3 Dark matter

The concept of dark matter was first suggested by Fritz Zwicky in 1933, whose observation of the Coma cluster revealed the problem of the missing mass. Even though many other evidences for the existence of dark matter have been found during the last decades, the nature of dark matter is still unknown up to the present. In the following sections we will briefly recapitulate some of the observational evidences, discuss the most famous ideas trying to explain dark matter and then focus on the production mechanism of WIMPs.

3.1 Observational evidence

As mentioned above Zwicky studied the velocity of galaxies in galaxy clusters based on their red shifts. By estimating the number of nebulae in the Coma cluster and their masses he got an estimate for the visible mass of the whole cluster. Supposing a homogeneous mass distribution over the cluster and using the virial theorem one can calculate the expected velocity of the objects on the edge of the cluster. When comparing this to the measured red shift, Zwicky found a huge discrepancy. Zwicky calculated that the total mass of the cluster would have to be 400 times bigger than the visible mass to match the velocities [19]. Today we know that this result is quantitatively quite inaccurate, but the fact that the matter in our universe is in large part dark still holds today.

A similar approach is to study the rotation curves of galaxies. These show the circular

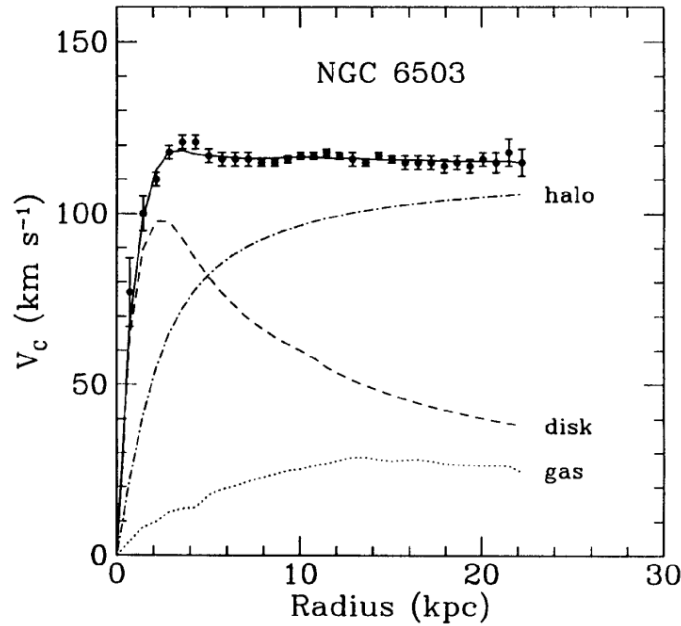


Figure 1: Galactic rotation curve for NGC 6503 showing disk and gas contribution plus the dark matter halo contribution needed to match the data[7]

velocity of the galaxy depending on the distance of the galactic center. In figure 1 the

line fitting the data points represents the velocity of the galaxy NGC 6503. The two lines labeled 'gas' and 'disk' shows the velocity that the visible matter would cause due to Kepler's gravitational laws. As one quickly realizes those two don't add up to the observed velocity. This is another evidence for the existence of dark matter. If one assumes a dark matter halo surrounding the galaxy, as indicated by the corresponding line in the plot, all contributions then add up to match the actual velocity.

Furthermore there are ways to determine the dark matter density in the universe without using kinetic analysis. The effect of gravitational lensing resulting from General Relativity provides the possibility to check the dark matter mass distribution predicted by other methods. So far they are in good agreement [14].

Also the process of structure formation needs the underlying assumption of dark matter to explain the large structures like galaxy clusters we observe today. In the early state of the universe energy was distributed homogeneously with only very small anisotropies, as we know by observation of the cosmic microwave background (CMB). However the domination of radiation in the early universe continuously diminished the anisotropies of visible matter. So if there would not have been any dark matter at the beginning of universe, no large scale structures could have been formed. But as dark matter does not interact with radiation dark structures developed under the influence of gravitation. In a later state of the universe matter gained domination about radiation, so visible matter formed structures on the basis of the dark matter structures.

Λ CDM model

The most acknowledged cosmological model today is the Λ CDM model, consisting of the cosmological constant Λ , cold dark matter (CDM) and the visible matter of the Standard Model of particle physics. When speaking of 'cold' in this context, one means particles with non-relativistic energies. The model is determined by six free parameters, two of them being the physical baryonic density $\Omega_b h^2$ and the physical dark matter density $\Omega_c h^2$. By measuring the CMB one can estimate the values of those parameters. The most accurate measurement of the CMB today is the one by the Planck satellite. When fitting those data with the Λ CDM model one receives $\Omega_b h^2 = 0.02237 \pm 0.00015$ and $\Omega_c h^2 = 0.1200 \pm 0.0012$ [9]. These results show that the abundance of dark matter is nearly six times as big as the one of visible matter. They also illustrate that the dark matter density is known quite accurately.

3.2 Candidates

Most of the existing suggestions for the constitution of dark matter can be categorized as either baryonic/non-baryonic and regarding their energy at the early universe as cold or hot dark matter.

Baryonic candidates are often summarized with the expression MACHOs (Massive Compact Halo Objects), including e.g. neutron stars, brown dwarfs and non-primordial black holes. Those could in principle contribute to the missing mass of rotation curves, but

obviously cannot explain structure formation in the early universe.

Hot dark matter is moving with ultrarelativistic velocities. Therefore only the larger fluctuations from the early universe would have outlived the radiation dominated stage. But to form the galactic structures we observe today also small scaled anisotropies had to be retained by dark matter. Hence the current scientific consent is that CDM accounts best for most of the observations.

There also exist theories fitting into none of these categories as they don't assume some kind of dark matter, but try to explain the evidences mentioned above by using alternate gravitational theories (e.g. MOND, Modified Newtonian Dynamics). However none of these theories is able to describe all observations with missing mass problems without proposing some amount of dark matter.

Non-baryonic cold dark matter candidates

As no particle within the Standard model qualifies as a reasonable dark matter candidate, one has to consider extensions of the Standard model to find an eligible candidate. Well known proposals are WIMPs (Weakly Interacting Massive Particles), Axions and sterile neutrinos.

To qualify as a WIMP, a particle has to be stable and only interact via weak and gravitational force. The candidate which motivates this thesis is the neutralino in the role of the lightest supersymmetric particle (LSP). It is massive, stable (because R-parity forbids a decay into SM-particles) and does not interact electromagnetically (as its neutral).

Axions are particles constructed to solve the strong CP problem. They also happen to be electrically neutral and if one chooses an adequate mass range they could be CDM constituents. Sterile neutrinos are the right-chiral extension to the left-chiral SM-neutrinos. Apart from completing the chiral structure that exists in the remaining part of the Standard Model, sterile neutrinos could also explain the small SM-neutrino mass and account for CDM, as they interact only via gravitation.

In the following sections we will consider the dark matter abundance assuming a supersymmetric model with a neutralino χ as LSP.

3.3 Boltzmann equation and freeze-out mechanism

Assuming a number of N supersymmetric particles χ_i their number density n_i can be described by the following differential equation (see e.g. [6] or [8]):

$$\begin{aligned} \frac{dn_i}{dt} = & -3Hn_i - \sum_{j=1}^N \langle \sigma_{ij} v_{ij} \rangle (n_i n_j - n_i^{eq} n_j^{eq}) \\ & - \sum_{j \neq i} [\langle \sigma'_{Xij} v_{ij} \rangle (n_i n_X - n_i^{eq} n_X^{eq}) - \langle \sigma'_{Xji} v_{ij} \rangle (n_j n_X - n_j^{eq} n_X^{eq})] \\ & - \sum_{j \neq i} [\Gamma_{ij} (n_i - n_i^{eq}) - \Gamma_{ji} (n_j - n_j^{eq})] \end{aligned} \quad (3.1)$$

The particles are sorted in ascending order of their masses $m_1 \leq m_2 \leq \dots \leq m_N$. There are four quantities that determine the decrease of the number density n_i over time:

- The expansion rate H of the universe,
- the direct annihilation cross section of two SUSY particles into ordinary matter

$$\sigma_{ij} = \sum_X \sigma(\chi_i \chi_j \rightarrow X),$$

- the scattering cross section with ordinary matter

$$\sigma'_{Xij} = \sum_Y \sigma(\chi_i X \rightarrow \chi_j Y),$$

- the decay rate into other supersymmetric particles with lower mass and SM particles

$$\Gamma_{ij} = \sum_X \Gamma(\chi_i \rightarrow \chi_j X).$$

The equilibrium density is defined as integral over the equilibrium distribution function. Assuming that $(m_i - \mu_i)/T \gg 1$, it is reasonable to use Maxwell-Boltzmann statistics as an approximation:

$$n_i^{eq} = \frac{g_i}{(2\pi)^3} \int d^3 \vec{p}_i e^{-\frac{E_i}{T}} \quad (3.2)$$

The computation of the relic density can be simplified by taking into account that all supersymmetric particles not wiped out by annihilation will end up as LSP. So the LSP abundance n can be understood as the sum of the number densities of all supersymmetric particles. Now summing up equation (3.1) over all supersymmetric particles $i = 1, \dots, N$ cancels the scattering cross sections σ'_{Xij} and decay rates Γ_{ij} and just leaves us with:

$$\frac{dn}{dt} = -3Hn - \sum_{i,j} \langle \sigma_{ij} v_{ij} \rangle (n_i n_j - n_i^{eq} n_j^{eq}) \quad (3.3)$$

A further simplification can be achieved by assuming that the supersymmetric particles stay in thermal equilibrium during their scatterings:

$$\frac{n_i}{n} \simeq \frac{n_i^{eq}}{n^{eq}} \quad (3.4)$$

Plugging this relation and the definition of the Hubble parameter $H = \frac{1}{a} \frac{da}{dt}$ into equation (3.3) this yields:

$$\frac{dn}{dt} + \frac{3}{a} \frac{da}{dt} n = \underbrace{\sum_{i,j} \langle \sigma_{ij} v_{ij} \rangle \frac{n_i^{eq}}{n^{eq}} \frac{n_j^{eq}}{n^{eq}}}_{\langle \sigma_{\text{eff}} v \rangle} (n_{eq}^2 - n^2) \quad (3.5)$$

The thermal average of the effective cross section $\langle \sigma_{\text{eff}} v \rangle$ now includes all possible annihilation cross sections of supersymmetric particles. We will have a closer look at it later. Before further analyzing the time evolution of the number density n it is instructive to introduce the dimensionless quantities² [17]

$$\text{comoving number density: } Y = \frac{n}{T^3} \quad (3.6)$$

$$\text{mass temperature ratio: } x = \frac{m}{T} \quad (3.7)$$

and rewrite the left hand side of equation (3.5), using that in the early radiation dominated universe $a \sim \frac{1}{T}$, so $\frac{d(aT)}{dt} = 0$. That leads to

$$\frac{dn}{dt} + \frac{3}{a} \frac{da}{dt} n = \frac{1}{a^3} \frac{d(na^3)}{dt} = \frac{d\left(\frac{n}{T^3}\right)}{dt} T^3 \quad (3.8)$$

and we can straightforwardly plug in the comoving number density:

$$\frac{dY}{dt} = T^3 \langle \sigma_{\text{eff}} v \rangle (Y_{eq}^2 - Y^2) \quad (3.9)$$

The advantage of using Y instead of n is that it cancels the expansion term of the original equation. The definition of Y is chosen such that it takes into account the Hubble expansion exactly, meaning that a constant comoving number density equals a constant number of WIMPs in the universe.

To incorporate also x into the equation, we need the time evolution $\frac{dx}{dt} = H(T)x$. Since in the radiation dominated era the relations $H(T)^2 \sim \rho T \sim T^4$ hold, the Hubble parameter as a function of mass m reads $H(T) = \frac{H(m)}{x^2}$ and therefore equation (3.9) results in

$$\frac{dY}{dx} = \frac{dY}{dt} \frac{1}{\frac{dx}{dt}} = T^3 \langle \sigma_{\text{eff}} v \rangle (Y_{eq}^2 - Y^2) \frac{1}{\frac{H(m)}{x}} \quad (3.10)$$

$$= \frac{m^3}{H(m)x^2} \langle \sigma_{\text{eff}} v \rangle (Y_{eq}^2 - Y^2) \quad (3.11)$$

We now want to estimate the time evolution of the comoving number density by examining equation (3.11). The prefactor $\frac{m^3 \langle \sigma_{\text{eff}} v \rangle}{H(m)}$ on the right hand side of the equation represents the ratio of effective annihilation rate and expansion rate of the universe $\frac{\Gamma}{H}$. In the early universe the annihilation rate exceeds the expansion rate $\Gamma \gg H$, so that the comoving number density Y traces the equilibrium density Y_{eq} very closely. The evolution of Y_{eq} is shown in figure 2 by the solid line. When the Hubble parameter grows gradually up to $H \approx \Gamma$, the prefactor in the evolution equation decreases. This leads Y to deviate from Y_{eq} . When finally $H \gg \Gamma$, the comoving number density remains constant. In the figure this stagnancy is illustrated by the dashed lines. The whole mechanism is called 'freeze

²There also exists the definition of $Y = n/s$ with s being the entropy. Note that these two definitions just differ by a factor, as $s \sim T^3$ assuming radiation domination.

out' and proceeds completely in the radiation dominated era of the universe. As one can see in the figure, the final comoving number density (relic density) depends on the thermal average of the effective annihilation cross section (called $\langle\sigma_A v\rangle$ in the figure). If this term is larger, it takes a longer time for H to reach Γ , so Y can follow Y_{eq} for a longer period of time. Since the equilibrium density declines with time, this leads to a lower relic density.

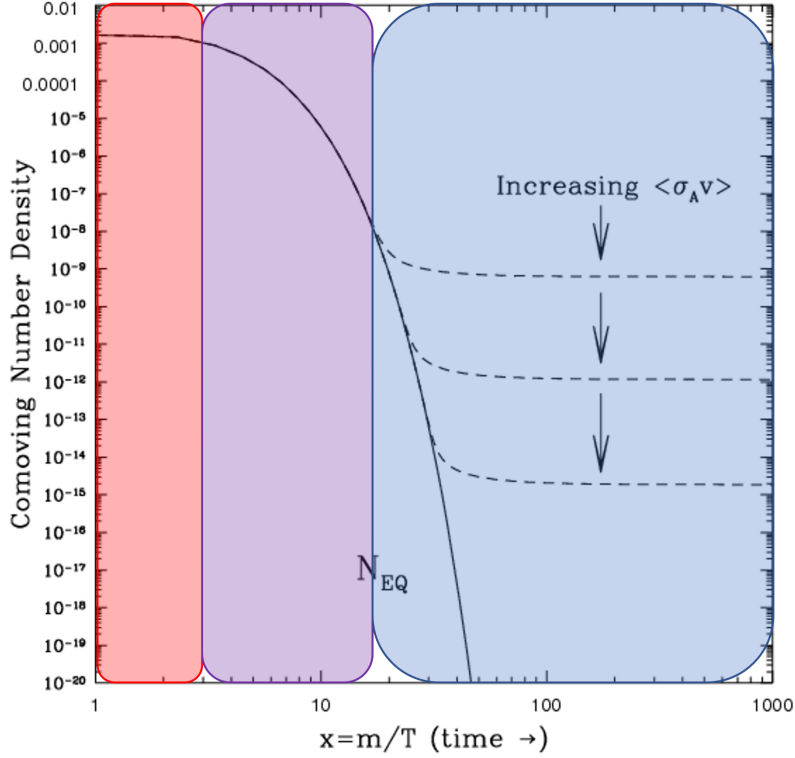


Figure 2: Solid line: expansion rate H never exceeds annihilation rate Γ . Dashed lines: freeze out of number density, when $H > \Gamma$. Red area: thermal equilibrium; Purple area: production rate exceeds annihilation rate; Blue area: expansion rate exceeds annihilation rate. Taken from [11]

To calculate the effective annihilation cross section

$$\langle q_{\text{eff}} v \rangle = \sum_{i,j} \langle \sigma_{ij} v_{ij} \rangle \frac{n_i^{eq} n_j^{eq}}{n^{eq} n^{eq}} \quad (3.12)$$

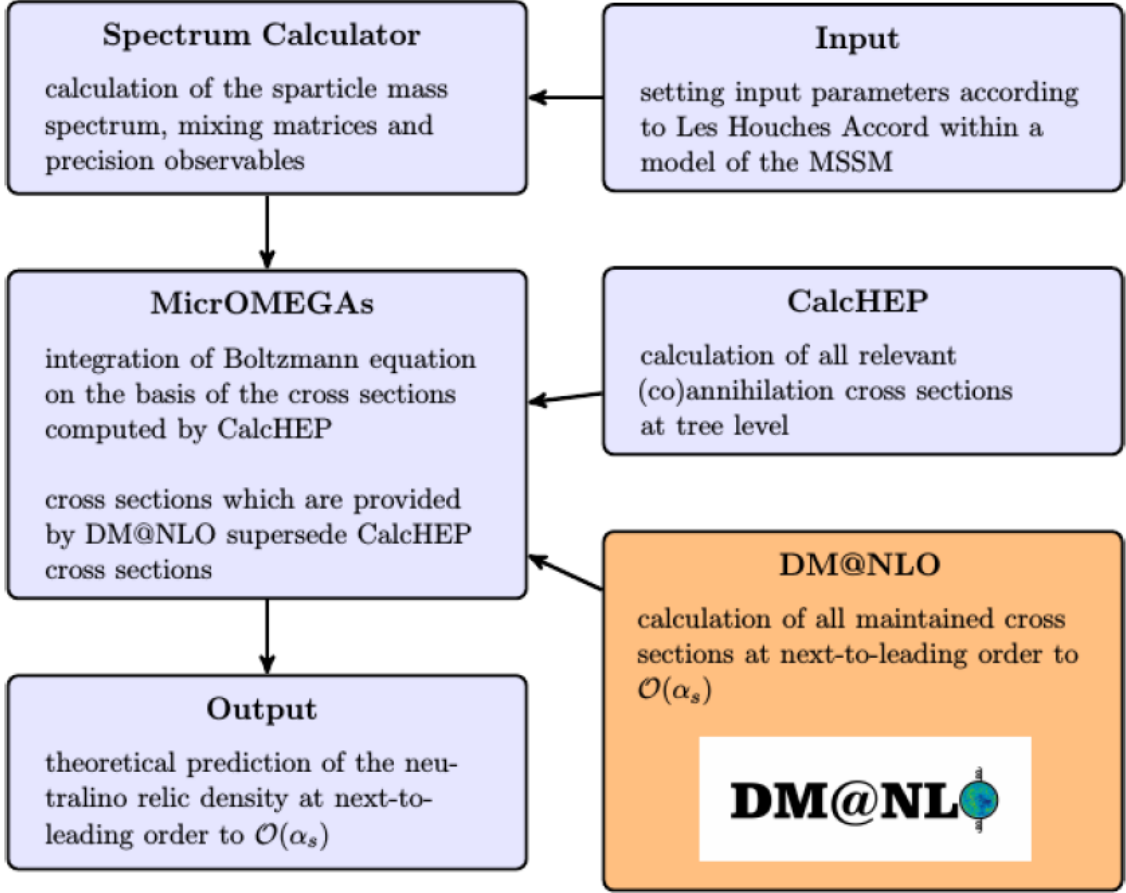
introduced in equation (3.5) one theoretically needs to compute all possible cross sections σ_{ij} . In practice however most of them are negligible, as one can see by recalling equation (3.2) for the equilibrium number density. Since WIMPs are cold dark matter candidates and therefore non-relativistic, the number density ratios appearing in $\langle q_{\text{eff}} v \rangle$

are proportional to

$$\frac{n_i^{eq}}{n^{eq}} \sim e^{-\frac{m_i - m_\chi}{T}}. \quad (3.13)$$

So only cross sections σ_{ij} with $(m_i - m_\chi) \ll 1$ and $(m_j - m_\chi) \ll 1$ are not heavily suppressed by the Boltzmann factor above. In this thesis we assume $(m_{\tilde{g}} - m_\chi) \ll 1$ and study the cross section $\sigma(\tilde{g}\tilde{g} \rightarrow gg)$.

4 DM@NLO



As pointed out in the previous chapter one needs to know the cross sections of all relevant annihilations and co-annihilations of SUSY particles to estimate relic density of the LSP. DM@NLO (Dark Matter at Next To Leading Order) now is a code calculating the next-to-leading order cross sections for all those processes. Figure 3 illustrates how the program is integrated into the software chain. As input one inserts the MSSM parameters describing the scenario of interest. These are evaluated by a spectrum calculator (in this work SPheno [15] was used) to gain the masses of the SUSY particles.

Then micrOMEGAs calculates the relic density of the LSP using the sparticle masses and cross sections as input. Instead of just using the tree level cross sections given by CalcHEP, DM@NLO now delivers the one loop corrections to yield a more accurate relic density.

5 Gluino Annihilation into Gluons

As argued before the cross section of the gluino annihilation into gluons can be relevant for calculating the relic density assuming that the gluino mass is just slightly bigger than the LSP mass. In this chapter first the cross section at tree level will be presented. Then there will be an overview of all first order corrections including propagator and vertex corrections, box and triangle diagrams and infrared radiation.

5.1 Leading Order Contributions

There are three tree level diagrams to be considered: annihilation via s-, t- and u-channel. Their Feynman diagrams are illustrated in figure 4.

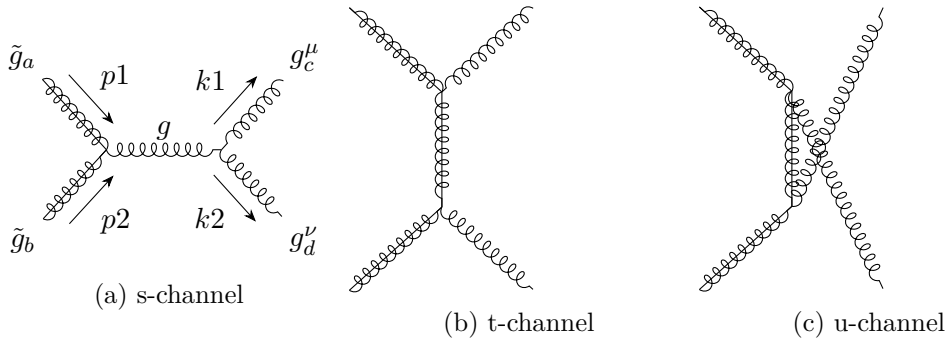


Figure 4: Tree level diagrams of gluino annihilation into gluons

When calculating the squares and interferences of the amplitudes there are two different possibilities for evaluating the polarization sums:

Physical polarization sum:

Use the gluon propagator in the lightcone gauge

$$\Pi_{R_\xi}^{\mu\nu}(p, n) = \frac{1}{p^2} \left(-g_{\mu\nu} + \frac{n^\mu p^\nu + p^\mu n^\nu}{n \cdot p} \right) \quad (5.1)$$

where n has to be chosen such that $n \cdot p \neq 0$ and $n^2 = 0$. Further use the physical polarization sum

$$\sum \varepsilon^\mu(k_1) \varepsilon^{\nu*}(k_2) = -g_{\mu\nu} + \frac{k_1^\mu k_2^\nu + k_2^\mu k_1^\nu}{k_1 \cdot k_2}. \quad (5.2)$$

In this case only the two physical polarizations transverse to the r-p-plane are taken into account. There is no need for ghosts to cancel unphysical modes.

Faddeev-Popov ghosts:

Use the gluon propagator of the form

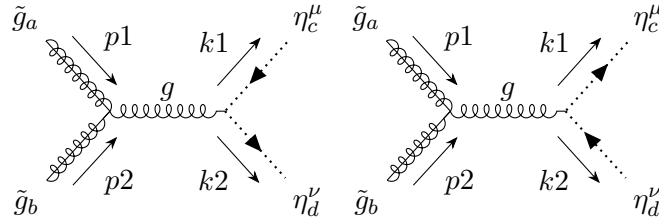
$$\Pi_{R_\xi}^{\mu\nu}(p) = \frac{1}{p^2} \left(-g_{\mu\nu} + (1 - \xi) \frac{p^\mu p^\nu}{p^2} \right) \quad (5.3)$$

where ξ fixes the gauge (e.g. $\xi = 1$ for Feynman gauge) and use the full polarization sum

$$\sum \varepsilon^\mu(k_1) \varepsilon^{\nu*}(k_2) = -g_{\mu\nu}. \quad (5.4)$$

In this case we sum over all four polarizations although two of them are not physical. In order to cancel those, ghosts are introduced. These are anti-commuting Lorentz scalars and thus they violate spin-statistics. This fact leads to the possibility of negative production probabilities which is necessary to compensate for the unphysical probabilities of the longitudinal modes.

In the end both methods should lead to the same result. When using ghost the following two diagrams have to be added to the tree level amplitude:



The associated amplitudes in Feynman gauge then read (all Feynman rules used for this thesis are listed in the Appendix):

$$M_s = \bar{v}(p_2) (-g_s f_{eba} \gamma_\rho) u(p_1) \left(-\frac{ig^{\rho\sigma} \delta_{ef}}{(p_1 + p_2)^2} \right) (-g_s f_{fcd}) \quad (5.5)$$

$$[(2k_1 + k_2)_\nu g_{\mu\sigma} + (k_2 - k_1)_\sigma g_{\mu\nu} - (k_1 + 2k_2)_\mu g_{\nu\sigma}] \varepsilon^{\mu*}(k_1) \varepsilon^{\nu*}(k_2) \quad (5.6)$$

$$M_t = \bar{v}(p_2) (-g_s f_{dbf} \gamma_\nu) \frac{i (\not{p}_1 - \not{k}_1 + m_{\tilde{g}}) \delta_{ef}}{(p_1 - k_1)^2 - m_{\tilde{g}}^2} (-g_s f_{cea} \gamma_\mu) u(p_1) \varepsilon^{\mu*}(k_1) \varepsilon^{\nu*}(k_2) \quad (5.7)$$

$$M_u = \bar{v}(p_2) (-g_s f_{cbf} \gamma_\nu) \frac{i (\not{p}_1 - \not{k}_2 + m_{\tilde{g}}) \delta_{ef}}{(p_1 - k_2)^2 - m_{\tilde{g}}^2} (-g_s f_{dea} \gamma_\mu) u(p_1) \varepsilon^{\nu*}(k_1) \varepsilon^{\mu*}(k_2) \quad (5.8)$$

$$M_{\text{ghost1}} = \bar{v}(p_2) (-g_s f_{eba} \gamma_\rho) u(p_1) \left(-\frac{ig^{\rho\sigma} \delta_{ef}}{(p_1 + p_2)^2} \right) (-g_s f_{fdc} k_{2\sigma}) \quad (5.9)$$

$$M_{\text{ghost2}} = \bar{v}(p_2) (-g_s f_{eba} \gamma_\rho) u(p_1) \left(-\frac{ig^{\rho\sigma} \delta_{ef}}{(p_1 + p_2)^2} \right) (-g_s f_{fcd} k_{1\sigma}) \quad (5.10)$$

Both squares of the ghost amplitudes can be pictorialized as

$$|M_{\text{ghost1}}|^2 = |M_{\text{ghost2}}|^2 =$$

The diagram shows the squares of the ghost amplitudes. It consists of two vertices connected by a gluon line. Each vertex has two external gluon lines and a ghost loop (dotted line) with arrows indicating the flow of the ghost number.

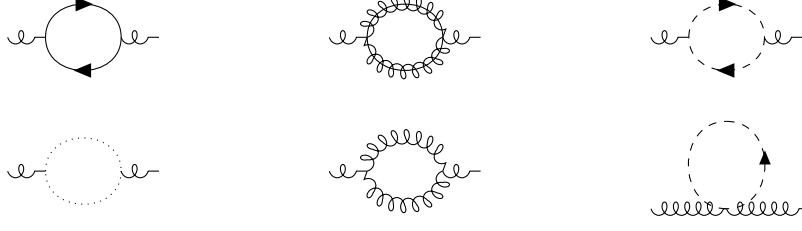


Figure 5: Corrections to the gluon propagator

since the loop direction does not matter in this case³. Therefore the full squared tree level amplitude can be written as

$$|M_{\text{tree}}|^2 = |M_s|^2 + |M_t|^2 + |M_u|^2 + 2\text{Re} \left(M_s M_t^\dagger + M_s M_u^\dagger + M_t M_u^\dagger \right) + 2|M_{\text{ghost}}|^2. \quad (5.11)$$

Those contributions read

$$|M_s|^2 = -N_C^2(N_C^2 - 1) \frac{4g_s^4}{s^2} \left(27m_{\tilde{g}}^4 - 19m_{\tilde{g}}^2(t + u) + 4(t^2 + u^2) + 3tu \right) \quad (5.12)$$

$$|M_t|^2 = -N_C^2(N_C^2 - 1) \frac{8g_s^4}{t^2} \left(m_{\tilde{g}}^4 + m_{\tilde{g}}^2(3t + u) - tu \right) \quad (5.13)$$

$$|M_u|^2 = -N_C^2(N_C^2 - 1) \frac{8g_s^4}{u^2} \left(m_{\tilde{g}}^4 + m_{\tilde{g}}^2(3u + t) - tu \right) \quad (5.14)$$

$$M_s M_t^\dagger = -\frac{N_C^2(N_C^2 - 1)}{2} \frac{8g_s^4}{st} \left(3m_{\tilde{g}}^4 - m_{\tilde{g}}^2(3t + u) + t^2 \right) \quad (5.15)$$

$$M_s M_u^\dagger = -\frac{N_C^2(N_C^2 - 1)}{2} \frac{8g_s^4}{su} \left(3m_{\tilde{g}}^4 - m_{\tilde{g}}^2(3u + t) + u^2 \right) \quad (5.16)$$

$$M_s M_t^\dagger = -\frac{N_C^2(N_C^2 - 1)}{2} \frac{8g_s^4}{tu} m_{\tilde{g}}^2 \left(2m_{\tilde{g}}^2 + t + u \right) \quad (5.17)$$

$$|M_{\text{ghost}}|^2 = N_C^2(N_C^2 - 1) \frac{2g_s^4}{s^2} \left(m_{\tilde{g}}^2 - t \right) \left(m_{\tilde{g}}^2 - u \right) \quad (5.18)$$

5.2 Next-to-leading order contributions

For the computation at one-loop level there are several contributions to be considered. In the tree-level diagrams the gluon and the gluino propagator are used, so both of them have to be corrected. For the gluon propagator there are six possible loops diagrams⁴, shown in figure 5. The gluino propagator has to be corrected by three loop diagrams (see figure 6). The corrected propagators are then incorporated into the tree level diagrams, as shown in figure 7.

Further there are three vertices to be corrected: the triple gluon vertex, the gluino-gluino-gluon vertex and the ghost-ghost-gluon vertex. All possible one-loop diagrams for

³You can also observe that switching between the two ghost diagrams is just a change of $t \leftrightarrow u$. Thus the result should be t-u-symmetric.

⁴The loop diagram with a four-point gluon vertex is already neglected here, as its amplitude vanishes.

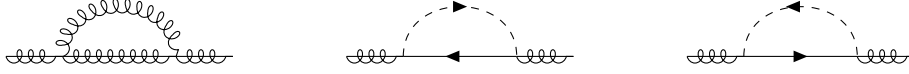


Figure 6: Gluino propagator corrections

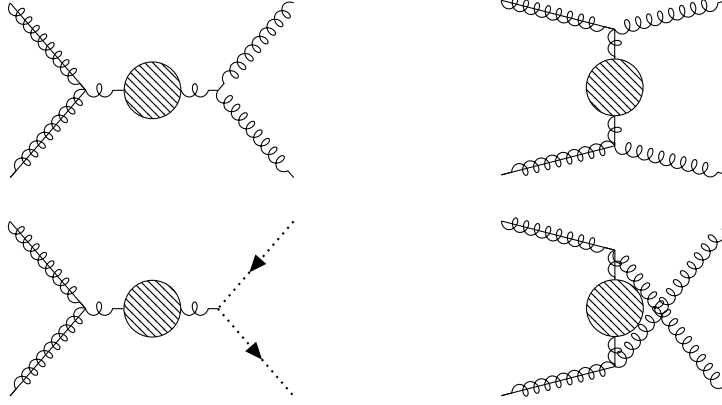


Figure 7: Contributions of propagator corrections to NLO

the triple gluon vertex can be found in [18]. The gluino-gluino-gluon vertex possesses six possible loop diagrams (figure 8), respecting different lepton number flow directions. The two loops of the ghost-ghost-gluon vertex are displayed in figure 9. All those vertex corrections are also computed off-shell and then inserted into the tree-level diagrams, as you can see in figure 10.

In a final step also those diagrams have to be considered, that do not factorize with tree level diagrams, namely triangle and box diagrams. When constructing box diagrams for the gluino annihilation into gluons, there has to be a fermion chain running through the loop connecting the two incoming gluinos. This chain can either consist of gluinos or

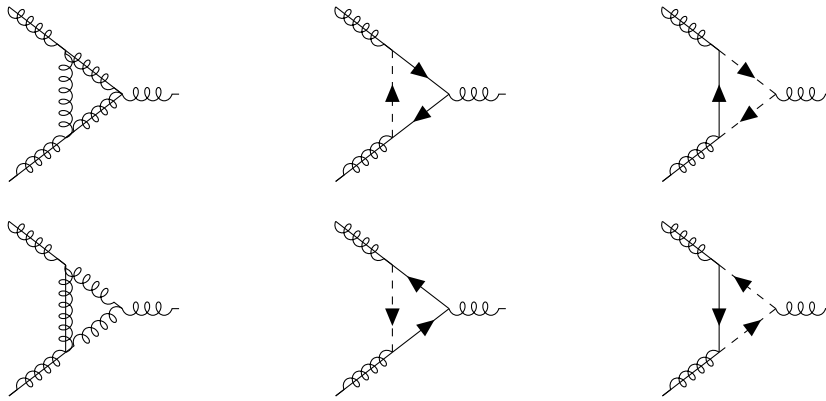


Figure 8: Gluino-gluino-gluon vertex corrections



Figure 9: Ghost-ghost-gluon vertex corrections

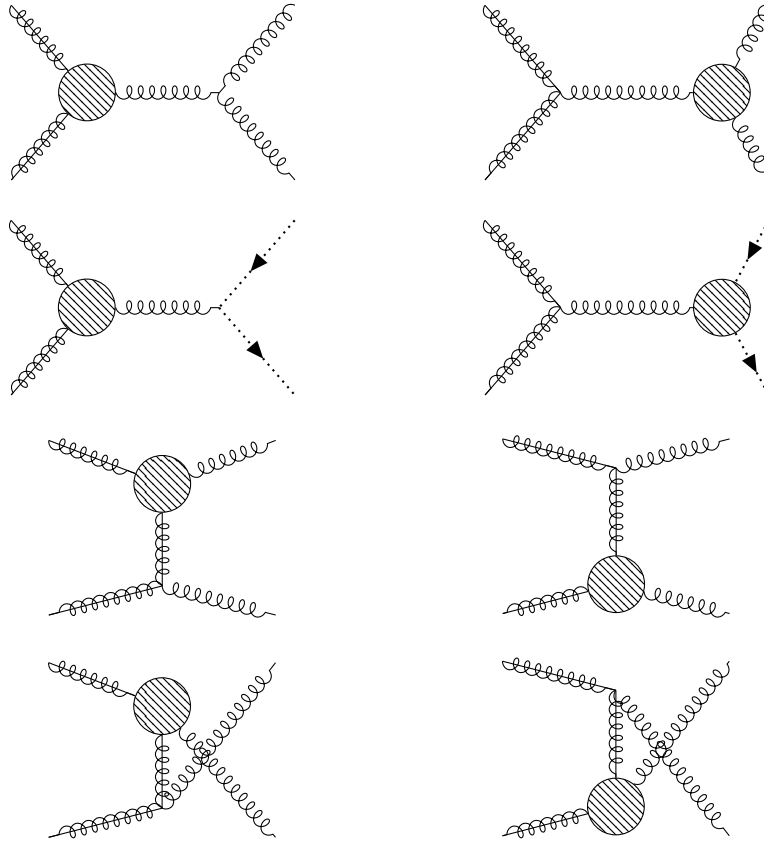


Figure 10: Contributions of vertex corrections to NLO

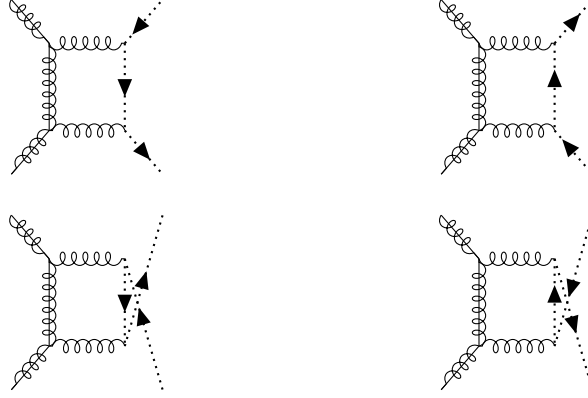


Figure 11: Ghost box diagrams

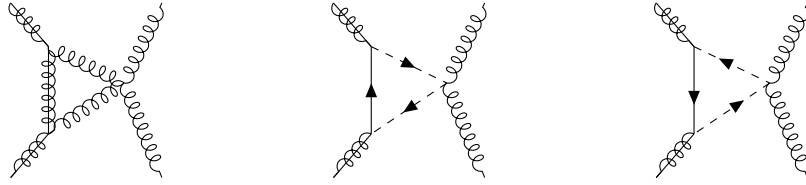


Figure 12: Triangle diagrams

quarks. Since in a box (and also in 'hourglass shaped' diagrams) there are always four propagators, either one, two or three of them can contribute to the fermion chain. When one now also considers the two possible lepton number flow directions in the loop and the possibility to exchange the two gluons in the final state, one counts 18 box/hourglass diagrams, as shown in figure 13.

When using the Faddeev-Popov formalism, one also has to take those box diagrams into account, that have ghost in the final states. Those four diagrams (figure 11) only differ in the direction of the ghost flow and the exchange of the two ghosts.

The last one-loop contributions to consider are the three triangle diagrams, displayed in figure 12

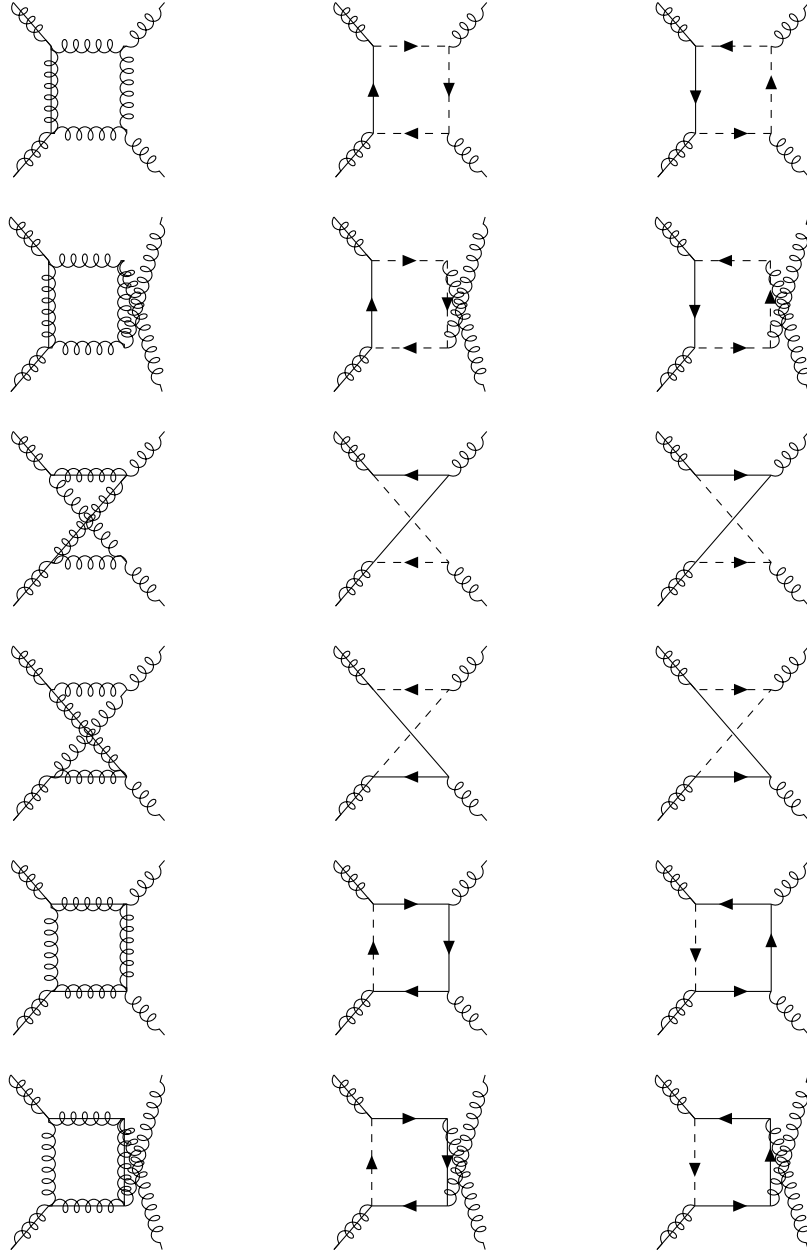


Figure 13: Box diagrams

1.+2. row: one fermion in the loop

3.+4. row: two fermions in the loop

5.+6. row: three fermions in the loop.

6 Color decomposition

As both gluons and gluinos carry color, it is important to characterize the color structure of the gluino annihilation process. In general, a two particle state corresponds to the tensor product of two representations, which can be decomposed using the Clebsch-Gordan decomposition:

$$R_{a_1} \otimes R_{a_2} = \bigoplus_{\alpha} R_{\alpha} \quad (6.1)$$

The corresponding Clebsch-Gordan coefficients C translate elements from the basis of the tensor product $e_{a_1 a_2}$ to the basis of the irreducible representations $e_{\alpha}^{R_{\alpha}}$:

$$e_{a_1 a_2} = \sum_{R_{\alpha}} C_{\alpha a_1 a_2}^{R_{\alpha}} e_{\alpha}^{R_{\alpha}} \quad (6.2)$$

Here R_{α} describes the irreducible representation and α represents all required indices for the basis of this representation. This will become clear considering the simple example of a quark-antiquark state. As quarks are N_C -dimensional fundamental representation of the $SU(N_C)$ the Clebsch-Gordan decomposition looks like

$$3 \otimes \bar{3} = 1 \oplus 8. \quad (6.3)$$

The corresponding Clebsch-Gordan coefficients are (see e.g. [18] for a calculation method)

$$C_{3\bar{3};ij}^1 = \frac{1}{\sqrt{N_C}} \delta_{ij} \quad i, j \in \{1, 2, 3\} \quad (6.4)$$

$$C_{3\bar{3};ij}^{8;a} = \sqrt{2} T_{ij}^a \quad a \in \{1, \dots, 8\} \quad (6.5)$$

Considering now a two gluon or two gluino state, which live in the $(N_C^2 - 1)$ -dimensional adjoint representation of the $SU(N_C)$ the tensor product decomposes to

$$8 \otimes 8 = 1 \oplus 8_A \oplus 8_S \oplus 10 \oplus \bar{10} \oplus 27. \quad (6.6)$$

The Clebsch-Gordan coefficients for the first three irreducible representations read:

$$C_{88;ab}^1 = \frac{1}{\sqrt{N_C^2 - 1}} \delta_{ab} \quad (6.7)$$

$$C_{88;ab}^{8_A;c} = \frac{1}{\sqrt{N_C}} i f_{abc} \quad (6.8)$$

$$C_{88;ab}^{8_S;c} = \sqrt{\frac{N_C}{N_C^2 - 4}} d_{abc} \quad (6.9)$$

The calculation of the remaining Clebsch-Gordan coefficients however is much more complicated, than for those above. We will follow [3]/[4] which involves using propagators to settle this later.

For the characterization of the color structure of a 2 to 2 process, the equivalent representations of initial (r) and final (R) state decompositions are paired up:

$$\{(r_\alpha, R_\alpha), (r_\beta, R_\beta), \dots\} \quad (6.10)$$

For a quark-antiquark scattering ($3 \otimes \bar{3} \rightarrow 3 \otimes \bar{3}$) this would mean

$$\{(1, 1), (8, 8)\} \quad (6.11)$$

while for the gluino annihilation into gluons ($8 \otimes 8 \rightarrow 8 \otimes 8$) this yields

$$\{(1, 1), (8_S, 8_S), (8_A, 8_S), (8_A, 8_A), (8_S, 8_A), (10, 10), (\bar{10}, \bar{10}), (27, 27)\}. \quad (6.12)$$

Multiplying the corresponding Clebsch-Gordan coefficients of those paired up representations leads to an orthogonal color basis of the process. By dividing by the square root of the dimension of the representation an orthonormal color basis is obtained⁵:

$$c_{a_1 a_2 a_3 a_4}^i = \frac{1}{\sqrt{\dim(R_\alpha)}} C_{\alpha a_1 a_2}^{r_\alpha} C_{\alpha a_3 a_4}^{R_\alpha} \quad (6.13)$$

Therefore the two color basis vectors for the quark-antiquark scattering are

$$c_{ijkl}^{(1,1)} = \frac{1}{N_C} \delta_{ij} \delta_{kl} \quad (6.14)$$

$$c_{ijkl}^{(8,8)} = \frac{2}{\sqrt{N_C^2 - 1}} T_{ij}^c T_{lk}^c. \quad (6.15)$$

Analogously the first five color basis vectors for the gluino annihilation into gluons read

$$c_{abcd}^{(1,1)} = \frac{1}{N_C^2 - 1} \delta_{ab} \delta_{cd} \quad (6.16)$$

$$c_{abcd}^{(8_S, 8_S)} = \frac{N_C}{(N_C^2 - 4) \sqrt{N_C^2 - 1}} d_{abe} d_{cde} \quad (6.17)$$

$$c_{abcd}^{(8_A, 8_S)} = \frac{1}{\sqrt{(N_C^2 - 4)(N_C^2 - 1)}} i f_{abe} d_{cde} \quad (6.18)$$

$$c_{abcd}^{(8_A, 8_A)} = \frac{1}{N_C \sqrt{N_C^2 - 1}} i f_{abe} i f_{dce} \quad (6.19)$$

$$c_{abcd}^{(8_S, 8_A)} = \frac{1}{\sqrt{(N_C^2 - 4)(N_C^2 - 1)}} d_{abe} i f_{dce} \quad (6.20)$$

⁵Notice, that the normalization factors for the color basis elements depend on the prefactors of the Clebsch-Gordan coefficients. For my choice of Clebsch-Gordan coefficients (6.13) is the suitable normalization

To derive the remaining part of the color basis, it is useful, to introduce color projectors. They are defined as the product of two Clebsch-Gordan coefficients of identical representations:

$$P_{abcd}^{R_\alpha} = C_{\alpha ab}^{R_\alpha} C_{\alpha cd}^{R_\alpha} \quad (6.21)$$

Color projectors possess some useful properties:

$$\text{completeness: } \sum_{\alpha} P_{abcd}^{R_\alpha} = \delta_{ac} \delta_{bd} = \mathbb{1} \quad (6.22)$$

$$\text{orthogonality: } P_{R_\alpha} \cdot P_{R_\beta} = 0 \quad (6.23)$$

$$\text{idempotence: } P_{R_\alpha} \cdot P_{R_\alpha} = P_{R_\alpha}, \quad (6.24)$$

where the application of one projector to another is defined by

$$P_{abcd} \cdot P_{efgh} = P_{abcd} P_{cdgh}. \quad (6.25)$$

For the completeness of $8 \otimes 8 \rightarrow 8 \otimes 8$ you need to sum over all six possible projectors (see Clebsch-Gordan decomposition in (6.6)):

$$\mathbb{1} = \delta_{ac} \delta_{bd} = P_1 + P_{8_A} + P_{8_S} + P_{10} + P_{\overline{10}} + P_{27} \quad (6.26)$$

The first three projectors you can read off the known Clebsch-Gordan coefficients (6.7) - (6.9):

$$P_1 = \frac{1}{N_C^2 - 1} \delta_{ab} \delta_{cd} \quad (6.27)$$

$$P_{8_A} = \frac{1}{N_C} i f_{abe} i f_{dce} \quad (6.28)$$

$$P_{8_S} = \frac{N_C}{N_C^2 - 4} d_{abe} d_{cde} \quad (6.29)$$

For deriving the missing three projectors we introduce the tensors

$$\Pi_d^u = \frac{1}{4} (\delta_{ac} \delta_{bd} + u d \delta_{ad} \delta_{bc}) + u \text{Tr}[T^a T^c T^b T^d] + d \text{Tr}[T^a T^d T^b T^c] \quad (6.30)$$

where $u, d \in \{+, -\}$ and notice that

$$\Pi_+^+ + \Pi_-^- + \Pi_+^- + \Pi_-^+ = \delta_{ac} \delta_{bd} = \mathbb{1}. \quad (6.31)$$

Furthermore, we notice that Π_{\pm}^{\pm} are symmetric under exchange of $a \leftrightarrow b$ while Π_{\mp}^{\pm} are antisymmetric under exchange of $a \leftrightarrow b$. By projecting the (anti)symmetric tensors Π_d^u onto the known (anti)symmetric projectors and subtracting those from the original tensors Π_d^u the remaining projectors can be found⁶:

$$P_{10} = \Pi_-^+ - \Pi_-^+ \cdot P_{8_A} \quad (6.32)$$

$$P_{\overline{10}} = \Pi_+^- - \Pi_+^- \cdot P_{8_A} \quad (6.33)$$

$$P_{27} = \Pi_+^+ - \Pi_+^+ - \Pi_+^+ \cdot P_1 - \Pi_+^+ \cdot P_{8_S} \quad (6.34)$$

⁶One might wonder, why one does not consider $P_0 = \Pi_-^- - \Pi_-^- - \Pi_-^- \cdot P_1 - \Pi_-^- \cdot P_{8_S}$. In a general $SU(N_C)$ you indeed would have to include this one as well, but for $N_C = 3$ it happens that the dimension of that representation is zero, as the index indicates.

After doing these calculations (see appendix C) one obtains the following projectors:

$$P_{10} = \frac{1}{4}(\delta_{ac}\delta_{bd} - \delta_{ad}\delta_{bc}) + \frac{1}{4}(d_{ace}if_{bde} + if_{ace}d_{bde}) - \frac{1}{2}\frac{1}{N_C}if_{abe}if_{dce} \quad (6.35)$$

$$P_{\overline{10}} = \frac{1}{4}(\delta_{ac}\delta_{bd} - \delta_{ad}\delta_{bc}) - \frac{1}{4}(d_{ace}if_{bde} + if_{ace}d_{bde}) - \frac{1}{2}\frac{1}{N_C}if_{abe}if_{dce} \quad (6.36)$$

$$P_{27} = \frac{1}{4}(\delta_{ac}\delta_{bd} + \delta_{ad}\delta_{bc}) + \frac{1}{4}(d_{ace}if_{bde} + if_{ace}d_{bde}) \quad (6.37)$$

$$- \frac{N_C - 1}{2N_C} \frac{1}{N_C^2 - 1} \delta_{ab}\delta_{cd} - \frac{N_C - 2}{2N_C} \frac{N_C}{N_C^2 - 4} d_{abe}d_{cde} \quad (6.38)$$

By including the normalization factors (see eq. (6.13)) the three remaining color basis vectors read

$$c_{abcd}^{(10,10)} = \frac{2}{\sqrt{(N_C^2 - 4)(N_C^2 - 1)}} P_{10} \quad (6.39)$$

$$c_{abcd}^{(\overline{10},\overline{10})} = \frac{2}{\sqrt{(N_C^2 - 4)(N_C^2 - 1)}} P_{\overline{10}} \quad (6.40)$$

$$c_{abcd}^{(27,27)} = \frac{2}{N_C \sqrt{(N_C + 3)(N_C - 1)}} P_{27}. \quad (6.41)$$

6.1 Color of tree level

Now that we derived the eight color basis vectors that span the color space in which the process takes place, it might be interesting to look at the tree level contributions again. By projecting the color basis vectors on the color part of the tree level amplitudes one can find the following linear combinations:

$$M_s^{\text{color}} = \sqrt{2}N_C \sqrt{N_C C_F} c_{abcd}^{(8_A, 8_A)} \quad (6.42)$$

$$M_t^{\text{color}} = N_C c_{abcd}^{(1,1)} + N_C \sqrt{\frac{N_C C_F}{2}} \left(c_{abcd}^{(8_S, 8_S)} + c_{abcd}^{(8_A, 8_A)} \right) \quad (6.43)$$

$$- \frac{N_C}{2} \sqrt{(N_C - 1)(N_C + 3)} c_{abcd}^{(27,27)} \quad (6.44)$$

$$M_u^{\text{color}} = N_C c_{abcd}^{(1,1)} + N_C \sqrt{\frac{N_C C_F}{2}} \left(c_{abcd}^{(8_S, 8_S)} - c_{abcd}^{(8_A, 8_A)} \right) \quad (6.45)$$

$$- \frac{N_C}{2} \sqrt{(N_C - 1)(N_C + 3)} c_{abcd}^{(27,27)} \quad (6.46)$$

The proportionality of M_s^{color} and $c^{(8_A, 8_A)}$ should not be surprising. Both color structures consist of two anti-symmetric structure constants and differ just by a normalization factor. The expressions of M_t^{color} and M_u^{color} are equal apart from the sign in front of $c^{(8_A, 8_A)}$. This is because the change of $u \leftrightarrow t$ does not alter the symmetric part of the color structure, but inverts the anti-symmetric one.

7 Next-to-leading order computations

While the computation of the squared tree level amplitudes is straightforward after deriving all necessary Feynman rules, the calculation of higher orders is more involved, as different types of divergencies appear on the way.

On one hand there are ultra-violet divergencies originating from unbounded integrals over loop momenta. How to deal with those is the main topic of this chapter. First we define the superficial degree of divergence. Then we use dimensional regularization to quantify the divergencies in the amplitudes explicitly. To simplify this process, Passarino-Veltman reduction is introduced. In the end we can renormalize the theory in order to prevent the divergencies from appearing in the result.

On the other hand different phenomena lead to infrared divergencies. When the energy of a massless particle in the final state is smaller than the detection threshold, this implicates a pole in the equations and therefore a divergence. Since those massless low-energetic particles are called soft, one often refers to this as soft singularity. Another possibility for gaining a pole is a massless particle in the final state, that is emitted in the same direction as another particle. Here one speaks about a collinear singularity.

Infrared divergencies emerge from loop integrals as well as from $2 \rightarrow 3$ processes with an additional massless gauge boson. In the case of gluino annihilation into gluons $\tilde{g}\tilde{g} \rightarrow gg$ one has to consider the diagrams for $\tilde{g}\tilde{g} \rightarrow ggg$ and $\tilde{g}\tilde{g} \rightarrow q\bar{q}g$ in order to cancel the infrared divergencies appearing in the loop calculations.

This chapter is mainly based on [12] and [16].

7.1 Superficial degree of divergence

For simplification we only consider one-particle irreducible (1PI) diagrams in this section. In these diagrams all internal momenta have a loop momentum going through them. Pictorially this means one cannot split the diagram by cutting just one line. The loop integrals of those diagrams look in a very simplified form like

$$iM \sim \int \frac{d^4q}{(2\pi)^4} \frac{1}{q^n} \quad (7.1)$$

where q is the momentum running in the loop and n depends on the specific diagram. We have neglected any on-shell momenta, masses and other constants here. The superficial degree of divergence \mathcal{D} is defined as the overall power of loop momenta q_i in the loop integrals, including those in the differentials d^4q_i , so in case of 1PI diagrams this means $\mathcal{D} = 4 - n$. As one can see in equation (7.1) the integral converges for $\mathcal{D} < 0$. In the case of $\mathcal{D} \geq 0$ there are two diverging behaviors to distinguish:

$$\int \frac{d^4q}{q^n} = \begin{cases} \lim_{q \rightarrow \infty} (\ln q) & , \mathcal{D} = 0 \\ \lim_{q \rightarrow \infty} (1/q^{\mathcal{D}}) & , \mathcal{D} > 0 \end{cases} \quad (7.2)$$

7.2 Dimensional Regularization

To somehow eliminate those divergencies one first has to parametrize them. A straightforward way to do this is by introducing a cut-off (meaning an upper bound of integration) Λ . Then the divergence is contained in a direct form in $\ln \Lambda$ or $1/\Lambda^D$ respectively by $\Lambda \rightarrow \infty$. However this method does not preserve Lorentz covariance, so usually another regularization technique is used.

The idea of dimensional regularization is to consider the loop integral in D dimensions first and take the limit $D \rightarrow 4$ in the end. As we saw above, the integral converges for $D < 0$, so if now the dimension is chosen $D < 4$, the diverging behavior of the integral will vanish. In the calculation one uses

$$D = 4 - 2\varepsilon \text{ with } \varepsilon \rightarrow 0 \quad (7.3)$$

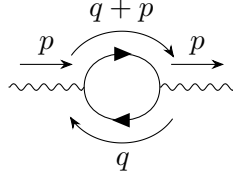
for dimensional regularization. This way the divergence is retained in an $1/\varepsilon$ pole. For equation (7.1) the approach of dimensional regularization looks like

$$\int \frac{d^4 q}{(2\pi)^4} \frac{1}{q^n} \rightarrow \mu^{2\varepsilon} \int \frac{d^D q}{(2\pi)^D} \frac{1}{q^n} \quad (7.4)$$

where μ is called the renormalization scale. It's dimension is mass, so that the overall dimension of the integral is conserved:

$$[\mu]^{2\varepsilon} \frac{[d^D q]}{[q]^n} = m^{4-D} \frac{m^D}{m^n} = \frac{[d^4 q]}{[q]^n} \quad (7.5)$$

To show how dimensional regularization works, the following QED vacuum polarization diagram will be considered:



The corresponding amplitude reads:

$$iM^{ab} = -(-ie)^2 \mu^{2\varepsilon} \int \frac{d^D q}{(2\pi)^D} \frac{i}{(q+p)^2 - m_q^2} \frac{i}{q^2 - m_q^2} \times \text{Tr}[\gamma^\mu (\not{q} + \not{p} + m_q) \gamma^\nu (\not{q} + m_q)] \quad (7.6)$$

After evaluating the trace, using Feynman parametrization, variable shifts and some special integrals including Γ -functions one will eventually end up with

$$iM^{ab} = \frac{-8e^2}{(4\pi)^{D/2}} \mu^{2\varepsilon} (p^2 g^{\mu\nu} - p^\mu p^\nu) \Gamma\left(2 - \frac{D}{2}\right) \int_0^1 dx x(1-x) \left(\frac{1}{m_e^2 - p^2 x(1-x)}\right)^{2-D/2} \quad (7.7)$$

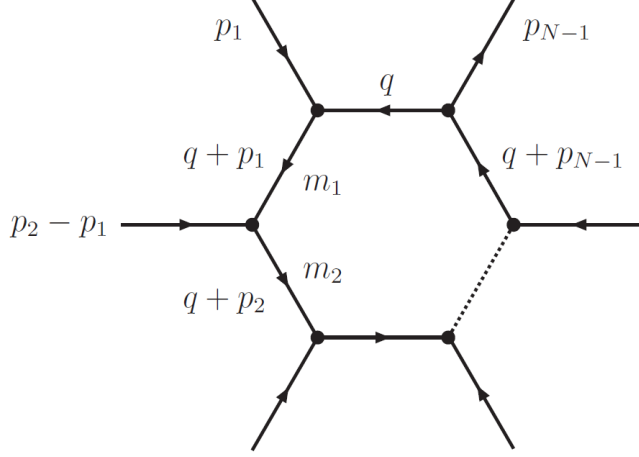


Figure 14: General one-loop integral. Taken from [12]

In the limit $\varepsilon \rightarrow 0$ this simplifies to

$$iM^{ab} = -i \left(g^{\mu\nu} - \frac{p^\mu p^\nu}{p^2} \right) \Pi_2(p^2) \quad (7.8)$$

with

$$\Pi_2(p^2) = \frac{e^2 p^2}{2\pi^2} \int_0^1 dx \, x(1-x) \left[\frac{1}{\varepsilon} + \ln \left(\frac{4\pi\mu^2}{m_e^2 - p^2 x(1-x)} \right) - \gamma_E \right] \quad (7.9)$$

Under the assumption of high energies $m_q^2 \ll -p^2$, electrons can be considered massless and this integral can simply be solved analytically. As one can see the divergence is now present explicitly in the $1/\varepsilon$ -pole while the rest of the amplitude is finite.

However performing this whole procedure (which was left out here for the sake of brevity) for every single one-loop process is not an efficient way of calculating the corrections. The next section presents a method to write every possible NLO-diagram as a function of some well classified scalar and tensor integrals with known divergencies and finite parts.

7.3 Passarino-Veltman integrals

Let us consider a general one-loop integral as shown in figure 14:

$$T_{\mu_1, \dots, \mu_m}^n(p_1, \dots, p_{n-1}, m_1, \dots, m_{n-1}) = \frac{(2\pi\mu)^{4-D}}{i\pi^2} \int d^D q \frac{q_{\mu_1} \dots q_{\mu_m}}{(q^2 - m_0^2 + i\varepsilon)[(q+p_1)^2 - m_1^2 + i\varepsilon] \dots [(q+p_{n-1})^2 - m_{n-1}^2 + i\varepsilon]} \quad (7.10)$$

where n is the number of propagators in the loop and m the number of loop momenta in

the nominator of the integral. Now we rename those integrals as following:

$$\begin{aligned}
T^1 &= A_0 & T_{\mu\nu}^1 &= A_{\mu\nu} \\
T^2 &= B_0 & T_\mu^2 &= B_\mu & T_{\mu\nu}^2 &= B_{\mu\nu} \\
T^3 &= C_0 & T_\mu^3 &= C_\mu & T_{\mu\nu}^3 &= C_{\mu\nu} & T_{\mu\nu\rho}^3 &= C_{\mu\nu\rho} \\
T^4 &= D_0 & T_\mu^4 &= D_\mu & T_{\mu\nu}^4 &= D_{\mu\nu} & T_{\mu\nu\rho}^4 &= D_{\mu\nu\rho}
\end{aligned}$$

The integrals in the first column are called scalar integrals, as there nominator is just a scalar. All the others are tensor integrals and can be completely reformulated as functions of the four scalar integrals and the momenta.

7.3.1 Scalar integrals

First we consider a general form of scalar integrals:

$$I_n(A) = \int d^D q \frac{1}{(q^2 - A + i\varepsilon)} \quad (7.11)$$

Every scalar integral can be brought into this form by using Feynman parametrization and shifting the integration variable in a clever way. One can show that

$$I_n(A) = i(-1)^n \pi^{D/2} \frac{\Gamma(n - D/2)}{\Gamma(n)} (A - i\varepsilon)^{D/2-n} \quad (7.12)$$

and use this result to calculate the specific scalar integrals.

With this knowledge the first integral is computed straightforwardly:

$$\begin{aligned}
A_0(m^2) &= \frac{(2\pi\mu)^{4-D}}{i\pi^2} \int d^D q \frac{1}{q^2 - m^2 + i\varepsilon} = \frac{(2\pi\mu)^{4-D}}{i\pi^2} I_1(m^2) \\
&= -(m^2 - i\varepsilon) \left(\frac{4\pi\mu^2}{m^2 - i\varepsilon} \right)^\varepsilon \Gamma(\varepsilon - 1) \\
&= m^2 \left(\underbrace{\frac{1}{\varepsilon_{UV}} - \gamma_E + \ln 4\pi - \ln \left(\frac{m^2}{\mu^2} \right)}_{\Delta} + 1 + \mathcal{O}(\varepsilon_{UV}) \right)
\end{aligned}$$

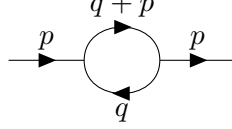
Here $D = 4 - 2\varepsilon$ was used⁷. In the last step a Taylor expansion around $\varepsilon = 0$ was performed. The Euler-Mascharoni constant is $\gamma_E = -\Gamma'(1)$. Sometimes the $1/\varepsilon$ -pole is summed up together with the constants that always appear in dimensional regularization as Δ . This will become clear when discussing different subtraction schemes for renormalization. For now we keep in mind that $A_0(m^2) = m^2\Delta + \text{finite terms} + \mathcal{O}(\varepsilon_{UV})$.

⁷To avoid confusion between the $i\varepsilon$ part in the denominator of propagators and the $\varepsilon = (4 - D)/2$ used in dimensional regularization, the subscripts ε_{UV} (or ε_{IR} respectively) are sometimes used for the latter.

The second scalar integral has the following form

$$B_0(p_1^2, m_0^2, m_1^2) = \frac{(2\pi\mu)^{4-D}}{i\pi^2} \int d^D q \frac{1}{(q^2 - m_0^2 + i\varepsilon)[(q+p_1)^2 - m_1^2 + i\varepsilon]} \quad (7.13)$$

and can be depicted as in the following Feynman diagram:



To recover the generic integral I_n from equation (14) Feynman parametrization (see A.3) is used:

$$B_0(p_1^2, m_0^2, m_1^2) = \frac{(2\pi\mu)^{4-D}}{i\pi^2} \int_0^1 dx \int d^D q \frac{1}{(q + xp_1)^2 - x^2 p_1^2 + x(p_1^2 - m_1^2 + m_0^2) - m_0^2 + i\varepsilon} \quad (7.14)$$

Since we integrate over all q the variable shift $q \rightarrow q - xp_1$ simply leads to

$$\begin{aligned} B_0(p_1^2, m_0^2, m_1^2) &= \frac{(2\pi\mu)^{4-D}}{i\pi^2} \int_0^1 dx \int d^D q \frac{1}{q^2 - x^2 p_1^2 + x(p_1^2 - m_1^2 + m_0^2) - m_0^2 + i\varepsilon} \\ &= \frac{(2\pi\mu)^{4-D}}{i\pi^2} \int_0^1 dx I_2(-x^2 p_1^2 + x(p_1^2 - m_1^2 + m_0^2) - m_0^2) \\ &= (4\pi\mu)^{2-D/2} \Gamma\left(\frac{4-D}{2}\right) \int_0^1 dx \left(x^2 p_1^2 - x(p_1^2 - m_1^2 + m_0^2) + m_0^2\right)^{D/2-2} \\ &= \frac{1}{\varepsilon_{UV}} - \gamma_E + \ln 4\pi - \int_0^1 dx \ln \left(\frac{x^2 p_1^2 - x(p_1^2 - m_1^2 + m_0^2) + m_0^2 - i\varepsilon}{\mu^2} \right) + \mathcal{O}(\varepsilon) \end{aligned} \quad (7.15)$$

Again we used the integral from equation (7.12), properties of the Γ -function and expanded around $\varepsilon = 0$. The first observation is that $B_0 = \Delta + \text{finite terms} + \mathcal{O}(\varepsilon)$. A special characteristic of the B_0 function is that the argument of the logarithm can be negative, which is why the latter has to be considered complex. By exploiting several identities for complex logarithms (see [12] for details) one can reformulate the result in a form, which separates real and imaginary part of B_0 :

$$\begin{aligned} B_0(p_1^2, m_0^2, m_1^2) &= \frac{1}{\varepsilon_{UV}} - \gamma_E + \ln 4\pi - \ln \left(\frac{m_0 m_1}{\mu^2} \right) + 2 + \frac{m_0 - m_1^2}{p_1^2} \ln \left(\frac{m_1}{m_0} \right) \\ &\quad + \frac{\sqrt{\lambda(p_1^2, m_0^2, m_1^2) + 4ip_1^2 \varepsilon}}{2p_1^2} \left[\ln \left(1 - \frac{1}{x_1} \right) - \ln \left(1 - \frac{1}{x_2} \right) \right] \end{aligned} \quad (7.16)$$

with the Källén function

$$\lambda(p_1^2, m_0^2, m_1^2) = \left(p_1^2 - (m_0 - m_1)^2 \right) \left(p_1^2 - (m_0 + m_1)^2 \right) \quad (7.17)$$

and the roots of the quadratic polynomial in the argument of the logarithm in (7.15)

$$x_{1,2} = \frac{1}{2p_1^2} \left(p_1^2 - m_1^2 + m_0^2 \pm \sqrt{(p_1^2 - m_1^2 + m_0^2)^2 - 4m_0^2 m_1^2 + i4p_1^2 \varepsilon} \right). \quad (7.18)$$

When one (or more) of the arguments of B_0 vanish one quickly notices that the result (7.15) is no longer defined. For those cases one has to deduce the integrals separately. For determining the renormalization constants later there is also need for the derivative of some of the integrals. The most important one is

$$\begin{aligned} \dot{B}_0 &= \frac{\partial B_0(p_1^2, m_0^2, m_1^2)}{\partial p_1^2} = \frac{1}{p_1^2(x_1 - x_2)} \cdot \\ &\cdot \left[(x_2 - x_1) + x_1(1 - x_1) \ln \left(1 - \frac{1}{x_1} \right) - x_2(1 - x_2) \ln \left(1 - \frac{1}{x_2} \right) \right] \end{aligned} \quad (7.19)$$

This expression is ultraviolet convergent, but for special argument sets an infrared divergence appears. When one of the particles in the loop is massless $m_1^2 = 0$ and the incoming momentum approaches the remaining mass $p_1^2 = m_0^2$, the derivative of B_0 can be evaluated to

$$\frac{\partial B_0(m^2, m^2, 0)}{\partial p_1^2} = \frac{1}{2m^2} \left(\Delta_{IR} + \ln \frac{m^2}{\mu^2} - 2 + \mathcal{O}(\varepsilon) \right) \quad (7.20)$$

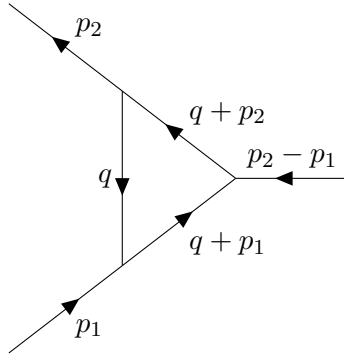
with

$$\Delta_{IR} = -\frac{1}{\varepsilon_{IR}} + \gamma_R - \ln 4\pi \quad (7.21)$$

The third scalar integral depends on six parameters:

$$\begin{aligned} C_0(p_1^2, (p_1 - p_2)^2, p_2^2, m_0^2, m_1^2, m_2^2) = \\ \frac{(2\pi\mu)^{4-D}}{i\pi^2} \int d^D q \frac{1}{(q^2 - m_0^2 + i\varepsilon)[(q + p_1)^2 - m_1^2 + i\varepsilon][(q + p_2)^2 - m_2^2 + i\varepsilon]} \end{aligned} \quad (7.22)$$

The corresponding Feynman diagram is:



After using a more complicated version of the Feynman parametrization (A.3) and manipulating the terms, one can again recover the general integral:

$$C_0 = \frac{(2\pi\mu)^{4-D}}{i\pi^2} 2 \int_0^1 dx \int_0^x dy I_3 \left(x^2 p_1^2 + y^2 p_2^2 + xy(p_0^2 - p_1^2 - p_2^2) \right. \\ \left. + x(m_0^2 - p_1^2 - m_1^2) + y(p_1^2 - p_0^2 + m_2^2 - m_0^2) + m_1^2 - i\varepsilon \right) \quad (7.23)$$

When now exploiting again (7.12) the important thing to notice is that I_n converges for $n \geq 3$. So while A_0 and B_0 possess divergent parts we wrote as $1/\varepsilon_{UV}$, the integrals C_0 and D_0 will have only finite terms. The computation of those is even more involved as the one of B_0 , so we refer to [12] to study the results.

7.3.2 Tensor integrals and reduction

After reproducing the calculations of the scalar integrals, let us have another look at the general tensor integral from the beginning:

$$T_{\mu_1, \dots, \mu_m}^n(p_1, \dots, p_{n-1}, m_1, \dots, m_{n-1}) = \frac{(2\pi\mu)^{4-D}}{i\pi^2} \int d^D q \frac{q_{\mu_1} \dots q_{\mu_m}}{(q^2 - m_0^2 + i\varepsilon)[(q + p_1)^2 - m_1^2 + i\varepsilon] \dots [(q + p_{n-1})^2 - m_{n-1}^2 + i\varepsilon]} \quad (7.24)$$

The integral is obviously symmetric under exchange of all Lorentz indices μ_1, \dots, μ_m . Therefore the result can contain only symmetric tensor structures made up of the metric tensor $g^{\mu\nu}$ and the 4-vectors $p_1^\mu, \dots, p_{n-1}^\mu$. When combining all possible tensor structures

for every tensor integral one ends up with:

$$\begin{aligned}
A^{\mu\nu} &= g^{\mu\nu} A_2 \\
B^\mu &= p_1^\mu B_1 \\
B^{\mu\nu} &= g^{\mu\nu} B_{00} + p_1^\mu p_1^\nu B_{11} \\
C^\mu &= p_1^\mu C_1 + p_2^\mu C_2 \\
C^{\mu\nu} &= g^{\mu\nu} C_{00} + p_1^\mu p_1^\nu C_{11} + (p_1^\mu p_2^\nu + p_2^\mu p_1^\nu) C_{12} + p_2^\mu p_2^\nu C_{22} \\
C_{\mu\nu\rho} &= (p_1^\mu g^{\nu\rho} + p_1^\nu g^{\mu\rho} + p_1^\rho g^{\mu\nu}) C_{001} + (p_2^\mu g^{\nu\rho} + p_2^\nu g^{\mu\rho} + p_2^\rho g^{\mu\nu}) C_{002} \\
&\quad + p_1^\mu p_1^\nu p_1^\rho C_{111} + (p_1^\mu p_1^\nu p_2^\rho + p_1^\mu p_2^\nu p_1^\rho + p_2^\mu p_1^\nu p_1^\rho) C_{112} \\
&\quad + (p_1^\mu p_2^\nu p_2^\rho + p_2^\mu p_2^\nu p_1^\rho + p_2^\mu p_1^\nu p_2^\rho) C_{122} + p_2^\mu p_2^\nu p_2^\rho C_{222} \\
D^\mu &= p_1^\mu D_1 + p_2^\mu D_2 + p_3^\mu D_3 \\
D^{\mu\nu} &= g_{\mu\nu} D_{00} + p_1^\mu p_1^\nu D_{11} + (p_1^\mu p_2^\nu + p_2^\mu p_1^\nu) D_{12} + (p_1^\mu p_3^\nu + p_3^\mu p_1^\nu) D_{13} \\
&\quad + p_2^\mu p_2^\nu D_{22} + (p_2^\mu p_3^\nu + p_3^\mu p_2^\nu) D_{23} + p_3^\mu p_3^\nu D_{33} \\
D^{\mu\nu\rho} &= (p_1^\mu g^{\nu\rho} + p_1^\nu g^{\mu\rho} + p_1^\rho g^{\mu\nu}) D_{001} + (p_2^\mu g^{\nu\rho} + p_2^\nu g^{\mu\rho} + p_2^\rho g^{\mu\nu}) D_{002} \\
&\quad + (p_3^\mu g^{\nu\rho} + p_3^\nu g^{\mu\rho} + p_3^\rho g^{\mu\nu}) D_{003} + p_1^\mu p_1^\nu p_1^\rho D_{111} \\
&\quad + (p_1^\mu p_1^\nu p_2^\rho + p_1^\mu p_2^\nu p_1^\rho + p_2^\mu p_1^\nu p_1^\rho) D_{112} + (p_1^\mu p_2^\nu p_2^\rho + p_2^\mu p_2^\nu p_1^\rho + p_2^\mu p_1^\nu p_2^\rho) D_{122} \\
&\quad + (p_1^\mu p_1^\nu p_3^\rho + p_1^\mu p_3^\nu p_1^\rho + p_3^\mu p_1^\nu p_1^\rho) D_{113} + (p_1^\mu p_3^\nu p_3^\rho + p_3^\mu p_1^\nu p_3^\rho + p_3^\mu p_3^\nu p_1^\rho) D_{133} \\
&\quad + p_2^\mu p_2^\nu p_2^\rho D_{222} + (p_2^\mu p_2^\nu p_3^\rho + p_2^\mu p_3^\nu p_2^\rho + p_3^\mu p_2^\nu p_2^\rho) D_{223} \\
&\quad + (p_2^\mu p_3^\nu p_3^\rho + p_3^\mu p_2^\nu p_3^\rho + p_3^\mu p_3^\nu p_2^\rho) D_{233} + p_3^\mu p_3^\nu p_3^\rho D_{333}
\end{aligned}$$

All the scalar coefficients B_1, C_{00}, \dots can be expressed through a combination of the scalar integrals described in the previous section. In the following this reduction of tensor integrals into scalar ones will be demonstrated using the example of B_1 .

We start with $p_1^\mu B_1 = B^\mu$ and multiply both sides of the equation with $p_{1\mu}$:

$$p_1^2 B_1 = \frac{(2\pi\mu)^{4-D}}{i\pi^2} \int d^D q \frac{p_1 \cdot q}{(q^2 - m_0^2 + i\varepsilon)[(q + p_1)^2 - m_1^2 + i\varepsilon]} \quad (7.25)$$

Now $p_1 \cdot q$ is rewritten by adding some zeros such that terms in nominator and denominator cancel:

$$\begin{aligned}
p_1^2 B_1 &= \frac{(2\pi\mu)^{4-D}}{i\pi^2} \int d^D q \frac{1}{2} \frac{[(q + p_1)^2 - m_1^2 + i\varepsilon] - (q^2 - m_0^2 + i\varepsilon) - (p_1^2 - m_1^2 + m_0^2)}{(q^2 - m_0^2 + i\varepsilon)[(q + p_1)^2 - m_1^2 + i\varepsilon]} \\
&= \frac{(2\pi\mu)^{4-D}}{i\pi^2} \frac{1}{2} \int d^D q \left[\frac{1}{q^2 - m_0^2 + i\varepsilon} - \frac{1}{[(q + p_1)^2 - m_1^2 + i\varepsilon]} \right. \\
&\quad \left. - \frac{p_1^2 - m_1^2 + m_0^2}{(q^2 - m_0^2 + i\varepsilon)[(q + p_1)^2 - m_1^2 + i\varepsilon]} \right] \\
&= \frac{1}{2} \left[A_0(m_0^2) - A_0(m_1^2) - (p_1^2 - m_1^2 + m_0^2) B_0(p_1^2, m_0^2, m_1^2) \right]
\end{aligned}$$

In the last step we found the scalar integrals A_0 and B_0 depending on different parameters. Using the results from the previous section leads to

$$\begin{aligned} B_1 &= \frac{1}{2p_1^2} \left(m_0^2 \Delta - m_1^2 \Delta - (p_1^2 - m_1^2 + m_0^2) \Delta \right) + \text{finite terms} + \mathcal{O}(\varepsilon) \\ &= -\frac{1}{2} \Delta + \text{finite terms} + \mathcal{O}(\varepsilon) \end{aligned} \quad (7.26)$$

For computing the other scalar coefficients one can proceed in a similar way. The following table summarizes the UV-divergent parts of the scalar integrals relevant for this thesis:

Integral	UV divergence
$A_0(m^2)$	$m^2 \Delta$
B_0	Δ
B_1	$-\frac{1}{2} \Delta$
$B_{00}(p^2, m_0^2, m_1^2)$	$-\left(\frac{p^2}{12} - \frac{1}{4}(m_0^2 + m_1^2)\right) \Delta$
B_{11}	$\frac{1}{3} \Delta$
C_{00}	$\frac{1}{4} \Delta$
C_{00i}	$-\frac{1}{12} \Delta$

7.4 Renormalization

By using dimensional regularization the divergencies of the integrals are expressed explicitly. The next goal is to subtract those divergencies by reformulating the theory. There are different subtraction schemes for that purpose that differ in their conventions about the finite terms.

The basic idea is to insert renormalization constants Z into the bare Lagrangian \mathcal{L}_0 of the theory to gain the renormalized Lagrangian \mathcal{L}_R and expand Z in the coupling constant. In lowest order $Z = 1$ and one regains the bare Lagrangian, which is valid for tree-level calculations. For one-loop calculations we expand up to first order $Z = 1 + \delta Z$. Thereby the renormalized Lagrangian obtains a second term aside from the tree level term: the so called counterterm which contains δZ . The key point is now to choose δZ such that the contribution from the counterterms cancels the divergent part of the loop calculations exactly.

The example of the photon field will illustrate the procedure. First a renormalization constant for the field is introduced and inserted into the Lagrangian:

$$A_\mu \rightarrow \sqrt{Z_3} A_\mu^a \quad (7.27)$$

$$\mathcal{L}_0 = -\frac{1}{4} (\partial_\mu A_\nu - \partial_\nu A_\mu)^2 \rightarrow \mathcal{L}_R = -\frac{1}{4} Z_3 (\partial_\mu A_\nu - \partial_\nu A_\mu)^2 \quad (7.28)$$

In this case the square root of the renormalization constant is used as a prefactor for the field, such that it appears linearly in the Lagrangian. Then the renormalization constant is expanded:

$$\mathcal{L}_R = -\frac{1}{4}(\partial_\mu A_\nu - \partial_\nu A_\mu)^2 - \frac{1}{8}\delta Z_3(\partial_\mu A_\nu - \partial_\nu A_\mu)^2 \quad (7.29)$$

The first term describes the photon field at tree level, while the second term is the counterterm. To determine the suitable δZ_3 one has to compute the contribution of the vacuum polarization diagram, as done in (7.8).

7.4.1 Minimal subtraction

In the minimal subtraction scheme (MS) the renormalization constant δZ is just the sum of the $1/\varepsilon$ contributions of each loop. When choosing the modified minimal subtraction ($\overline{\text{MS}}$), also the $\ln 4\pi - \gamma_E$ is eliminated by δZ . Looking back to the previous chapter, this is now the reason for introducing the variable $\Delta = \frac{1}{\varepsilon} + \ln 4\pi - \gamma_E$, so that one can easily subtract the Δ -parts of the contributing diagrams in $\overline{\text{MS}}$.

The renormalization constant for the photon field in the different schemes read

$$\delta Z_3^{MS} = -\frac{e^2}{16\pi^2} \frac{1}{\varepsilon} \quad (7.30)$$

$$\delta Z_3^{\overline{MS}} = -\frac{e^2}{16\pi^2} \left(\frac{1}{\varepsilon} + \ln 4\pi - \gamma_E \right) = -\frac{e^2}{16\pi^2} \Delta \quad (7.31)$$

7.4.2 On-shell subtraction

The corrected photon propagator at first order is the sum of the tree level propagator, the polarization diagram and the counterterm, which can be expressed as

$$iG^{\mu\nu} = -\frac{i}{p^2} \left(g^{\mu\nu} - \frac{p^\mu p^\nu}{p^2} \right) \left(1 - \frac{\Pi(p^2)}{p^2} \right). \quad (7.32)$$

with

$$\Pi(p^2) = \Pi_2(p^2) + p^2 \delta Z_3 \quad (7.33)$$

, where Π_2 describes the one-loop contribution as defined in (7.8). The on-shell scheme now requires the renormalized mass to agree with the physical mass and further the residuum to match unity:

$$\text{Re} [\Pi(p^2)] \Big|_{p^2=m^2} = 0 \quad (7.34)$$

$$\lim_{p^2 \rightarrow m^2} \frac{\Pi(p^2)}{p^2 - m^2} = 1 \quad (7.35)$$

By expanding $\Pi(p^2)$ around m^2 and using the first condition one can reformulate the second condition to

$$\text{Re} \left[\frac{\partial}{\partial p^2} \Pi(p^2) \right] \Big|_{p^2=m^2} = 0. \quad (7.36)$$

In the exemplary case of the massless photon this leads to

$$\text{Re} \left[\frac{\partial}{\partial p^2} \left(\Pi_2(p^2) + p^2 \delta Z_3 \right) \right] \Big|_{p^2=0} = \text{Re} \left[\dot{\Pi}_2(p^2) \right] \Big|_{p^2=0} + \delta Z_3 = 0 \quad (7.37)$$

so the photon renormalization constant in the on-shell scheme is defined as

$$\delta Z_3 = -\text{Re} \left[\dot{\Pi}_2(p^2) \right] \Big|_{p^2=0} \quad (7.38)$$

In the following section all renormalization constants used for this thesis are listed. These can be looked up for example in [5].

7.4.3 Gluon sector

The renormalization constant for the gluon field is introduced in a similar way the one for the photon field in the previous section.

$$A_\mu^a \rightarrow \sqrt{Z_g} A_\mu^a = \left(1 + \frac{1}{2} \delta Z_g\right) A_\mu^a \quad (7.39)$$

The kinetic gluon term in the Lagrangian also gains a counterterm:

$$\mathcal{L}_R = -\frac{1}{4} \left(\partial_\mu A_\nu - \partial_\nu A_\mu + g f^{abc} A_\mu^b A_\nu^c \right)^2 - \frac{1}{8} \delta Z_g \left(\partial_\mu A_\nu - \partial_\nu A_\mu + g f^{abc} A_\mu^b A_\nu^c \right)^2 \quad (7.40)$$

which leads to the propagator counterterm

$$\text{diagram} = i\delta Z_g \delta_{ab} (p^2 g^{\mu\nu} - p^\mu p^\nu)$$

To determine the renormalization constant δZ_g one has to compute all diagrams contributing to the gluon vacuum polarization. The general form used to express those self energies is

$$\Pi_{ab}^{\mu\nu} = -\frac{i}{4\pi^2}\delta_{ab}\left[\left(g^{\mu\nu} - \frac{p^\mu p^\nu}{p^2}\right)^2 \Pi^T(p^2) + \frac{p^\mu p^\nu}{p^2}\Pi^L(p^2)\right] \quad (7.41)$$

The advantage of this expression is, that the longitudinal part vanishes when being sandwiched between the propagators, so that the renormalized two-point function reduces to the same as in the photon case (7.32) with

$$\Pi(p^2) = \Pi^T(p^2) + p^2 \delta Z_q \quad (7.42)$$

The individual contributions for the gluon self energy can be found in D.1.1. The on-shell renormalization conditions are the same as in the photon case

$$\text{Re} \left[\Pi(p^2) \right] \Big|_{p^2=0} = 0 \quad \text{and} \quad (7.43)$$

$$\frac{\partial}{\partial p^2} \Pi(p^2)_{p^2=0} = 0 \quad (7.44)$$

and therefore lead to the gluon renormalization constant

$$\delta Z_{\tilde{g}} = -\text{Re} \left[\frac{\partial}{\partial p^2} \Pi^T(p^2) \right]_{p^2=0} \quad (7.45)$$

In the code of DM@NLO the gluon propagator counterterm is implemented via the formula

$$M = -i\varepsilon_\mu(p) \left(g^{\mu\nu} A(p^2) + \frac{p^\mu p^\nu}{p^2} B(p^2) \right) \varepsilon_\nu^* \quad (7.46)$$

with

$$A = \delta Z_g p^2 \quad (7.47)$$

$$B = -\delta Z_g. \quad (7.48)$$

7.4.4 Ghost sector

For renormalizing the ghost-gluon-vertex later we also need a renormalization constant for the ghost and anti-ghost field:

$$c^a \rightarrow \sqrt{Z} c^a = \left(1 + \frac{1}{2} \delta Z_c \right) c^a \quad (7.49)$$

$$\bar{c}^a \rightarrow \sqrt{Z} \bar{c}^a = \left(1 + \frac{1}{2} \delta Z_c \right) \bar{c}^a \quad (7.50)$$

There is only one contribution to the ghost self energy, which can be generally written as

$$\Pi_{ab} = \delta_{ab} i \Pi^c(p^2) \quad (7.51)$$

which leads to the renormalization constant

$$\delta Z_c = -\text{Re} \left[\frac{\partial}{\partial p^2} \Pi^T(p^2) \right]_{p^2=0} \quad (7.52)$$

7.4.5 Gluino sector

Renormalizing the gluino field is a bit more involved as one has to pay attention to the left and right handed parts of the field:

$$\psi_{\tilde{g}} \rightarrow \left(1 + \frac{1}{2} \delta Z_{\tilde{g}}^L P_L + \frac{1}{2} \delta Z_{\tilde{g}}^R P_R \right) \psi_{\tilde{g}} \quad (7.53)$$

Since gluinos are massive particles, there is also need for mass renormalization constant:

$$m_{\tilde{g}} \rightarrow \left(1 + \frac{\delta m_{\tilde{g}}}{m_{\tilde{g}}} \right) m_{\tilde{g}} = m_{\tilde{g}} + \delta m_{\tilde{g}} \quad (7.54)$$

Note the different definition for the increment of the mass renormalization constant $\delta m_{\tilde{g}}$, which already includes the gluino mass itself.

Inserting those two definitions into the kinetic and the mass term of the Lagrangian yields:

$$\mathcal{L}_R = \frac{i}{2} \bar{\Psi}_{\tilde{g}}^a \not{\partial} \Psi_{\tilde{g}}^a + \frac{i}{4} \left(\delta Z_{\tilde{g}}^L P_L + \delta Z_{\tilde{g}}^R P_R \right) \bar{\Psi}_{\tilde{g}}^a \not{\partial} \Psi_{\tilde{g}}^a - \frac{1}{2} m_{\tilde{g}} \bar{\Psi}_{\tilde{g}}^a \Psi_{\tilde{g}}^a - \frac{1}{2} \delta m_{\tilde{g}} \bar{\Psi}_{\tilde{g}}^a \Psi_{\tilde{g}}^a \quad (7.55)$$

The two-point functions can be written as

$$\Pi_{ab}(p^2) = \delta_{ab} i \left[\Pi_{ab}^{SL}(p^2) P_L + \Pi_{ab}^{SR}(p^2) P_R + \Pi_{ab}^{VL}(p^2) \not{p} P_L + \Pi_{ab}^{VR}(p^2) \not{p} P_R \right] \quad (7.56)$$

and to receive the gluino propagator counterterm one chooses

$$\Pi_{ab}^{SL} = -(\delta m_{\tilde{g}} + \delta Z_{\tilde{g}}^L) \quad (7.57)$$

$$\Pi_{ab}^{SR} = -(\delta m_{\tilde{g}} + \delta Z_{\tilde{g}}^R) \quad (7.58)$$

$$\Pi_{ab}^{VL} = \delta Z_{\tilde{g}}^L \quad (7.59)$$

$$\Pi_{ab}^{VR} = \delta Z_{\tilde{g}}^R. \quad (7.60)$$

The two renormalization conditions in this case read

$$\text{Re} \left[\Pi(p^2) \right] \Big|_{p^2=m_{\tilde{g}}^2} = 0 \quad (7.61)$$

$$\text{Re} \left[\frac{d}{d\not{p}} \Pi(p^2) \right] \Big|_{p^2=m_{\tilde{g}}^2} = 0 \quad (7.62)$$

with

$$\begin{aligned} \Pi(p^2) = \Pi_{ab}(p^2) + \frac{1}{2} \not{p} \left[\left(\delta Z_{\tilde{g}}^L + \delta Z_{\tilde{g}}^{L\dagger} \right) P_L + \left(\delta Z_{\tilde{g}}^R + \delta Z_{\tilde{g}}^{R\dagger} \right) P_R \right] \\ - \frac{1}{2} \left[\left(\delta Z_{\tilde{g}}^L + \delta Z_{\tilde{g}}^{R\dagger} \right) P_L + \left(\delta Z_{\tilde{g}}^R + \delta Z_{\tilde{g}}^{L\dagger} \right) P_R \right] m_{\tilde{g}} - \delta m_{\tilde{g}} \end{aligned} \quad (7.63)$$

Those lead to the following renormalization constants:

$$\delta Z_{\tilde{g}}^L = \text{Re} \left[-\Pi_{ab}^{VL} - m_{\tilde{g}}^2 \left(\dot{\Pi}_{ab}^{VL} + \dot{\Pi}_{ab}^{VR} \right) - m_{\tilde{g}} \left(\dot{\Pi}_{ab}^{SL} + \dot{\Pi}_{ab}^{SR} \right) \right] \quad (7.64)$$

$$\delta Z_{\tilde{g}}^R = \text{Re} \left[-\Pi_{ab}^{VR} - m_{\tilde{g}}^2 \left(\dot{\Pi}_{ab}^{VL} + \dot{\Pi}_{ab}^{VR} \right) - m_{\tilde{g}} \left(\dot{\Pi}_{ab}^{SL} + \dot{\Pi}_{ab}^{SR} \right) \right] \quad (7.65)$$

$$\delta m_{\tilde{g}} = \frac{1}{2} \text{Re} \left[\Pi_{ab}^{SL}(p^2) + \Pi_{ab}^{SR}(p^2) + m_{\tilde{g}} \left(\Pi_{ab}^{VL}(p^2) + \Pi_{ab}^{VR}(p^2) \right) \right] \quad (7.66)$$

In the appendix D.1.3 all 1-loop contributions to the gluino self energy are given. Studying those one recognizes $\Pi_{ab}^{SL}(p^2) = \Pi_{ab}^{SR}(p^2)$ as well as $\Pi_{ab}^{VL}(p^2) = \Pi_{ab}^{VR}(p^2)$ when summing over both squark „chirality states,, $i = 1, 2$. This implies $\delta Z_{\tilde{g}}^L = \delta Z_{\tilde{g}}^R$ after the summation.

7.4.6 Correction of α_s

Also the strong coupling constant has to be renormalized properly by introducing a renormalization constant

$$g_s \rightarrow (1 + \delta g_s) g_s \quad (7.67)$$

with the following divergent contribution:

$$\delta g_s = \frac{g_s^2}{32\pi^2} (n_f - 3C_V) \Delta \quad (7.68)$$

7.4.7 Vertex counterterms

After having derived the renormalization constants for the relevant fields, masses, couplings and propagators it is time to think about the counterterms for the propagators and vertices.

For most of the vertices one can make use of the fact, that the counterterm factorizes the vertex at tree level. The triple gluon vertex counterterm can therefore be written as

$$M_{3g,\text{counter}} = \delta Z_{3g} M_{3g,\text{tree}} \quad (7.69)$$

with the factor

$$\delta Z_{3g} = \delta g_s + \frac{3}{2} \delta Z_g. \quad (7.70)$$

The counterterm of the ghost-gluon-vertex is build up in a similar way using the factor

$$\delta Z_{\eta\eta g} = \delta g_s + \delta Z_C + \frac{1}{2} \delta Z_g \quad (7.71)$$

in front of the tree-level amplitude.

Again the vertex including gluinos is a bit more involved. First one has to split up the tree-level amplitude of the gluino-gluon-vertex in its left and right-chiral parts:

$$M_{\tilde{g}\tilde{g}g,\text{tree}} = P_L M_{\tilde{g}\tilde{g}g,\text{tree},L} + P_R M_{\tilde{g}\tilde{g}g,\text{tree},R} \quad (7.72)$$

Then the left and right-chiral parts of the counterterm factorize the corresponding parts of the tree level:

$$M_{\tilde{g}\tilde{g}g,\text{counter}} = \delta Z_{\tilde{g}\tilde{g}g}^L P_L M_{\tilde{g}\tilde{g}g,\text{tree}}^L + \delta Z_{\tilde{g}\tilde{g}g}^R P_R M_{\tilde{g}\tilde{g}g,\text{tree}}^R \quad (7.73)$$

The respective factors read:

$$\begin{aligned} \delta Z_{\tilde{g}\tilde{g}g}^L &= \delta g_s + \frac{1}{2} \left(\delta Z_g + \delta Z_{\tilde{g}}^L + \delta Z_{\tilde{g}}^{L*} \right) \\ \delta Z_{\tilde{g}\tilde{g}g}^R &= \delta g_s + \frac{1}{2} \left(\delta Z_g + \delta Z_{\tilde{g}}^R + \delta Z_{\tilde{g}}^{R*} \right) \end{aligned} \quad (7.74)$$

But as the tree-level vertex itself is not sensitive to chirality ($M_{\tilde{g}\tilde{g}g,\text{tree}}^L = M_{\tilde{g}\tilde{g}g,\text{tree}}^R$) and we learned that $\delta Z_{\tilde{g}}^L = \delta Z_{\tilde{g}}^R$ earlier, one can simplify the counterterm to

$$M_{\tilde{g}\tilde{g}g,\text{counter}} = \delta Z_{\tilde{g}\tilde{g}g}^{L,R} M_{\tilde{g}\tilde{g}g,\text{tree}} \quad (7.75)$$

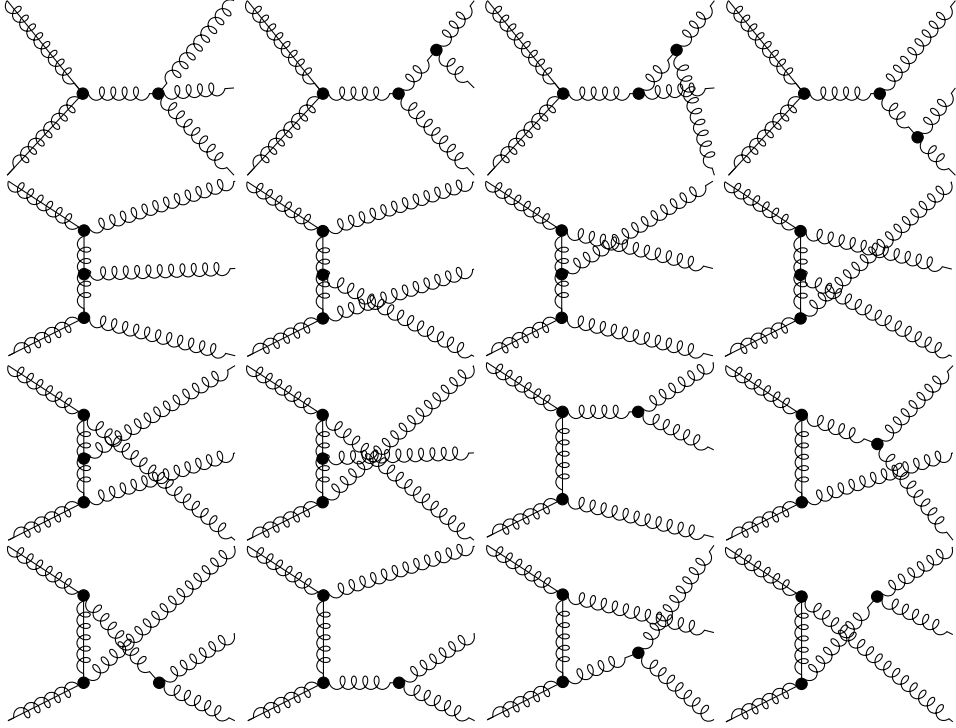


Figure 15: $\tilde{g}\tilde{g} \rightarrow ggg$ for real corrections

7.5 Infrared divergencies

As mentioned before there appear not only ultraviolet divergencies in the one-loop corrections, but also infrared divergencies. Those cancel by including the $2 \rightarrow 3$ process with an additional massless gauge boson and considering it soft or collinear with another final state particle (or both).

In the case of gluino annihilation into gluons it is not sufficient to just examine the process of $\tilde{g}\tilde{g} \rightarrow ggg$ (see figure 15). As the infrared divergencies also occur through corrections with quark/squark-loops, they will depend on the fermion number N_f , which can not be matched by a process involving no quarks. So in addition one also has to include the soft and collinear divergencies of $\tilde{g}\tilde{g} \rightarrow q\bar{q}g$ (see figure 16) and therefore also all one-loop corrections of $\tilde{g}\tilde{g} \rightarrow q\bar{q}$. For a detailed derivation of a similar case see [18].

When using ghost, one also has to take all possible $\tilde{g}\tilde{g} \rightarrow c\bar{c}g$ processes into account. As there are two possibilities for the ghost directions for all of the three options of the gluon final state, that gives a total of six different final state possibilities that all have to be considered. The corresponding diagrams of this six classes are depicted in figures 17 to 22.

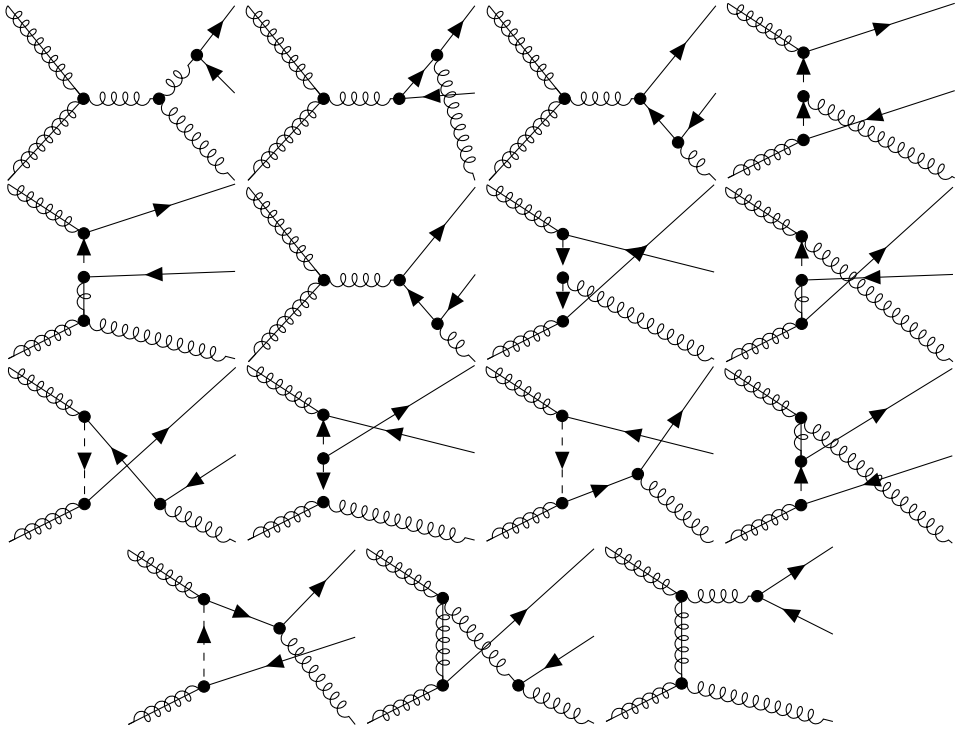


Figure 16: $\tilde{g}\tilde{g} \rightarrow q\bar{q}g$

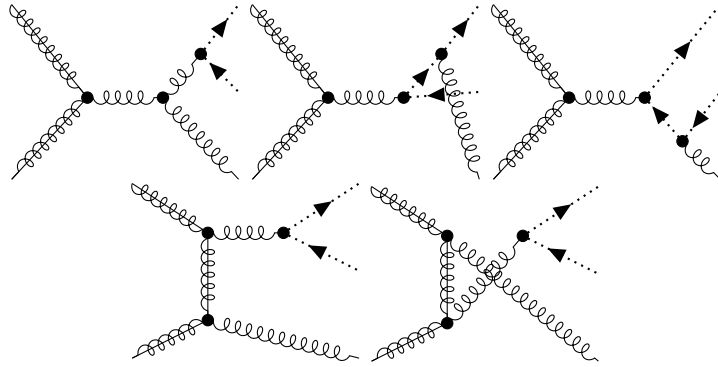


Figure 17: First class of $\tilde{g}\tilde{g} \rightarrow c\bar{c}g$

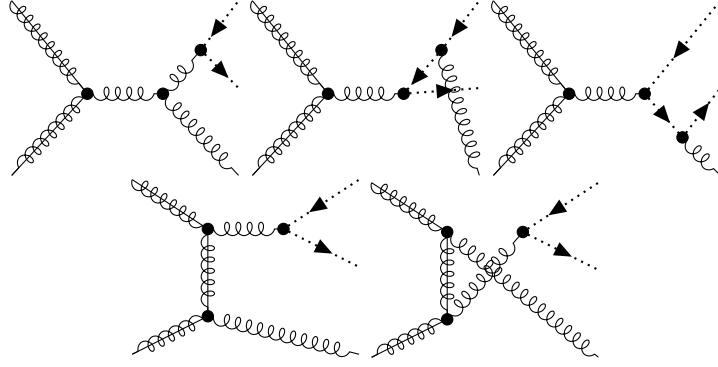


Figure 18: Second class of $\tilde{g}\tilde{g} \rightarrow c\bar{c}g$

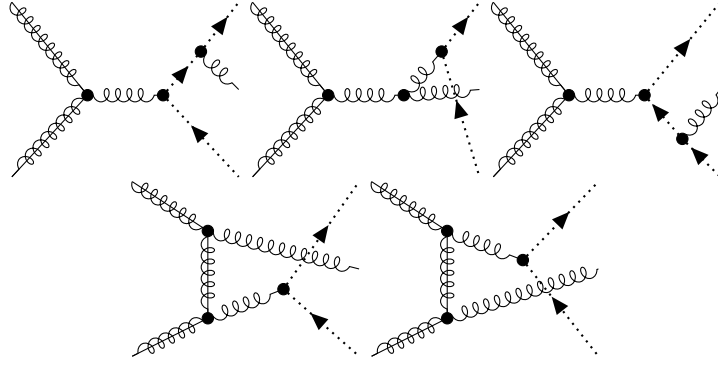


Figure 19: Third class of $\tilde{g}\tilde{g} \rightarrow c\bar{c}g$

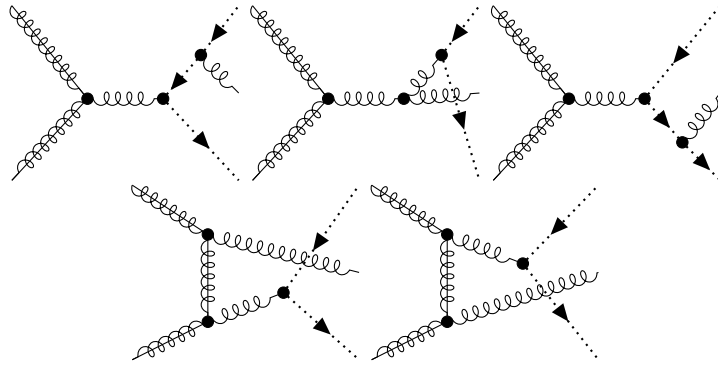


Figure 20: Fourth class of $\tilde{g}\tilde{g} \rightarrow c\bar{c}g$

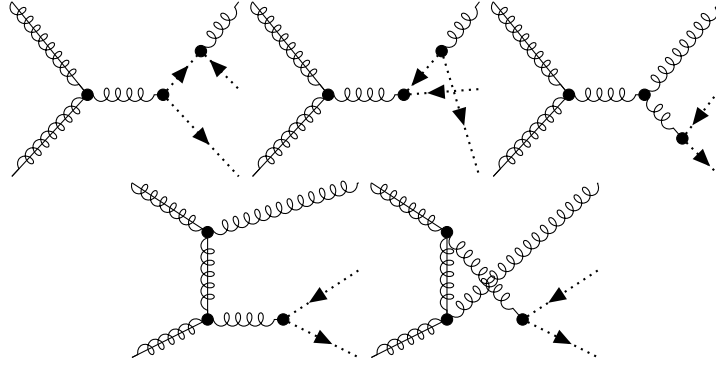


Figure 21: Fifth class of $\tilde{g}\tilde{g} \rightarrow c\bar{c}g$

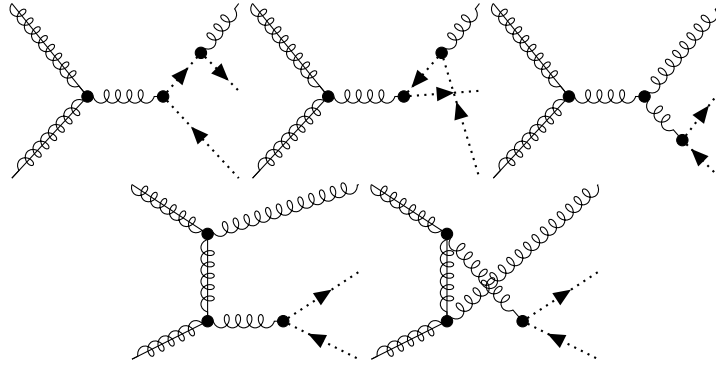


Figure 22: Sixth class of $\tilde{g}\tilde{g} \rightarrow c\bar{c}g$

8 Numerical results

After calculating all virtual corrections at NLO for the gluino annihilation into gluons and implementing them into DM@NLO, the cross sections of the NLO contributions can be calculated. As an exemplary case we use the following parameter scenario:

	$\tan \beta$	M_1	M_2	M_3	A_t	A_b	A_τ
Szenario I	1.55	1430,00	2093,52	1267,80	2755,29	2320,90	-1440,33

	μ	m_{A^0}	$M_{\tilde{l}_L}$	$M_{\tilde{\tau}_L}$	$M_{\tilde{l}_R}$	$M_{\tilde{\tau}_R}$	$M_{\tilde{q}_L}$
Szenario I	-3952,55	3624,81	3134,07	1503,88	2102,53	1780,39	3796,00

	$M_{\tilde{q}_{3L}}$	$M_{\tilde{u}_R}$	$M_{\tilde{t}_R}$	$M_{\tilde{d}_R}$	$M_{\tilde{b}_R}$	Q_{SUSY}
Szenario I	2535,04	3995,01	1620,00	3133,22	3303,77	1784,638

This scenario leads to a MSSM with a neutralino as the LSP and the gluino as the NLSP being just slightly heavier. Furthermore this parameter constellation predicts the relic density measured by Planck.

The upper part of figure 15 plots the tree level cross section of the process in black and the corrections through propagators, vertices and box diagrams in the respective colors. The plot beneath shows the relative values of the corrections in comparison to the tree level cross section. Disregarding the diverging behavior for small momenta, all contributions can be observed to be smaller than the tree level cross section as they should. The sign of the box corrections changes with increasing momentum.

One should keep in mind that those are only preliminary results, as they are UV-convergent but still contain infrared divergencies. The divergence of vertex and box corrections for small momenta is caused by diagrams with a gluon exchange. To fix this behavior the resummation of this soft gluons at next-to-leading logarithmic accuracy is necessary.

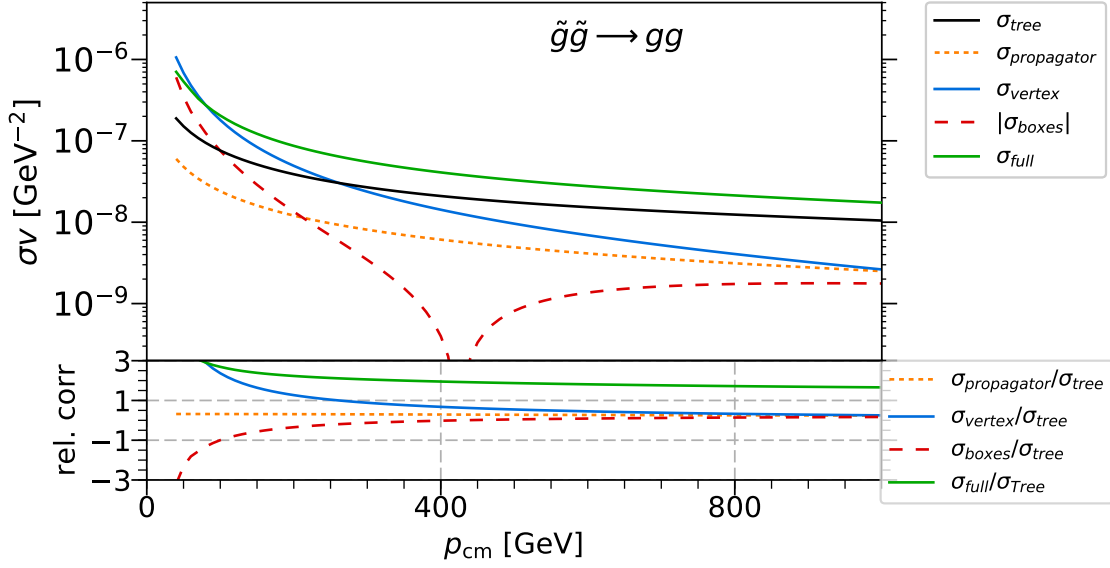


Figure 23: Total virtual corrections at NLO for $\tilde{g}\tilde{g} \rightarrow gg$ and ratio of corrections to tree level contribution

9 Conclusion

In this thesis the virtual corrections of gluino annihilation into gluons at next-to-leading order were derived. By using Passarino-Veltman integrals all propagator and vertex corrections as well as box diagrams were set up. After calculating the self-energies of gluon and gluino the required renormalization constants for the fields were derived. With these the counterterms for all propagators and box diagrams could be written. By implementing all those results in the code of DM@NLO, one is enabled to calculate the cross section of the process with higher accuracy than before. However one should consider, that the full NLO calculation is still incomplete. As next steps the cancellation of infrared divergencies would have to be ensured, followed by the resummation of the soft gluons.

The counterterms, self energies, vertex corrections and box diagrams derived for this thesis can all be found in the appendix.

A Collection of Formulas

A.1 Dirac Algebra in D Dimensions

A.1.1 Dirac Matrices

$$\{\gamma^\mu, \gamma^\nu\} = 2g^{\mu\nu} \quad (\text{A.1})$$

$$\gamma_\mu p^\mu = \not{p} \quad (\text{A.2})$$

$$\gamma^\mu \gamma_\mu = D \quad (\text{A.3})$$

$$\gamma^\alpha \gamma^\mu \gamma_\alpha = (2 - D)\gamma^\mu \quad (\text{A.4})$$

$$\gamma^\alpha \gamma^\mu \gamma^\nu \gamma_\alpha = 4g^{\mu\nu} - (4 - D)\gamma^\mu \gamma^\nu \quad (\text{A.5})$$

$$\gamma^\alpha \gamma^\mu \gamma^\nu \gamma^\rho \gamma_\alpha = -2\gamma^\rho \gamma^\nu \gamma^\mu + (4 - D)\gamma^\mu \gamma^\nu \gamma^\rho \quad (\text{A.6})$$

A.1.2 Completeness Relations

$$\sum_s u_s(p) \bar{u}_s(p) = \not{p} + m \quad (\text{A.7})$$

$$\sum_s v_s(p) \bar{v}_s(p) = \not{p} - m \quad (\text{A.8})$$

$$\sum_{\lambda=1}^4 \epsilon_{(\lambda)}^\mu(k) \cdot \epsilon_{(\lambda)}^{\nu*}(k) = -g^{\mu\nu} \quad (\text{A.9})$$

A.1.3 Traces

$$\text{Tr}[\gamma^\alpha \gamma^\beta \gamma^\mu] = 0 \quad (\text{A.10})$$

$$\text{Tr}[\gamma^\alpha \gamma^\beta \gamma^\mu \gamma^\nu \gamma^\lambda] = 0 \quad (\text{A.11})$$

$$\text{Tr}[\gamma^\mu \gamma^\nu] = 4g^{\mu\nu} \quad (\text{A.12})$$

$$\text{Tr}[\gamma^\alpha \gamma^\beta \gamma^\mu \gamma^\nu] = 4(g^{\alpha\beta} g^{\mu\nu} - g^{\alpha\mu} g^{\beta\nu} + g^{\alpha\nu} g^{\beta\mu}) \quad (\text{A.13})$$

A.1.4 Dirac Equation

$$(\not{p} - m)u(p) = 0 \quad (\text{A.14})$$

$$(\not{p} + m)v(p) = 0 \quad (\text{A.15})$$

$$\bar{u}(p)(\not{p} - m) = 0 \quad (\text{A.16})$$

$$\bar{v}(p)(\not{p} + m) = 0 \quad (\text{A.17})$$

A.2 SU(N) Algebra

$$[T^a, T^b] = f^{abc}T^c \quad (\text{A.18})$$

$$C_F = \frac{N_C^2 - 1}{2N_C} \quad (\text{A.19})$$

$$T_F = \frac{1}{2} \quad (\text{A.20})$$

$$\delta_{ii} = N_C \quad (\text{A.21})$$

$$\delta^{aa} = N_C^2 - 1 \quad (\text{A.22})$$

$$f_{abe}f_{ecd} + f_{cbe}f_{aed} + f_{dbe}f_{ace} = 0 \text{ (Jacobi identity)} \quad (\text{A.23})$$

$$f_{abe}d_{cde} + f_{ace}d_{bde} + f_{ade}d_{bce} = 0 \quad (\text{A.24})$$

$$f_{eab} \cdot f_{gab} = N\delta_{eg} \quad (\text{A.25})$$

$$d_{abc}d_{abd} = \frac{N_C^2 - 4}{N_C}\delta_{cd} \quad (\text{A.26})$$

$$f^{abc} = -2i \text{Tr}(T^a[T^b, T^c]) \quad (\text{A.27})$$

$$\sum_a T_{ij}^a T_{kl}^a = \frac{1}{2} \left(\delta_{il}\delta_{jk} - \frac{1}{N} \delta_{ij}\delta_{kl} \right) \quad (\text{A.28})$$

$$\text{Tr}[T^a T^b] = \frac{1}{2}\delta^{ab} \quad (\text{A.29})$$

$$\text{Tr}[T^a T^b T^c] = \frac{1}{4}(d^{abc} + if^{abc}) \quad (\text{A.30})$$

$$\text{Tr}[T^a T^b T^c T^d] = \frac{1}{4N}\delta_{ab}\delta_{cd} + \frac{1}{8}(d_{abe} + if_{abe})(d_{cde} + if_{cde}) \quad (\text{A.31})$$

$$d_{caf}d_{fbd}d_{dec} = \frac{N_C^2 - 12}{2N_C}d_{abe} \quad (\text{A.32})$$

$$d_{caf}d_{fbd}if_{dec} = \frac{N_C^2 - 4}{2N_C}if_{abe} \quad (\text{A.33})$$

$$d_{caf}if_{fbd}if_{dec} = \frac{N_C}{2}d_{abe} \quad (\text{A.34})$$

$$if_{caf}if_{fbd}if_{dec} = \frac{N_C}{2}if_{abe} \quad (\text{A.35})$$

A.3 Feynman parametrization

$$\frac{1}{AB} = \int_0^1 dx \frac{1}{[A + (B - A)x]^2} \quad (\text{A.36})$$

$$\frac{1}{ABC} = 2 \int_0^1 dx \int_0^x dy \frac{1}{[a(x - y) + b(1 - x) + cy]^3} \quad (\text{A.37})$$

B Feynman rules

B.1 Propagators

Gluon propagator (when using ghosts)

$$g_a^\mu \xrightarrow{p} g_b^\nu = i\delta_{ab} \frac{-g^{\mu\nu} + (1-\xi) \frac{p^\mu p^\nu}{p^2}}{p^2 + i\varepsilon} \quad (\text{B.1})$$

Ghost propagator

$$c_a \xrightarrow{p} c_b = \frac{i\delta_{ab}}{p^2 + i\varepsilon} \quad (\text{B.2})$$

Gluino propagator

$$\tilde{g}_a \xrightarrow{p} \tilde{g}_b = i\delta_{ab} \frac{\not{p} + m_{\tilde{g}}}{p^2 - m_{\tilde{g}}^2 + i\varepsilon} \quad (\text{B.3})$$

Quark propagator

$$q_s^\alpha \xrightarrow{p} q_t^\beta = i\delta_{st} \delta^{\alpha\beta} \frac{\not{p} + m_{q^\alpha}}{p^2 - m_{q^\alpha}^2 + i\varepsilon} \quad (\text{B.4})$$

Squark propagator

$$\tilde{q}_{i,s}^\alpha \xrightarrow{p} \tilde{q}_{j,t}^\beta = \frac{i\delta_{ij} \delta_{st} \delta^{\alpha\beta}}{p^2 - m_{\tilde{q}_i}^2 + i\varepsilon} \quad (\text{B.5})$$

B.2 Couplings

Triple-gluon vertex

$$g_a^\mu \xrightarrow{k_1} \begin{array}{c} g_b^\nu \\ \nearrow k_2 \\ \nwarrow k_3 \\ g_c^\rho \end{array} = if_{abc} i g_s [(k_1 - k_2)^\rho g^{\mu\nu} + (k_2 - k_3)^\mu g^{\nu\rho} + (k_3 - k_1)^\nu g^{\mu\rho}] \quad (\text{B.6})$$

2-ghost-gluon vertex

$$g_a^\mu \xrightarrow{k} \begin{array}{c} \bar{c}_b \\ \nearrow k \\ \searrow k \\ c_c \end{array} = if_{abc} i g_s k^\mu \quad (\text{B.7})$$

2-gluino-gluon vertex

$$\begin{array}{c}
 \bar{\tilde{g}}_b \\
 \diagup \\
 g_a^\mu \text{---} \text{wavy line} \\
 \diagdown \\
 \tilde{g}_c
 \end{array}
 = i f_{abc} i g_s \gamma^\mu
 \quad (B.8)$$

2-quark-gluon vertex

$$\begin{array}{c}
 \bar{q}_s^\beta \\
 \diagup \\
 g_a^\mu \text{---} \text{wavy line} \\
 \diagdown \\
 q_r^\alpha
 \end{array}
 = -T_{rs}^\alpha i g_s \delta^{\alpha\beta} \gamma^\mu
 \quad (B.9)$$

2-squark-gluon vertex

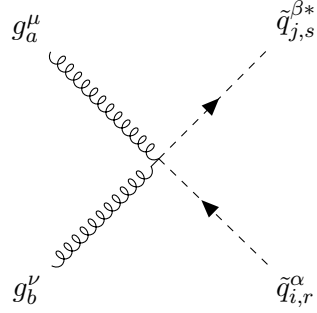
$$\begin{array}{c}
 k1 \nearrow \tilde{q}_{j,s}^{\beta*} \\
 g_a^\mu \text{---} \text{wavy line} \\
 k2 \searrow \tilde{q}_{i,r}^\alpha
 \end{array}
 = -T_{rs}^\alpha i g_s \delta^{\alpha\beta} \delta_{ij} (k1 - k2)^\mu
 \quad (B.10)$$

Quark-squark-gluon vertices

$$\begin{array}{c}
 \tilde{q}_{i,s}^{\beta*} \\
 \diagup \\
 g_a^\mu \text{---} \text{wavy line} \\
 \diagdown \\
 q_r^\alpha
 \end{array}
 = -T_{rs}^\alpha i \sqrt{2} g_s \delta^{\alpha\beta} (R_{i1}^\alpha P_R - R_{i2}^\alpha P_L)
 \quad (B.11)$$

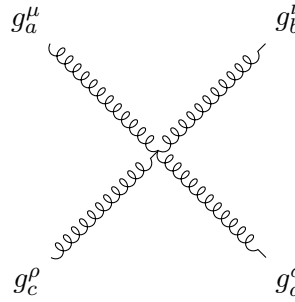
$$\begin{array}{c}
 \tilde{q}_{i,s}^\beta \\
 \diagup \\
 g_a^\mu \text{---} \text{wavy line} \\
 \diagdown \\
 \bar{q}_r^\alpha
 \end{array}
 = -T_{rs}^\alpha i \sqrt{2} g_s \delta^{\alpha\beta} (R_{i1}^\alpha P_L - R_{i2}^\alpha P_R)
 \quad (B.12)$$

2-squark-2-gluon vertex



$$= \{T^a, T^b\}_{sr} i g_s^2 \delta^{\alpha\beta} \delta_{ij} \quad (\text{B.13})$$

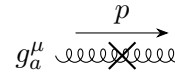
4-gluon vertex



$$= -i g_s^2 [f_{abe} f_{cde} (g^{\mu\rho} g^{\nu\sigma} - g^{\mu\sigma} g^{\nu\rho}) + f_{ace} f_{bde} (g^{\mu\nu} g^{\rho\sigma} - g^{\mu\sigma} g^{\nu\rho}) + f_{ade} f_{bce} (g^{\mu\nu} g^{\rho\sigma} - g^{\mu\rho} g^{\nu\sigma})] \quad (\text{B.14})$$

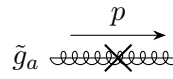
B.3 Counterterms

Gluon propagator



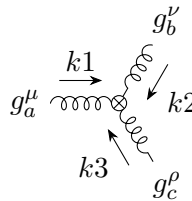
$$g_a^\mu \xrightarrow{p} g_b^\nu = -i \delta_{ab} (p^2 g^{\mu\nu} - p^\mu p^\nu) \delta Z_g \quad (\text{B.15})$$

Gluino propagator



$$\tilde{g}_a \xrightarrow{p} \tilde{g}_b = i \delta_{ab} \left[-(\delta m_{\tilde{g}} + \delta Z_{\tilde{g}}^L) P_L - (\delta m_{\tilde{g}} + \delta Z_{\tilde{g}}^R) P_R + \not{p} (\delta Z_{\tilde{g}}^L P_L + \delta Z_{\tilde{g}}^R P_R) \right] \quad (\text{B.16})$$

Triple-gluon vertex



$$g_a^\mu \xrightarrow{k1} g_b^\nu \xrightarrow{k2} g_c^\rho \xrightarrow{k3} = i f_{abc} i g_s [(k_1 - k_2)^\rho g^{\mu\nu} + (k_2 - k_3)^\mu g^{\nu\rho} + (k_3 - k_1)^\nu g^{\mu\rho}] \delta Z_{3g} \quad (\text{B.17})$$

with

$$\delta Z_{3g} = \delta g_s + \frac{3}{2} \delta Z_g \quad (\text{B.18})$$

2-gluino-gluon vertex

$$g_a^\mu \text{---} \circ \begin{array}{c} \nearrow \\ \searrow \end{array} \begin{array}{l} \tilde{g}_b \\ \tilde{g}_c \end{array} = \delta Z_{\tilde{g}\tilde{g}}^{L/R} i f_{abc} i g_s \gamma^\mu \quad (\text{B.19})$$

with

$$\delta Z_{\tilde{g}\tilde{g}\tilde{g}}^{L/R} = \delta g_s + \frac{1}{2} \left(\delta Z_g + \delta Z_{\tilde{g}}^{L/R} + \delta Z_{\tilde{g}}^{L/R*} \right) \quad (\text{B.20})$$

C Calculations for color basis

These results of these calculations are used to derive the color basis in chapter 6.

$$\text{Tr}[T^a T^c T^b T^d] + \text{Tr}[T^c T^a T^d T^b] = \left(\frac{1}{4N_C} \delta_{ac} \delta_{bd} + \frac{1}{8} (d_{ace} d_{bde} + d_{ace} i f_{bde} + i f_{ace} d_{bde} + i f_{ace} i f_{bde}) \right) \quad (\text{C.1})$$

$$+ \left(\frac{1}{4N_C} \delta_{ca} \delta_{db} + \frac{1}{8} (d_{cae} d_{dbe} + d_{cae} i f_{dbe} + i f_{cae} d_{dbe} + i f_{cae} i f_{dbe}) \right) \quad (\text{C.2})$$

$$= \frac{1}{2N_C} \delta_{ac} \delta_{bd} + \frac{1}{4} (d_{ace} d_{bde} + i f_{ace} i f_{bde}) \quad (\text{C.3})$$

$$\text{Tr}[T^a T^c T^b T^d] - \text{Tr}[T^c T^a T^d T^b] = \left(\frac{1}{4N_C} \delta_{ac} \delta_{bd} + \frac{1}{8} (d_{ace} d_{bde} + d_{ace} i f_{bde} + i f_{ace} d_{bde} + i f_{ace} i f_{bde}) \right) \quad (\text{C.4})$$

$$-\left(\frac{1}{4N_C}\delta_{ca}\delta_{db} + \frac{1}{8}(d_{cae}d_{dbe} + d_{cae}if_{dbe} + if_{cae}d_{dbe} + if_{cae}if_{dbe})\right) \quad (\text{C.5})$$

$$= \frac{1}{4} (d_{ace} i f_{bde} + i f_{ace} d_{bde}) \quad (\text{C.6})$$

$$\Pi_{\pm}^{\pm} \cdot P_1 = \left(\frac{1}{4} (\delta_{ac} \delta_{bd} + \delta_{ad} \delta_{bc}) \pm \text{Tr}[T^a T^c T^b T^d] \pm \text{Tr}[T^a T^d T^b T^c] \right) \frac{1}{N_C^2 - 1} \delta_{cd} \delta_{fg} \quad (\text{C.7})$$

$$= \left(\frac{1}{4} (\delta_{ac} \delta_{bd} + \delta_{ad} \delta_{bc}) \pm \frac{1}{2N_C} \delta_{ac} \delta_{bd} \pm \frac{1}{4} (d_{ace} d_{bde} + i f_{ace} i f_{bde}) \right) \frac{1}{N_C^2 - 1} \delta_{cd} \delta_{fg} \quad (\text{C.8})$$

$$= \left(\frac{1}{4}(\delta_{ab} + \delta_{ab}) \pm \frac{1}{2N_C} \delta_{ab} \pm \frac{1}{4} \left(\frac{N_C^2 - 4}{N_C} - N_C \right) \delta_{ab} \right) \frac{1}{N_C^2 - 1} \delta_{fg} \quad (\text{C.9})$$

$$= \frac{N_C \mp 1}{2N_C} P_1 \quad (\text{C.10})$$

$$\Pi_{\mp}^{\pm} \cdot P_{8_A} = \left(\frac{1}{4}(\delta_{ac}\delta_{bd} - \delta_{ad}\delta_{bc}) \pm \text{Tr}[T^a T^c T^b T^d] \mp \text{Tr}[T^a T^d T^b T^c] \right) \frac{1}{N_C} i f_{cde} i f_{gfe} \quad (\text{C.11})$$

$$= \left(\frac{1}{4}(\delta_{ac}\delta_{bd} - \delta_{ad}\delta_{bc}) \pm \frac{1}{4} (d_{ach} i f_{bdh} + i f_{ach} d_{bdh}) \right) \frac{1}{N_C} i f_{cde} i f_{gfe} \quad (\text{C.12})$$

$$= \frac{1}{4}(f_{abe} - f_{bae}) \pm \frac{1}{4} \left(\frac{N_C}{2} d_{abe} - \frac{N_C}{2} d_{abe} \right) \frac{1}{N_C} i f_{gfe} \quad (\text{C.13})$$

$$= \frac{1}{2} P_{8_A} \quad (\text{C.14})$$

$$\Pi_{\pm}^{\pm} \cdot P_{8_S} = \left(\frac{1}{4}(\delta_{ac}\delta_{bd} + \delta_{ad}\delta_{bc}) \pm \text{Tr}[T^a T^c T^b T^d] \pm \text{Tr}[T^a T^d T^b T^c] \right) \frac{N_C}{N_C^2 - 4} d_{cde} d_{gfe} \quad (\text{C.15})$$

$$= \left(\frac{1}{4}(\delta_{ac}\delta_{bd} + \delta_{ad}\delta_{bc}) \pm \frac{1}{2N_C} \delta_{ac}\delta_{bd} \pm \frac{1}{4} (d_{ach} d_{bdh} + i f_{ach} i f_{bdh}) \right) \frac{N_C}{N_C^2 - 4} d_{cde} d_{gfe} \quad (\text{C.16})$$

$$= \left(\frac{1}{4}(d_{abe} + d_{abe}) \pm \frac{1}{2N_C} d_{abe} \pm \frac{1}{4} \left(\frac{N_C^2 - 12}{2N_C} - \frac{N_C}{2} \right) d_{abe} \right) \frac{N_C}{N_C^2 - 4} d_{gfe} \quad (\text{C.17})$$

$$= \frac{N_C \mp 2}{2N_C} P_{8_S} \quad (\text{C.18})$$

$$P_{10} = \Pi_{-}^{+} - \frac{1}{2} P_{8_A} \quad (\text{C.19})$$

$$= \frac{1}{4}(\delta_{ac}\delta_{bd} - \delta_{ad}\delta_{bc}) + \frac{1}{4} (d_{ace} i f_{bde} + i f_{ace} d_{bde}) - \frac{1}{2} \frac{1}{N_C} i f_{abe} i f_{dce} \quad (\text{C.20})$$

$$P_{\overline{10}} = \Pi_{+}^{-} - \frac{1}{2} P_{8_A} \quad (\text{C.21})$$

$$= \frac{1}{4}(\delta_{ac}\delta_{bd} - \delta_{ad}\delta_{bc}) - \frac{1}{4} (d_{ace} i f_{bde} + i f_{ace} d_{bde}) - \frac{1}{2} \frac{1}{N_C} i f_{abe} i f_{dce} \quad (\text{C.22})$$

$$P_{27} = \Pi_{+}^{+} - \frac{N_C - 1}{2N_C} P_1 - \frac{N_C - 2}{2N_C} P_{8_S} \quad (\text{C.23})$$

$$= \frac{1}{4}(\delta_{ac}\delta_{bd} + \delta_{ad}\delta_{bc}) + \frac{1}{4} (d_{ace} i f_{bde} + i f_{ace} d_{bde}) \quad (\text{C.24})$$

$$- \frac{N_C - 1}{2N_C} \frac{1}{N_C^2 - 1} \delta_{ab} \delta_{cd} - \frac{N_C - 2}{2N_C} \frac{N_C}{N_C^2 - 4} d_{abe} d_{cde} \quad (\text{C.25})$$

D Virtual corrections

Here all self energies, vertex corrections and amplitudes of the box diagrams are listed.

D.1 Self energies

To retain the definition of the Passarino-Veltman integrals use

$$\mu^{4-D} \int \frac{d^D q}{(2\pi)^D} = \frac{i}{(4\pi)^2} \frac{(2\pi\mu)^{4-D}}{i\pi^2} \int d^D q \quad (\text{D.1})$$

for the self energies.

D.1.1 Gluon self energy

The general amplitude can be written as

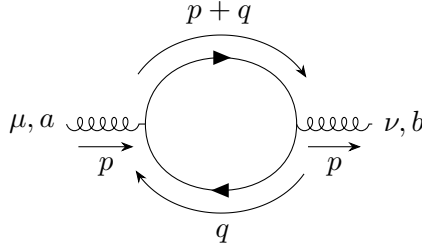
$$\Pi_{ab}^{\mu\nu} = -\delta_{ab} \frac{i}{(4\pi)^2} \left[\left(g^{\mu\nu} - \frac{p^\mu p^\nu}{p^2} \right)^2 \Pi^T(p^2) + \frac{p^\mu p^\nu}{p^2} \Pi^L(p^2) \right] \quad (\text{D.2})$$

$$= -iF_{\text{color}} \delta_{ab} \left(g^{\mu\nu} A(p^2) + \frac{p^\mu p^\nu}{p^2} B(p^2) \right) \quad (\text{D.3})$$

Π^T and Π^B can be regained from A,B by

$$\Pi^T(p^2) = F_{\text{color}} (4\pi)^2 A \quad (\text{D.4})$$

$$\Pi^B(p^2) = F_{\text{color}} (4\pi)^2 (A + B) \quad (\text{D.5})$$



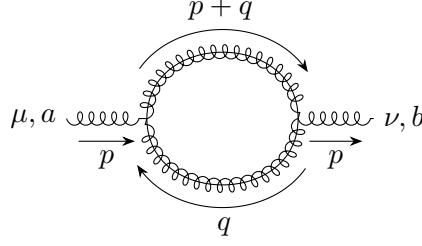
Quark loop

$$M = \mu^{4-D} \int \frac{d^D q}{(2\pi)^D} (-1) T_{sr}^a (-ig_s \gamma^\mu) \frac{i(\not{p} + \not{q} + m_q)}{(p+q)^2 - m_q^2} T_{rs}^b (-ig_s \gamma^\nu) \frac{i(\not{q} + m_q)}{q^2 - m_q^2} \quad (\text{D.6})$$

$$A(p^2) = \frac{g_s^2}{(4\pi)^2} (8B_{00} - 4p^2 B_1 - 4A_0(m_q^2)) \quad (\text{D.7})$$

$$B(p^2) = \frac{g_s^2}{(4\pi)^2} 8p^2 (B_1 + B_{11}) \quad (\text{D.8})$$

$$F_{\text{color}} = T_F \quad (\text{D.9})$$



Gluino loop

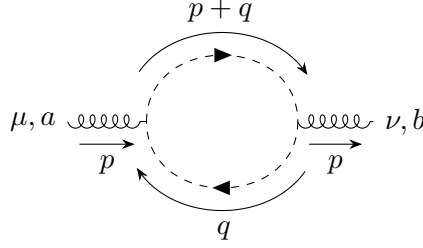
$$M = \mu^{4-D} \int \frac{d^D q}{(2\pi)^D} \frac{1}{2} (-1) i f_{acd} i g_s \gamma^\mu \frac{i(\not{p} + \not{q} + m_q)}{(p+q)^2 - m_q^2} i f_{bdc} i g_s \gamma^\nu \frac{i(\not{q} + m_q)}{q^2 - m_q^2} \quad (\text{D.10})$$

The factor of $\frac{1}{2}$ in the amplitude is a symmetry factor due to the Majorana nature of gluino.

$$A(p^2) = \frac{1}{2} \frac{g_s^2}{(4\pi)^2} (8B_{00} - 4p^2 B_1 - 4A_0(m_g^2)) \quad (\text{D.11})$$

$$B(p^2) = \frac{1}{2} \frac{g_s^2}{(4\pi)^2} 8p^2 (B_1 + B_{11}) \quad (\text{D.12})$$

$$F_{color} = N_C \quad (\text{D.13})$$



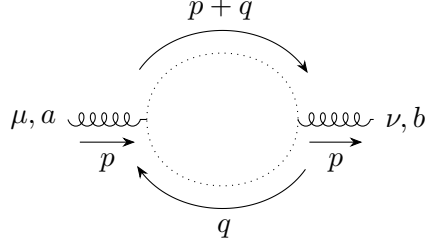
Squark loop

$$M = \mu^{4-D} \int \frac{d^D q}{(2\pi)^D} T_{sr}^a (-i g_s (p+2q)^\mu) \frac{i}{(p+q)^2 - m_{\tilde{q}}^2} T_{rs}^b (-i g_s (p+2q)^\nu) \frac{i}{q^2 - m_{\tilde{q}}^2} \quad (\text{D.14})$$

$$A(p^2) = \frac{g_s^2}{(4\pi)^2} (-4B_{00}) \quad (\text{D.15})$$

$$B(p^2) = \frac{g_s^2}{(4\pi)^2} (-p^2) (4B_{11} + 4B_1 + B_0) \quad (\text{D.16})$$

$$F_{color} = T_F \quad (\text{D.17})$$



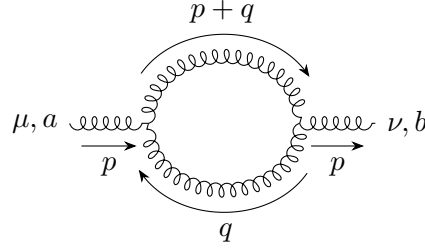
Ghost loop

$$M = \mu^{4-D} \int \frac{d^D q}{(2\pi)^D} (-1) i f_{acd} i g_s (p+q)^\mu \frac{i}{(p+q)^2 - m_{\bar{q}}^2} i f_{dcb} i g_s q^\nu \frac{i}{q^2 - m_{\bar{q}}^2} \quad (\text{D.18})$$

$$A(p^2) = \frac{g_s^2}{(4\pi)^2} B_{00} \quad (\text{D.19})$$

$$B(p^2) = \frac{g_s^2}{(4\pi)^2} p^2 (B_1 + B_{11}) \quad (\text{D.20})$$

$$F_{color} = N_C \quad (\text{D.21})$$



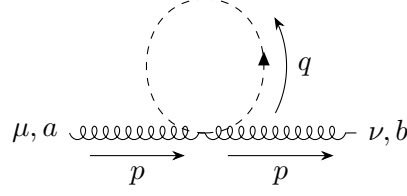
Gluon loop

$$M = \mu^{4-D} \int \frac{d^D q}{(2\pi)^D} \frac{1}{2} i f_{dcb} i g_s (g^{\mu\rho} (p-q)^\sigma + g^{\rho\sigma} (p+2q)^\mu - g^{\sigma\mu} (2p+q)^\rho) \frac{-i}{(p+q)^2} i f_{dcb} i g_s \left(g_\rho^\nu (p-q)_\sigma + g_{\rho\sigma} (p+2q)^\nu - g_\sigma^\nu (2p+q)_\rho \right) \frac{-i}{q^2} \quad (\text{D.22})$$

$$A(p^2) = \frac{1}{2} \frac{g_s^2}{(4\pi)^2} \left(-10B_{00} - p^2 (2B_1 + 5B_0 + \frac{2}{3}) \right) \quad (\text{D.23})$$

$$B(p^2) = \frac{1}{2} \frac{g_s^2}{(4\pi)^2} (-p^2) (10B_{11} + 10B_1 - 2B_0 - \frac{2}{3}) \quad (\text{D.24})$$

$$F_{color} = N_C \quad (\text{D.25})$$



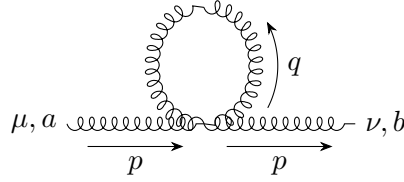
4-point vertex squark loop

$$M = \mu^{4-D} \int \frac{d^D q}{(2\pi)^D} \{T^a, T^b\}_{rr} i g_s^2 g^{\mu\nu} \frac{i}{q^2 - m_{\tilde{q}}^2} \quad (\text{D.26})$$

$$A(p^2) = \frac{g_s^2}{(4\pi)^2} A_0(m_q^2) \quad (\text{D.27})$$

$$B(p^2) = 0 \quad (\text{D.28})$$

$$F_{color} = 2T_F \quad (\text{D.29})$$



4-point vertex gluon loop

$$M = 0 \quad (\text{D.30})$$

$$A(p^2) = 0 \quad (\text{D.31})$$

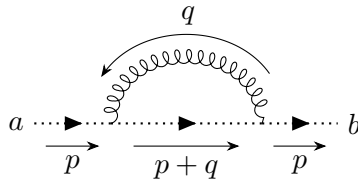
$$B(p^2) = 0 \quad (\text{D.32})$$

D.1.2 Ghost

The general form of the ghost self energy reads

$$\Pi_{ab} = \delta_{ab} i \Pi^c(p^2) \quad (\text{D.33})$$

$$= F_{color} \delta_{ab} i A(p^2) \quad (\text{D.34})$$



Gluon-ghost loop

$$M = \mu^{4-D} \int \frac{d^D q}{(2\pi)^D} i f_{cda} i g_s \gamma_\mu \frac{-i}{q^2} \frac{i}{(p+q)^2} i f_{cbd} i g_s \gamma^\mu \quad (\text{D.35})$$

$$A(p^2) = -\frac{g_s^2}{(4\pi)^2} \frac{1}{2} p^2 B_0 \quad (\text{D.36})$$

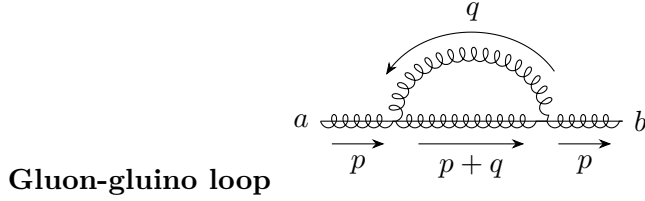
$$F_{color} = N_C \quad (\text{D.37})$$

D.1.3 Gluino self energy

The general form of the gluino self energy reads

$$\Pi_{ab} = \delta_{ab} i \left[\Pi_{ab}^{SL} P_L + \Pi_{ab}^{SR} P_R + \Pi_{ab}^{VL} \not{p} P_L + \Pi_{ab}^{VR} \not{p} P_R \right] \quad (\text{D.38})$$

$$= F_{color} \delta_{ab} i \left[A_L P_L + A_R P_R + B_L \not{p} P_L + B_R \not{p} P_R \right] \quad (\text{D.39})$$

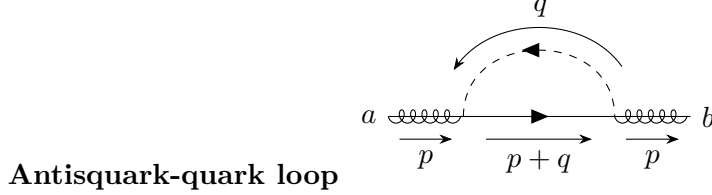


$$M = \mu^{4-D} \int \frac{d^D q}{(2\pi)^D} i f_{dcb} i g_s \gamma_\mu \frac{-i (\not{p} + \not{q} + m_{\tilde{g}})}{q^2 (q+p)^2 - m_{\tilde{g}}^2} i f_{acd} i g_s \gamma^\mu \quad (\text{D.40})$$

$$A_L = A_R = - \frac{g_s^2}{(4\pi)^2} m_{\tilde{g}} (4B_0 - 2) \quad (\text{D.41})$$

$$B_L = B_R = \frac{g_s^2}{(4\pi)^2} (2B_0 + 2B_1 - 1) \quad (\text{D.42})$$

$$F_{color} = N_C \quad (\text{D.43})$$



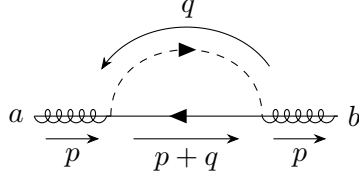
$$M = \mu^{4-D} \int \frac{d^D q}{(2\pi)^D} T_{rs}^b (-i\sqrt{2}g_s (R_{i1}P_R - R_{i2}P_L)) \frac{-i}{q^2 - m_{\tilde{q}}^2} \frac{i(\not{p} + \not{q} + m_q)}{(q+p)^2 - m_q^2} T_{sr}^a (i\sqrt{2}g_s (R_{i1}P_R - R_{i2}P_L)) \quad (\text{D.44})$$

$$A_L = A_R = - \frac{g_s^2}{(4\pi)^2} 2m_q R_{i1} R_{i2} B_0 \quad (\text{D.45})$$

$$B_L = \frac{g_s^2}{(4\pi)^2} R_{i2}^2 2(B_0 + B_1) \quad (\text{D.46})$$

$$B_R = \frac{g_s^2}{(4\pi)^2} R_{i1}^2 2(B_0 + B_1) \quad (\text{D.47})$$

$$F_{color} = T_F \quad (\text{D.48})$$



Squark-antiquark loop

$$M = \mu^{4-D} \int \frac{d^D q}{(2\pi)^D} T_{sr}^b (-i\sqrt{2}g_s(R_{i1}P_L - R_{i2}P_R)) \frac{-i}{q^2 - m_{\tilde{q}}} \frac{i(\not{p} + \not{q} + m_q)}{(q+p)^2 - m_q^2} T_{rs}^a (i\sqrt{2}g_s(R_{i1}P_L - R_{i2}P_R)) \quad (\text{D.49})$$

$$A_L = A_R = -\frac{g_s^2}{(4\pi)^2} 2m_q R_{i1} R_{i2} B_0 \quad (\text{D.50})$$

$$B_L = \frac{g_s^2}{(4\pi)^2} R_{i1}^2 2(B_0 + B_1) \quad (\text{D.51})$$

$$B_R = \frac{g_s^2}{(4\pi)^2} R_{i2}^2 2(B_0 + B_1) \quad (\text{D.52})$$

$$F_{color} = T_F \quad (\text{D.53})$$

D.2 Vertex Corrections

For the vertex correction the following equation can be used to regain the definition of the Passarino-Veltman integrals:

$$\mu^{4-D} \mu^{\frac{4-D}{2}} \int \frac{d^D q}{(2\pi)^D} = \mu^{\frac{4-D}{2}} \frac{i}{(4\pi)^2} \frac{(2\pi\mu)^{4-D}}{i\pi^2} \int d^D q \quad (\text{D.54})$$

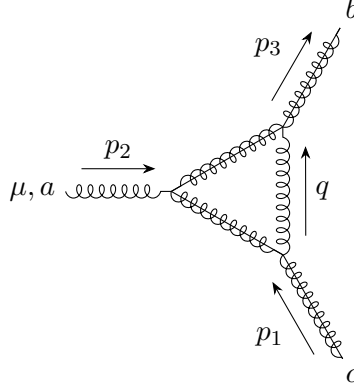
D.2.1 Gluino-gluon Vertex

The Gluino-gluon vertex at NLO can generally be written as:

$$\begin{aligned} M = & F_{color} \mu^{\frac{4-D}{2}} \frac{i}{4\pi^2} \left[\gamma^\mu \left(A_L^1 P_L + A_R^1 P_R \right) + (p_1 - p_3)^\mu \left(A_L^2 P_L + A_R^2 P_R \right) \right. \\ & + (p_1 + p_3)^\mu \left(A_L^3 P_L + A_R^3 P_R \right) + \gamma^\mu \left(B_L^1 P_L + B_R^1 P_R \right) (\not{p}_1 - m_{\tilde{g}}) \\ & + (p_1 - p_3)^\mu \left(B_L^2 P_L + B_R^2 P_R \right) (\not{p}_1 - m_{\tilde{g}}) + (p_1 + p_3)^\mu \left(B_L^3 P_L + B_R^3 P_R \right) (\not{p}_1 - m_{\tilde{g}}) \\ & + (\not{p}_3 - m_{\tilde{g}}) \gamma^\mu \left(C_L^1 P_L + C_R^1 P_R \right) + (\not{p}_3 - m_{\tilde{g}}) (p_1 - p_3)^\mu \left(C_L^2 P_L + C_R^2 P_R \right) \\ & + (\not{p}_3 - m_{\tilde{g}}) (p_1 + p_3)^\mu \left(C_L^3 P_L + C_R^3 P_R \right) + (\not{p}_3 - m_{\tilde{g}}) \gamma^\mu \left(D_L^1 P_L + D_R^1 P_R \right) (\not{p}_1 - m_{\tilde{g}}) \\ & + (\not{p}_3 - m_{\tilde{g}}) (p_1 - p_3)^\mu \left(D_L^2 P_L + D_R^2 P_R \right) (\not{p}_1 - m_{\tilde{g}}) \\ & \left. + (\not{p}_3 - m_{\tilde{g}}) (p_1 + p_3)^\mu \left(D_L^3 P_L + D_R^3 P_R \right) (\not{p}_1 - m_{\tilde{g}}) \right] \quad (\text{D.55}) \end{aligned}$$

The use of this notation is, that the B coefficients vanish, if p_1 is on-shell and the C coefficients vanish, if p_3 is on-shell.

Gluino-gluon loops



$$M = \mu^{\frac{4-D}{2}} \int \frac{d^D q}{(2\pi)^D} i f_{ebd} i g_s \gamma_\nu \frac{i(\not{p}_3 - \not{q} + m_{\tilde{g}})}{(p_3 - q)^2 - m_{\tilde{g}}^2} i f_{adf} i g_s \gamma_\mu \frac{i(\not{p}_1 - \not{q} + m_{\tilde{g}})}{(p_1 - q)^2 - m_{\tilde{g}}^2} i f_{efc} i g_s \gamma^\nu \frac{-i}{q^2} \quad (\text{D.56})$$

$$A_L^1 = A_R^1 = g_s^3 \left(2B_0 - 2m_{\tilde{g}}^2 C_0 + (4p_1 \cdot p_3 + 2m_{\tilde{g}}^2)(C_0 + C_1 + C_2) - 4C_{00} + 2p_1^1 C_1 + 2p_3^2 C_2 - 1 \right) \quad (\text{D.57})$$

$$A_L^2 = A_R^2 = (4m_{\tilde{g}}(C_1 - C_2) + (-2)m_{\tilde{g}}(C_1 - C_2 + C_{11} - C_{22})) \quad (\text{D.58})$$

$$A_L^3 = A_R^3 = g_s^3 (-2)m_{\tilde{g}}(C_1 + C_2 + C_{11} + 2C_{12} + C_{22}) \quad (\text{D.59})$$

$$B_L^1 = B_R^1 = g_s^3 2m_{\tilde{g}}(C_0 + C_1 + C_2) \quad (\text{D.60})$$

$$B_L^2 = B_R^2 = g_s^3 2(C_0 + C_2 - C_{11} + C_{12}) \quad (\text{D.61})$$

$$B_L^3 = B_R^3 = g_s^3 (-2)(C_0 + 2C_1 + C_2 + C_{11} + C_{12}) \quad (\text{D.62})$$

$$C_L^1 = C_R^1 = g_s^3 2m_{\tilde{g}}(C_0 + C_1 + C_2) \quad (\text{D.63})$$

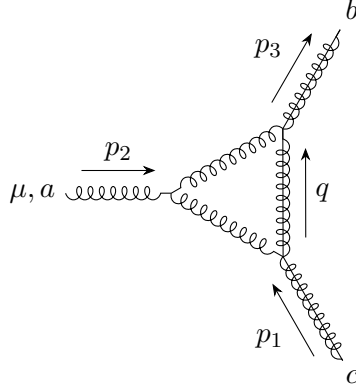
$$C_L^2 = C_R^2 = g_s^3 2(-C_0 - C_1 - C_{12} + C_{22}) \quad (\text{D.64})$$

$$C_L^3 = C_R^3 = g_s^3 (-2)(C_0 + C_1 + 2C_2 + C_{12} + C_{22}) \quad (\text{D.65})$$

$$D_L^1 = D_R^1 = g_s^3 2(C_0 + C_1 + C_1) \quad (\text{D.66})$$

$$D_L^2 = D_R^2 = D_L^3 = D_R^3 = 0 \quad (\text{D.67})$$

$$F_{color} = \frac{N_C}{2} \quad (\text{D.68})$$



$$\begin{aligned}
M = \mu^{\frac{4-D}{2}} \int \frac{d^D q}{(2\pi)^D} & i f_{dbe} i g_s \gamma_\rho \frac{i(\not{q} + m_{\tilde{g}})}{q^2 - m_{\tilde{g}}^2} i f_{fec} i g_s \gamma_\nu \frac{-i}{(p_3 - q)^2} \frac{-i}{(p_1 - q)^2} \\
& i f_{adf} i g_s (g^{\mu\nu} (p_3 - 2p_q + q)^\rho + g^{\nu\rho} (p_1 + p_3 - 2q)^\mu + g^{\rho\mu} (p_1 - 2p_3 + q)^\nu)
\end{aligned} \tag{D.69}$$

$$A_L^1 = A_R^1 = -g_s^3 \left(2B_0 + 8m_{\tilde{g}}^2 C_0 + (4p_1 \cdot 3 - 3m_{\tilde{g}}^2)(C_1 + C_2) + p_1^2 C_1 + p_3^2 C_2 + 4C_{00} - 1 \right) \tag{D.70}$$

$$A_L^2 = A_R^2 = -g_s^3 (4m_{\tilde{g}}(C_1 - C_2) + 2m_{\tilde{g}}(C_{11} - C_{22})) \tag{D.71}$$

$$A_L^3 = A_R^3 = -g_s^3 (2m_{\tilde{g}}(C_1 + C_3) + 2m_{\tilde{g}}(C_{11} + 2C_{12} + C_{22})) \tag{D.72}$$

$$B_L^1 = B_R^1 = -g_s^3 (3m_{\tilde{g}}(C_0 + C_1 + C_2)) \tag{D.73}$$

$$B_L^2 = B_R^2 = -g_s^3 (2C_1 + C_2 + 2(C_{11} - C_{12})) \tag{D.74}$$

$$B_L^3 = B_R^3 = -g_s^3 (-C_2 + 2(C_{11} + C_{22})) \tag{D.75}$$

$$C_L^1 = C_R^1 = -g_s^3 3m_{\tilde{g}}(C_0 + C_1 + C_2) \tag{D.76}$$

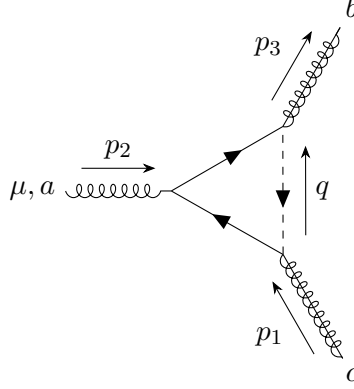
$$C_L^2 = C_R^2 = -g_s^3 (-C_1 - 2C_2 + 2(C_{12} - C_{22})) \tag{D.77}$$

$$C_L^3 = C_R^3 = -g_s^3 (-C_1 + 2(C_{12} + C_{22})) \tag{D.78}$$

$$D_L^1 = D_R^1 = -g_s^3 3(C_1 + C_2) \tag{D.79}$$

$$F_{color} = -\frac{N_C}{2} \tag{D.80}$$

Quark-squark loops



$$M = \mu^{\frac{4-D}{2}} \int \frac{d^D q}{(2\pi)^D} T_{rs}^b(-ig_s\sqrt{2})(R_{i1}P_L - R_{i2}P_R) \frac{i(\not{p}_3 - \not{q} + m_q)}{(p_3 - q)^2 - m_q^2} T_{st}^a(-ig_s\gamma^\mu) \frac{i(\not{p}_1 - \not{q} + m_q)}{(p_1 - q)^2 - m_q^2} T_{tr}^c(-ig_s\sqrt{2})(R_{i1}P_R - R_{i2}P_L) \frac{i}{q^2 - m_{\tilde{q}}^2} \quad (\text{D.81})$$

$$A_L^1 = g_s^3 \left[\left((2C_{00} - B_0) + (m_q^2 - m_{\tilde{q}}^2)C_0 - m_{\tilde{g}}^2(C_1 + C_2) \right) R_{i2}^2 \right. \quad (\text{D.82})$$

$$\left. - m_{\tilde{g}}^2(C_0 + C_1 + C_2)R_{i1}^2 - 2m_{\tilde{g}}m_q C_0 R_{i1}R_{i2} \right] \quad (\text{D.83})$$

$$A_R^1 = g_s^3 \left[\left((2C_{00} - B_0) + (m_q^2 - m_{\tilde{q}}^2)C_0 - m_{\tilde{g}}^2(C_1 + C_2) \right) R_{i1}^2 \right. \quad (\text{D.84})$$

$$\left. - m_{\tilde{g}}^2(C_0 + C_1 + C_2)R_{i2}^2 - 2m_{\tilde{g}}m_q C_0 R_{i1}R_{i2} \right] \quad (\text{D.85})$$

$$A_L^2 = g_s^3 \left[m_{\tilde{g}}(C_{12} - C_{22} - C_2)R_{i2}^2 + m_{\tilde{g}}(C_{11} - C_{12} + C_1)R_{i1}^2 - m_q(C_1 - C_2)R_{i1}R_{i2} \right] \quad (\text{D.86})$$

$$A_L^2 = g_s^3 \left[m_{\tilde{g}}(C_{12} - C_{22} - C_2)R_{i1}^2 + m_{\tilde{g}}(C_{11} - C_{12} + C_1)R_{i2}^2 - m_q(C_1 - C_2)R_{i1}R_{i2} \right] \quad (\text{D.87})$$

$$A_L^3 = g_s^3 \left[m_{\tilde{g}}(C_{12} + C_{22} + C_2)R_{i2}^2 + m_{\tilde{g}}(C_{11} + C_{12} + C_1)R_{i1}^2 - m_q C_1 C_2 R_{i1}R_{i2} \right] \quad (\text{D.88})$$

$$A_R^3 = g_s^3 \left[m_{\tilde{g}}(C_{12} + C_{22} + C_2)R_{i1}^2 + m_{\tilde{g}}(C_{11} + C_{12} + C_1)R_{i2}^2 - m_q C_1 C_2 R_{i1}R_{i2} \right] \quad (\text{D.89})$$

$$B_L^1 = g_s^3 \left[m_{\tilde{g}}(C_0 + C_1 + C_2)R_{i1}^2 - m_q C_0 R_{i1} R_{i2} \right] \quad (\text{D.90})$$

$$B_R^1 = g_s^3 \left[m_{\tilde{g}}(C_0 + C_1 + C_2)R_{i2}^2 - m_q C_0 R_{i1} R_{i2} \right] \quad (\text{D.91})$$

$$B_L^2 = g_s^3 (C_{11} - C_{12} + C_1) R_{i1}^2 \quad (\text{D.92})$$

$$B_R^2 = g_s^3 (C_{11} - C_{12} + C_1) R_{i2}^2 \quad (\text{D.93})$$

$$B_L^3 = g_s^3 (C_{11} + C_{12} + C_1) R_{i1}^2 \quad (\text{D.94})$$

$$B_R^3 = g_s^3 (C_{11} + C_{12} + C_1) R_{i2}^2 \quad (\text{D.95})$$

$$C_L^1 = g_s^3 \left[m_{\tilde{g}}(C_0 + C_1 + C_2)R_{i1}^2 - m_q C_0 R_{i1} R_{i2} \right] \quad 6 \quad (\text{D.96})$$

$$C_R^1 = g_s^3 \left[m_{\tilde{g}}(C_0 + C_1 + C_2)R_{i2}^2 - m_q C_0 R_{i1} R_{i2} \right] \quad (\text{D.97})$$

$$C_L^2 = g_s^3 (C_{11} - C_{12} + C_2) R_{i2}^2 \quad (\text{D.98})$$

$$C_R^2 = g_s^3 (C_{11} - C_{12} + C_2) R_{i1}^2 \quad (\text{D.99})$$

$$C_L^3 = g_s^3 (C_{11} + C_{12} + C_2) R_{i2}^2 \quad (\text{D.100})$$

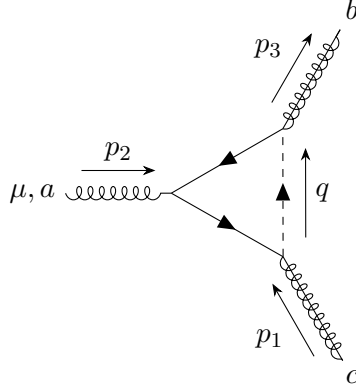
$$C_R^3 = g_s^3 (C_{11} + C_{12} + C_2) R_{i1}^2 \quad (\text{D.101})$$

$$D_L^1 = g_s^3 (C_0 + C_1 + C_2) R_{i1}^2 \quad (\text{D.102})$$

$$D_R^1 = g_s^3 (C_0 + C_1 + C_2) R_{i2}^2 \quad (\text{D.103})$$

$$D_L^2 = D_R^2 = D_L^3 = D_R^3 \quad (\text{D.104})$$

$$F_{color} = -\frac{1}{4} \quad (\text{D.105})$$



$$M = \mu^{\frac{4-D}{2}} \int \frac{d^D q}{(2\pi)^D} T_{sr}^b (-ig_s \sqrt{2}) (R_{i1} P_R - R_{i2} P_L) \frac{i(\not{p}_3 - \not{q} + m_q)}{(p_3 - q)^2 - m_q^2} T_{ts}^a i g_s \gamma^\mu$$

$$\frac{i(\not{p}_1 - \not{q} + m_q)}{(p_1 - q)^2 - m_q^2} T_{rt}^c (-ig_s \sqrt{2}) (R_{i1} P_L - R_{i2} P_R) \frac{i}{q^2 - m_q^2}$$
(D.106)

$$A_L^1 = -g_s^3 \left[\left((2C_{00} - B_0) + (m_q^2 - m_{\bar{q}}^2) C_0 - m_{\bar{q}}^2 (C_1 + C_2) \right) R_{i1}^2 \right.$$
(D.107)

$$\left. - m_{\bar{q}}^2 (C_0 + C_1 + C_2) R_{i2}^2 - 2m_{\bar{q}} m_q C_0 R_{i1} R_{i2} \right]$$
(D.108)

$$A_R^1 = -g_s^3 \left[\left((2C_{00} - B_0) + (m_q^2 - m_{\bar{q}}^2) C_0 - m_{\bar{q}}^2 (C_1 + C_2) \right) R_{i2}^2 \right.$$
(D.109)

$$\left. - m_{\bar{q}}^2 (C_0 + C_1 + C_2) R_{i1}^2 - 2m_{\bar{q}} m_q C_0 R_{i1} R_{i2} \right]$$
(D.110)

$$A_L^2 = -g_s^3 \left[m_{\bar{q}} (C_{12} - C_{22} - C_2) R_{i1}^2 + m_{\bar{q}} (C_{11} - C_{12} + C_1) R_{i2}^2 - m_q (C_1 - C_2) R_{i1} R_{i2} \right]$$
(D.111)

$$A_L^2 = -g_s^3 \left[m_{\bar{q}} (C_{12} - C_{22} - C_2) R_{i2}^2 + m_{\bar{q}} (C_{11} - C_{12} + C_1) R_{i1}^2 - m_q (C_1 - C_2) R_{i1} R_{i2} \right]$$
(D.112)

$$A_L^3 = -g_s^3 \left[m_{\bar{q}} (C_{12} + C_{22} + C_2) R_{i1}^2 + m_{\bar{q}} (C_{11} + C_{12} + C_1) R_{i2}^2 - m_q C_1 C_2 R_{i1} R_{i2} \right]$$
(D.113)

$$A_R^3 = -g_s^3 \left[m_{\bar{q}} (C_{12} + C_{22} + C_2) R_{i2}^2 + m_{\bar{q}} (C_{11} + C_{12} + C_1) R_{i1}^2 - m_q C_1 C_2 R_{i1} R_{i2} \right]$$
(D.114)

$$B_L^1 = -g_s^3 \left[m_{\tilde{g}}(C_0 + C_1 + C_2)R_{i2}^2 - m_q C_0 R_{i1} R_{i2} \right] \quad (\text{D.115})$$

$$B_R^1 = -g_s^3 \left[m_{\tilde{g}}(C_0 + C_1 + C_2)R_{i1}^2 - m_q C_0 R_{i1} R_{i2} \right] \quad (\text{D.116})$$

$$B_L^2 = -g_s^3 (C_{11} - C_{12} + C_1)R_{i2}^2 \quad (\text{D.117})$$

$$B_R^2 = -g_s^3 (C_{11} - C_{12} + C_1)R_{i1}^2 \quad (\text{D.118})$$

$$B_L^3 = -g_s^3 (C_{11} + C_{12} + C_1)R_{i2}^2 \quad (\text{D.119})$$

$$B_R^3 = -g_s^3 (C_{11} + C_{12} + C_1)R_{i1}^2 \quad (\text{D.120})$$

$$C_L^1 = -g_s^3 \left[m_{\tilde{g}}(C_0 + C_1 + C_2)R_{i2}^2 - m_q C_0 R_{i1} R_{i2} \right] \quad (\text{D.121})$$

$$C_R^1 = -g_s^3 \left[m_{\tilde{g}}(C_0 + C_1 + C_2)R_{i1}^2 - m_q C_0 R_{i1} R_{i2} \right] \quad (\text{D.122})$$

$$C_L^2 = -g_s^3 (C_{11} - C_{12} + C_2)R_{i1}^2 \quad (\text{D.123})$$

$$C_R^2 = -g_s^3 (C_{11} - C_{12} + C_2)R_{i2}^2 \quad (\text{D.124})$$

$$C_L^3 = -g_s^3 (C_{11} + C_{12} + C_2)R_{i1}^2 \quad (\text{D.125})$$

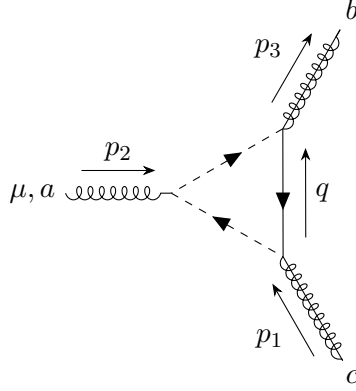
$$C_R^3 = -g_s^3 (C_{11} + C_{12} + C_2)R_{i2}^2 \quad (\text{D.126})$$

$$D_L^1 = -g_s^3 (C_0 + C_1 + C_2)R_{i2}^2 \quad (\text{D.127})$$

$$D_R^1 = -g_s^3 (C_0 + C_1 + C_2)R_{i1}^2 \quad (\text{D.128})$$

$$D_L^2 = D_R^2 = D_L^3 = D_R^3 \quad (\text{D.129})$$

$$F_{color} = \frac{1}{4} \quad (\text{D.130})$$



$$M = \mu^{\frac{4-D}{2}} \int \frac{d^D q}{(2\pi)^D} T_{rs}^b(-i\sqrt{2}g_s)(R_{i1}P_R - R_{i2}P_L) \frac{i(\not{q} + m_q)}{q^2 - m_q^2} T_{tr}^c(-i\sqrt{2}g_s)(R_{i1}P_L - R_{i2}P_R) \\ T_{st}^a g_s (p_1 + p_3 - 2q)^\mu \frac{i}{(p_3 - q)^2} \frac{i}{(p_1 - q)^2} \quad (\text{D.131})$$

$$A_L^1 = g_s^3(-4R_{i1}^2)C_{00} \quad (\text{D.132})$$

$$A_R^1 = g_s^3(-4R_{i2}^2)C_{00} \quad (\text{D.133})$$

$$A_L^2 = g_s^3 \left(2m_q(C_2 - C_1)R_{i1}R_{i2} - 2m_{\bar{g}}(C_{11} - C_{12})R_{i2}^2 - 2m_{\bar{g}}(C_{12} - C_{22})R_{i1}^2 \right) \quad (\text{D.134})$$

$$A_R^2 = g_s^3 \left(2m_q(C_2 - C_1)R_{i1}R_{i2} - 2m_{\bar{g}}(C_{11} - C_{12})R_{i1}^2 - 2m_{\bar{g}}(C_{12} - C_{22})R_{i2}^2 \right) \quad (\text{D.135})$$

$$A_L^3 = g_s^3 \left(-2m_q(C_0 + C_1 + C_2)R_{i1}R_{i2} - 2m_{\bar{g}}(C_1 + C_{11} + C_{12})R_{i2}^2 - 2m_{\bar{g}}(C_2 + C_{12} + C_{22})R_{i1}^2 \right) \quad (\text{D.136})$$

$$A_R^3 = g_s^3 \left(-2m_q(C_0 + C_1 + C_2)R_{i1}R_{i2} - 2m_{\bar{g}}(C_1 + C_{11} + C_{12})R_{i1}^2 - 2m_{\bar{g}}(C_2 + C_{12} + C_{22})R_{i2}^2 \right) \quad (\text{D.137})$$

$$B_L^1 = B_R^1 = 0 \quad (\text{D.138})$$

$$B_L^2 = -g_s^3 2(C_{11} - C_{12})R_{i2}^2 \quad (\text{D.139})$$

$$B_R^2 = -g_s^3 2(C_{11} - C_{12})R_{i1}^2 \quad (\text{D.140})$$

$$B_L^3 = -g_s^3 2(C_1 + C_{11} + C_{12})R_{i2}^2 \quad (\text{D.141})$$

$$B_R^3 = -g_s^3 2(C_1 + C_{11} + C_{12})R_{i1}^2 \quad (\text{D.142})$$

$$C_L^1 = C_R^1 = 0 \quad (\text{D.143})$$

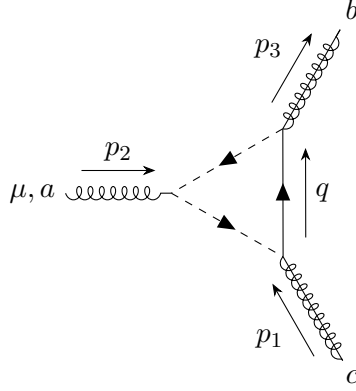
$$C_L^2 = -g_s^3 2(C_{12} - C_{22})R_{i1}^2 \quad (\text{D.144})$$

$$C_R^2 = -g_s^3 2(C_{12} - C_{22})R_{i2}^2 \quad (\text{D.145})$$

$$C_L^3 = -g_s^3 2(C_2 + C_{12} + C_{22})R_{i1}^2 \quad (\text{D.146})$$

$$C_R^3 = -g_s^3 2(C_2 + C_{12} + C_{22})R_{i2}^2 \quad (\text{D.147})$$

$$D_L^1 = D_R^1 = D_L^2 = D_R^2 = D_L^3 + D_R^3 = 0 \quad (\text{D.148})$$



$$M = \mu^{\frac{4-D}{2}} \int \frac{d^D q}{(2\pi)^D} T_{sr}^b(-i\sqrt{2}g_s)(R_{i1}P_L - R_{i2}P_R) \frac{i(q + m_q)}{q^2 - m_q^2} T_{rt}^c(-i\sqrt{2}g_s)(R_{i1}P_R - R_{i2}P_L) \\ T_{ts}^a(-g_s(p_1 + p_3 - 2q)^\mu) \frac{i}{(p_3 - q)^2} \frac{i}{(p_1 - q)^2} \quad (\text{D.149})$$

$$A_L^1 = g_s^3 4R_{i2}^2 C_{00} \quad (\text{D.150})$$

$$A_R^1 = g_s^3 4R_{i1}^2 C_{00} \quad (\text{D.151})$$

$$A_L^2 = -g_s^3 \left(2m_q(C_2 - C_1)R_{i1}R_{i2} - 2m_{\tilde{g}}(C_{11} - C_{12})R_{i1}^2 - 2m_{\tilde{g}}(C_{12} - C_{22})R_{i2}^2 \right) \quad (\text{D.152})$$

$$A_R^2 = -g_s^3 \left(2m_q(C_2 - C_1)R_{i1}R_{i2} - 2m_{\tilde{g}}(C_{11} - C_{12})R_{i2}^2 - 2m_{\tilde{g}}(C_{12} - C_{22})R_{i1}^2 \right) \quad (\text{D.153})$$

$$A_L^3 = -g_s^3 \left(-2m_q(C_0 + C_1 + C_2)R_{i1}R_{i2} - 2m_{\tilde{g}}(C_1 + C_{11} + C_{12})R_{i1}^2 - 2m_{\tilde{g}}(C_2 + C_{12} + C_{22})R_{i2}^2 \right) \quad (\text{D.154})$$

$$A_R^3 = g_s^3 \left(-2m_q(C_0 + C_1 + C_2)R_{i1}R_{i2} - 2m_{\tilde{g}}(C_1 + C_{11} + C_{12})R_{i2}^2 - 2m_{\tilde{g}}(C_2 + C_{12} + C_{22})R_{i1}^2 \right) \quad (\text{D.155})$$

$$B_L^1 = B_R^1 = 0 \quad (\text{D.156})$$

$$B_L^2 = g_s^3 2(C_{11} - C_{12})R_{i1}^2 \quad (\text{D.157})$$

$$B_R^2 = g_s^3 2(C_{11} - C_{12})R_{i2}^2 \quad (\text{D.158})$$

$$B_L^3 = g_s^3 2(C_1 + C_{11} + C_{12})R_{i1}^2 \quad (\text{D.159})$$

$$B_R^3 = g_s^3 2(C_1 + C_{11} + C_{12})R_{i2}^2 \quad (\text{D.160})$$

$$C_L^1 = C_R^1 = 0 \quad (\text{D.161})$$

$$C_L^2 = g_s^3 2(C_{12} - C_{22})R_{i2}^2 \quad (\text{D.162})$$

$$C_R^2 = g_s^3 2(C_{12} - C_{22})R_{i1}^2 \quad (\text{D.163})$$

$$C_L^3 = g_s^3 2(C_2 + C_{12} + C_{22})R_{i2}^2 \quad (\text{D.164})$$

$$C_R^3 = g_s^3 2(C_2 + C_{12} + C_{22})R_{i1}^2 \quad (\text{D.165})$$

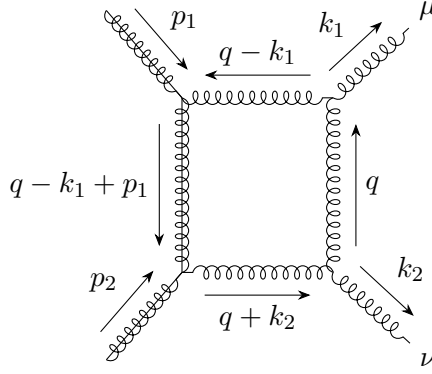
$$D_L^1 = D_R^1 = D_L^2 = D_R^2 = D_L^3 + D_R^3 = 0 \quad (\text{D.166})$$

D.3 Box diagrams

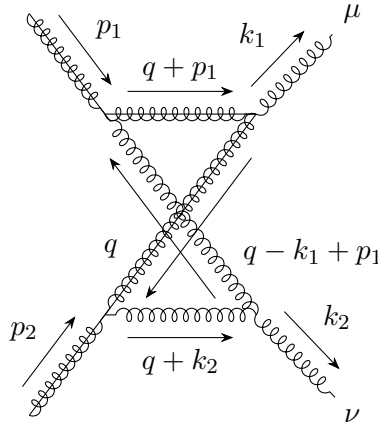
As the contributions of the box diagrams were computed via FeynCalc, here follows a list of all box amplitudes without the declaration of any coefficients. Note that all those boxes also have to be taken into account with exchanged final states. To regain the form of the definition of Passarino-Veltman integrals, one can use:

$$\mu^{2(4-D)} \int \frac{d^D q}{(2\pi)^D} = \mu^{4-D} \frac{i}{4\pi^2} \frac{(2\pi\mu)^{4-D}}{i\pi^2} \int d^D q \quad (\text{D.167})$$

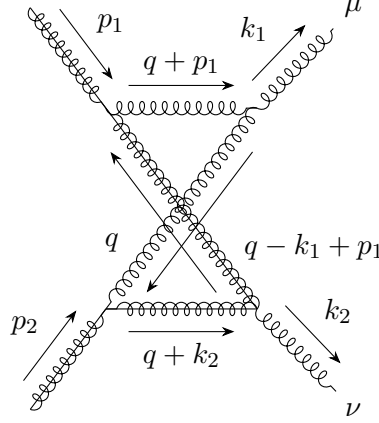
Gluon-gluino loops



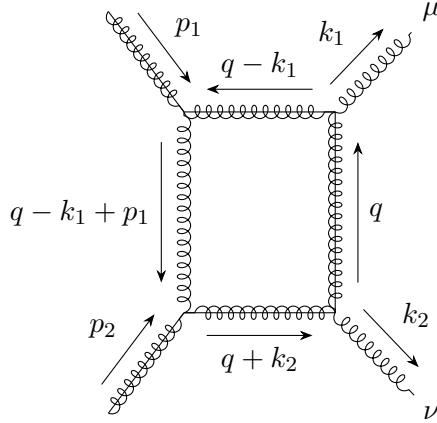
$$\begin{aligned} M = & \mu^{2(4-D)} \int \frac{d^D q}{(2\pi)^D} \bar{v}(p_2) i f_{bef} i g_s \gamma^\rho \frac{i(q + \cancel{p_1} - \cancel{k_1} + m_{\tilde{g}})}{(q + p_1 - k_1)^2 - m_{\tilde{g}}^2} i f_{eah} i g_s \gamma^\tau u(p_1) \frac{-i}{(q - k_1^2)} \\ & i f_{hcg} i g_s [(2q - k_1)^\mu g^{\sigma\tau} + (2k_1 - q)^\sigma g^{\mu\tau} - (q + k_1)^\tau g^{\mu\sigma}] \frac{-i}{q^2} \\ & i f_{gdf} i g_s [(2q + k_2)^\nu g^{\rho\sigma} + (k_2 - q)^\rho g^{\nu\sigma} - (q + 2k_2)^\sigma g^{\nu\rho}] \\ & \frac{-i}{(q + k_2)^2} \varepsilon_\mu^*(k_1) \varepsilon_\nu^*(k_2) \end{aligned} \quad (\text{D.168})$$



$$\begin{aligned}
M = \mu^{2(4-D)} \int \frac{d^D q}{(2\pi)^D} & \bar{v}(p_2) i f_{ibh} i g_s \gamma^\rho \frac{i(\not{q} + \not{p}_1 - \not{k}_1 + m_{\tilde{g}})}{(q + p_1 - k_1)^2 - m_{\tilde{g}}^2} i f_{chg} i g_s \gamma^\mu \frac{i(\not{q} + \not{p}_1 + m_{\tilde{g}})}{(q + p_1)^2 - m_{\tilde{g}}^2} \\
& i f_{fga} i g_s \gamma^\sigma u(p_1) i f_{ifd} i g_s [(-q - 2k_2)_\sigma g_{\rho\nu} + (2q + k_2)_\nu g_{\rho\sigma} + (-q + k_2)_\rho g_{\nu\sigma} \\
& \frac{-i}{(q + k_2)^2} \frac{-i}{q^2} \varepsilon_\mu^*(k_1) \varepsilon_\nu^*(k_2)
\end{aligned} \tag{D.169}$$

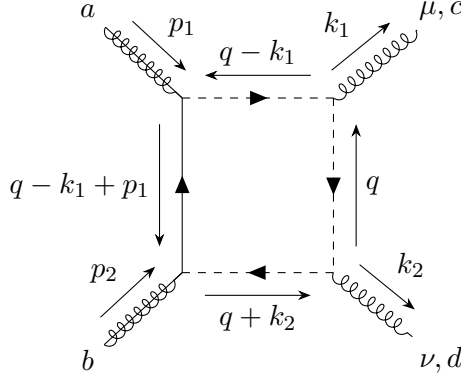


$$\begin{aligned}
M = \mu^{2(4-D)} \int \frac{d^D q}{(2\pi)^D} & \bar{v}(p_2) i f_{ibh} i g_s \gamma^\rho \frac{i(\not{q} + \not{k}_2 + m_{\tilde{g}})}{(q + k_2)^2 - m_{\tilde{g}}^2} i f_{ifd} i g_s \gamma^\mu \frac{i(\not{q} + \not{p}_1 + m_{\tilde{g}})}{(q + p_1)^2 - m_{\tilde{g}}^2} \\
& i f_{fga} i g_s \gamma^\sigma u(p_1) i f_{ibh} i g_s [(q + p_1 - 2k_2)_\sigma g_{\mu\rho} + (-2q - 2p_1 + k_1)_\mu g_{\rho\sigma} + (q + p_1 + k_1)_\rho g_{\mu\sigma}] \\
& \frac{-i}{(q + k_2)^2} \frac{-i}{q^2} \varepsilon_\mu^*(k_1) \varepsilon_\nu^*(k_2)
\end{aligned} \tag{D.170}$$

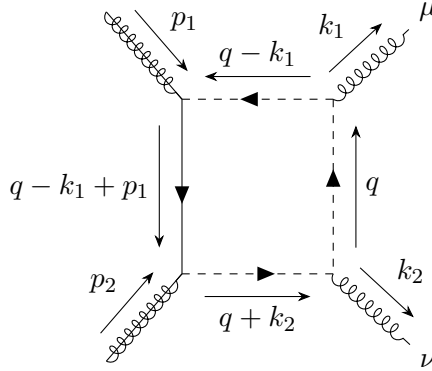


$$\begin{aligned}
M = \mu^{2(4-D)} \int \frac{d^D q}{(2\pi)^D} & \bar{v}(p_2) i f_{bfe} i g_s \gamma_\rho \frac{i(-\not{q} - \not{k}_2 + m_{\tilde{g}})}{(q + k_2)^2 - m_{\tilde{g}}^2} i f_{fgd} i g_s \gamma^\nu \frac{i(-\not{q} + m_{\tilde{g}})}{q^2 - m_{\tilde{g}}^2} i f_{ghc} i g_s \gamma^\mu \\
& \frac{i(\not{k}_1 - \not{q} + m_{\tilde{g}})}{(q - k_1)^2 - m_{\tilde{g}}^2} i f_{hae} i g_s \gamma^\rho u(p_1) \frac{-i}{(q - k_1 + p_1)^2} \varepsilon_\mu^*(k_1) \varepsilon_\nu^*(k_2)
\end{aligned} \tag{D.171}$$

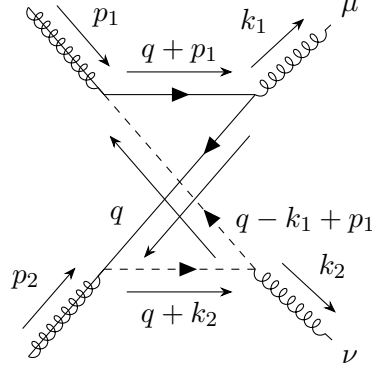
Quark-squark loops



$$\begin{aligned}
M = \mu^{2(4-D)} \int \frac{d^D q}{(2\pi)^D} & \bar{v}(p_2) T_{rs}^b (-i\sqrt{2}g_s) (R_{i1}P_R - R_{i2}P_L) \frac{i(\not{q} + \not{p}_1 - \not{k}_1 + m_{\tilde{q}})}{(q + p_1 - k_1)^2 - m_{\tilde{q}}^2} T_{ur}^a \\
& (-i\sqrt{2}g_s) (R_{i1}P_L - R_{i2}P_R) u(p_1) \frac{i}{(q - k_1)^2 - m_{\tilde{q}}^2} T_{tu}^c (-ig_s) (-2q + k_1)^\mu \\
& \frac{i}{q^2 - m_{\tilde{q}}^2} T_{st}^d (-ig_s) (-2q - k_2)^\nu \frac{i}{(q + k_2)^2 - m_{\tilde{q}}^2} \varepsilon_\mu^*(k_1) \varepsilon_\nu^*(k_2)
\end{aligned} \tag{D.172}$$



$$\begin{aligned}
M = & \mu^{2(4-D)} \int \frac{d^D q}{(2\pi)^D} \bar{v}(p_2) T_{sr}^b (-i\sqrt{2}g_s) (R_{i1}P_L - R_{i2}P_R) \frac{i(\not{q} + \not{p}_1 - \not{k}_1 + m_q)}{(q + p_1 - k_1)^2 - m_q^2} T_{ru}^a \\
& (-i\sqrt{2}g_s) (R_{i1}P_R - R_{i2}P_L) u(p_1) \frac{i}{(q - k_1)^2 - m_{\bar{q}}^2} T_{ut}^c (-ig_s) (2q - k_1)^\mu \\
& \frac{i}{q^2 - m_{\bar{q}}^2} T_{ts}^d (-ig_s) (2q + k_2)^\nu \frac{i}{(q + k_2)^2 - m_{\bar{q}}^2} \varepsilon_\mu^*(k_1) \varepsilon_\nu^*(k_2)
\end{aligned} \tag{D.173}$$



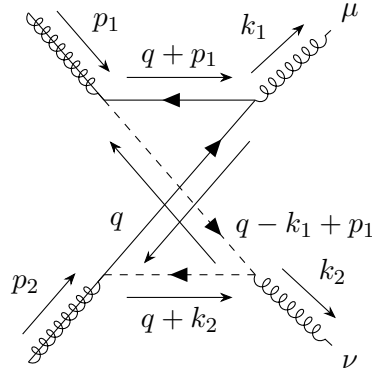
$$\begin{aligned}
M = & F_{\text{color}} g_s^2 \mu^{2(4-D)} \int \frac{d^D q}{(2\pi)^D} \bar{v}(p_2) \boxed{2} \frac{\not{q} + \not{p}_1 - \not{k}_1 + m_q}{(q + p_1 - k_1)^2 - m_q^2} \gamma^\mu \frac{\not{q} + \not{p}_1 + m_q}{(q + p_1)^2 - m_q^2} \boxed{1} u(p_1) \\
& (2q + k_2)^\mu \frac{i}{q^2 - m_{\bar{q}}^2} \frac{i}{(q + k_2)^2 - m_{\bar{q}}^2} \varepsilon_\mu^*(k_1) \varepsilon_\nu^*(k_2)
\end{aligned} \tag{D.174}$$

with

$$\boxed{1} = -i\sqrt{2}g_s (R_{i1}P_R - R_{i2}P_L) \tag{D.175}$$

$$\boxed{2} = -i\sqrt{2}g_s (R_{i1}P_L - R_{i2}P_R) \tag{D.176}$$

$$F_{\text{color}} = \text{Tr}[T^a T^d T^b T^c] \tag{D.177}$$

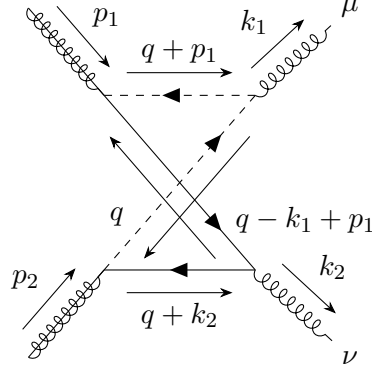


with

$$\boxed{1} = -i\sqrt{2}g_s(R_{i1}P_L - R_{i2}P_R) \quad (\text{D.178})$$

$$\boxed{2} = -i\sqrt{2}g_s(R_{i1}P_R - R_{i2}P_L) \quad (\text{D.179})$$

$$F_{\text{color}} = \text{Tr}[T^a T^c T^b T^d] \quad (\text{D.180})$$



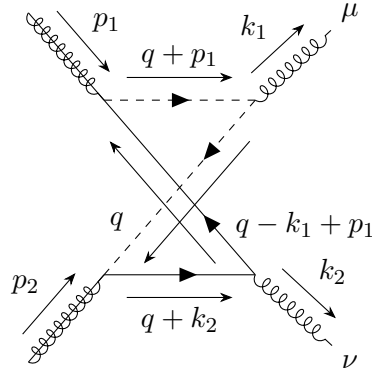
$$M = F_{\text{color}} g_s^2 \mu^{2(4-D)} \int \frac{d^D q}{(2\pi)^D} \bar{v}(p_2) \boxed{2} \frac{-\not{q} - \not{k}_2 + m_q}{(q+k_2)^2 - m_q^2} \gamma^\nu \frac{-\not{q} + m_q}{q^2 - m_q^2} \boxed{1} u(p_1) \\ (2q+k_2)^\mu \varepsilon_\mu^*(k_1) \varepsilon_\nu^*(k_2) \frac{i}{(q+p_1)^2 - m_q^2} \frac{i}{(q-k_1+p_1)^2 - m_q^2} \quad (\text{D.181})$$

with

$$\boxed{1} = -i\sqrt{2}g_s(R_{i1}P_R - R_{i2}P_L) \quad (\text{D.182})$$

$$\boxed{2} = -i\sqrt{2}g_s(R_{i1}P_L - R_{i2}P_R) \quad (\text{D.183})$$

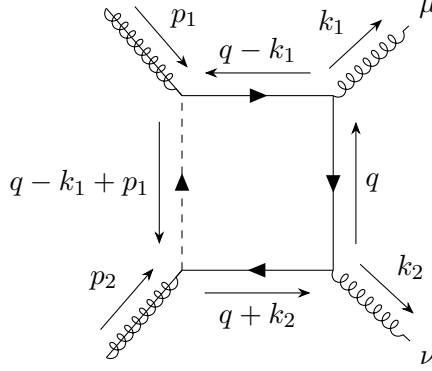
$$F_{\text{color}} = \text{Tr}[T^a T^d T^b T^c] \quad (\text{D.184})$$



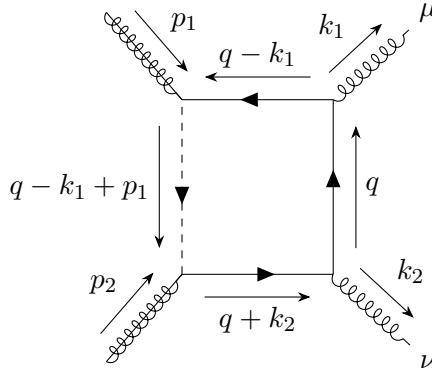
$$\boxed{1} = -i\sqrt{2}g_s(R_{i1}P_L - R_{i2}P_R) \quad (\text{D.185})$$

$$\boxed{2} = -i\sqrt{2}g_s(R_{i1}P_R - R_{i2}P_L) \quad (\text{D.186})$$

$$F_{\text{color}} = \text{Tr}[T^a T^c T^b T^d] \quad (\text{D.187})$$

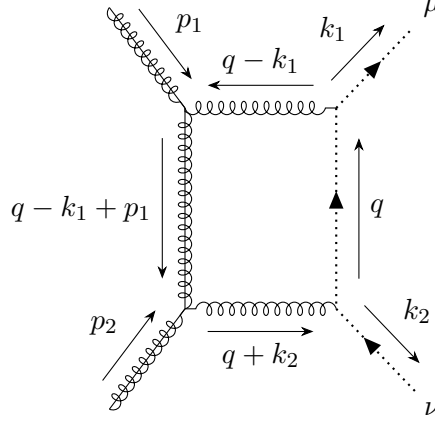


$$\begin{aligned}
M = & \mu^{2(4-D)} \int \frac{d^D q}{(2\pi)^D} \bar{v}(p_2) T_{rs}^b (-i\sqrt{2}g_s) (R_{i1}P_L - R_{i2}P_R) \frac{i(\not{k}_1 - \not{q} + m_q)}{(-q - k_2)^2 - m_q^2} T_{st}^d (-ig_s \gamma^\nu) \\
& \frac{i(-\not{q} + m_q)}{q^2 - m_q^2} T_{tu}^c (-ig_s \gamma^\mu) \frac{i(\not{k}_1 - \not{q})}{(q - k_1^2) - m_q^2} T_{ur}^a (-i\sqrt{2}g_s) (R_{i1}P_R - R_{i2}P_L) \\
& u(p_1) \frac{i}{(q - k_1 + p_1)^2 - m_q^2} \varepsilon_\mu^*(k_1) \varepsilon_\nu^*(k_2)
\end{aligned} \tag{D.188}$$



$$\begin{aligned}
M = & \mu^{2(4-D)} \int \frac{d^D q}{(2\pi)^D} \bar{v}(p_2) T_{sr}^b (-i\sqrt{2}g_s) (R_{i1}P_R - R_{i2}P_L) \frac{i(\not{k}_1 - \not{q} + m_q)}{(-q - k_2)^2 - m_q^2} T_{ts}^d ig_s \gamma^\nu \\
& \frac{i(-\not{q} + m_q)}{q^2 - m_q^2} T_{ut}^c ig_s \gamma^\mu \frac{i(\not{k}_1 - \not{q})}{(q - k_1^2) - m_q^2} T_{ru}^a (-i\sqrt{2}g_s) (R_{i1}P_L - R_{i2}P_R) \\
& u(p_1) \frac{i}{(q - k_1 + p_1)^2 - m_q^2} \varepsilon_\mu^*(k_1) \varepsilon_\nu^*(k_2)
\end{aligned} \tag{D.189}$$

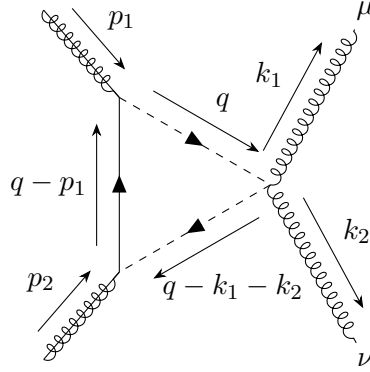
Ghost boxes



$$M = \mu^{2(4-D)} \int \frac{d^D q}{(2\pi)^D} \bar{v}(p_2) i f_{bef} i g_s \gamma^\rho \frac{i(q + \cancel{p_1} - k_1 + m_{\tilde{g}})}{(q + p_1 - k_1)^2 - m_{\tilde{g}}^2} i f_{eah} i g_s \gamma^\tau u(p_1) \quad (D.190)$$

$$i f_{hcg} i g_s k_1^\mu i f_{gdf} i g_s q^\nu \frac{-i}{(q + k_2)^2} \frac{i}{q^2} \frac{-i}{(q - k_1^2)}$$

Triangles



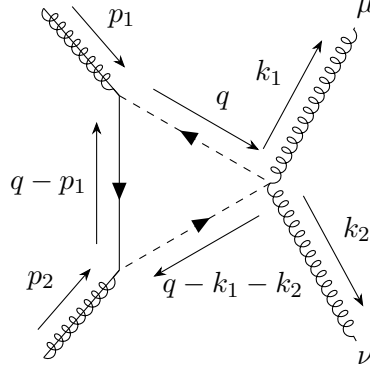
$$M = (\text{Tr}[T^a T^b T^d T^c] + \text{Tr}[T^a T^b T^c T^d]) g_s^2 \mu^{2(4-D)} \int \frac{d^D q}{(2\pi)^D} \bar{v}(p_2) \boxed{2} \frac{i(q - \cancel{p_1})}{(q - p_1)^2 - m_{\tilde{g}}^2} \boxed{1} u(p_1) i g_s^2 g^{\mu\nu} \quad (D.191)$$

$$\frac{i}{q^2} \frac{i}{(q - k_1 - k_2)^2} \varepsilon_\mu^*(k_1) \varepsilon_\nu^*(k_2)$$

with

$$\boxed{1} = -i\sqrt{2}g_s(R_{i1}P_L - R_{i2}P_R) \quad (D.192)$$

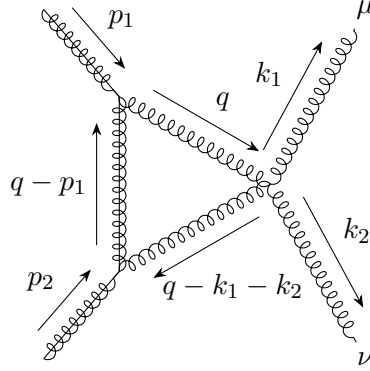
$$\boxed{2} = -i\sqrt{2}g_s(R_{i1}P_R - R_{i2}P_L) \quad (D.193)$$



with

$$\boxed{1} = -i\sqrt{2}g_s(R_{i1}P_R - R_{i2}P_L) \quad (\text{D.194})$$

$$\boxed{2} = -i\sqrt{2}g_s(R_{i1}P_L - R_{i2}P_R) \quad (\text{D.195})$$



$$\begin{aligned}
M = & \mu^{2(4-D)} \int \frac{d^D q}{(2\pi)^D} \bar{v}(p_2) i f_{fbh} i g_s \gamma^\rho \frac{i(\not{q} + \not{p}_1 - \not{k}_1 + m_{\tilde{g}})}{(q + p_1 - k_1)^2 - m_{\tilde{g}}^2} i f_{gha} i g_s \gamma^\sigma u(p_1) (-i g_s) \\
& [f_{gce} f_{fde} (g^{\sigma\rho} g^{\mu\nu} - g^{\sigma\nu} g^{\rho\mu}) + f_{gfe} f_{cde} (g^{\mu\nu} g^{\rho\sigma} - g^{\sigma\nu} g^{\rho\mu}) + f_{gde} f_{cfe} (g^{\sigma\mu} g^{\rho\nu} - g^{\sigma\rho} g^{\mu\nu})] \\
& \frac{-i}{q^2} \frac{-i}{(q - k_1 - k_2)^2} \varepsilon_\mu^*(k_1) \varepsilon_\nu^*(k_2)
\end{aligned} \quad (\text{D.196})$$

References

- [1] Ian Aitchison. *Supersymmetry in Particle Physics*. 2007.
- [2] Ian J R Aitchison. *Supersymmetry and the MSSM: An Elementary Introduction*. 2005. arXiv: [hep-ph/0505105](https://arxiv.org/abs/hep-ph/0505105) [hep-ph].
- [3] Yu. L. Dokshitzer. *QCD for beginners*. 1997.
- [4] Yu. L. Dokshitzer and G. Marchesini. “Soft gluons at large angles in hadron collisions”. In: (2005).
- [5] Helmut Eberl. “Strahlungskorrekturen im minimalen supersymmetrischen Standardmodell”. PhD thesis. 1998.
- [6] Joakim Edsjö and Paolo Gondolo. “Neutralino relic density including coannihilations”. In: *Physical Review D* 56.4 (Aug. 1997), pp. 1879–1894. DOI: [10.1103/PhysRevD.56.1879](https://doi.org/10.1103/PhysRevD.56.1879). URL: <https://doi.org/10.1103/PhysRevD.56.1879>.
- [7] K. Freese. “Review of Observational Evidence for Dark Matter in the Universe and in upcoming searches for Dark Stars”. In: *EAS Publications Series* 36 (2009), pp. 113–126. DOI: [10.1051/eas/0936016](https://doi.org/10.1051/eas/0936016). URL: <https://doi.org/10.1051/eas/0936016>.
- [8] Kim Griest and David Seckel. “Three exceptions in the calculation of relic abundances”. In: *Phys. Rev. D* 43 (1991), pp. 3191–3203. DOI: [10.1103/PhysRevD.43.3191](https://doi.org/10.1103/PhysRevD.43.3191).
- [9] Particle Data Group. “Review of Particle Physics”. In: *Progress of Theoretical and Experimental Physics* 2020.8 (Aug. 2020). 083C01. ISSN: 2050-3911. DOI: [10.1093/ptep/ptaa104](https://doi.org/10.1093/ptep/ptaa104). eprint: <https://academic.oup.com/ptep/article-pdf/2020/8/083C01/34673722/ptaa104.pdf>. URL: <https://doi.org/10.1093/ptep/ptaa104>.
- [10] Julia Harz. “Supersymmetric QCD Corrections and Phenomenological Studies in Relation to Coannihilation of Dark Matter”. In: ().
- [11] Edward W. Kolb and Michael S. Turner. *The Early Universe*. Vol. 69. 1990. ISBN: 978-0-201-62674-2. DOI: [10.1201/9780429492860](https://doi.org/10.1201/9780429492860).
- [12] Karol Kovarik. “Hitchhiker’s Guide To Renormalization”. In: (unpublished).
- [13] M. Kuroda. *Complete Lagrangian of MSSM*. 1999. DOI: [10.48550/ARXIV.HEP-PH/9902340](https://arxiv.org/abs/hep-ph/9902340). URL: <https://arxiv.org/abs/hep-ph/9902340>.
- [14] Priyamvada Natarajan et al. “Mapping substructure in the HST Frontier Fields cluster lenses and in cosmological simulations”. In: *Monthly Notices of the Royal Astronomical Society* 468 (Feb. 2017). DOI: [10.1093/mnras/stw3385](https://doi.org/10.1093/mnras/stw3385).
- [15] W. Porod. “SPheno, a program for calculating supersymmetric spectra, SUSY particle decays and SUSY particle production at ee- colliders”. In: *Computer Physics Communications* 153.2 (June 2003), pp. 275–315. DOI: [10.1016/s0010-4655\(03\)00222-4](https://doi.org/10.1016/s0010-4655(03)00222-4). URL: [https://doi.org/10.1016/s0010-4655\(03\)00222-4](https://doi.org/10.1016/s0010-4655(03)00222-4).

- [16] Matthew D. Schwartz. *Quantum Field Theory and the Standard Model*. Cambridge University Press, 2014.
- [17] Flip Tanedo. “Defense Against the Dark Arts - Notes on dark matter and particle physics”. In: (2011).
- [18] Luca Wiggering. *Squark annihilation into a pair of gluons in the MSSM*. 2021.
- [19] F. Zwicky. “Die Rotverschiebung von extragalaktischen Nebeln”. In: *Helv. Phys. Acta* 6 (1933), pp. 110–127. DOI: 10.1007/s10714-008-0707-4.

Declaration of Academic Integrity

I hereby confirm that this thesis on Gluino annihilation into gluons at next-to-leading order is solely my own work and that I have used no sources or aids other than the ones stated. All passages in my thesis for which other sources, including electronic media, have been used, be it direct quotes or content references, have been acknowledged as such and the sources cited.

(date and signature of student)

I agree to have my thesis checked in order to rule out potential similarities with other works and to have my thesis stored in a database for this purpose.

(date and signature of student)